

**Psychoactive Substances  
as Substrates or Inhibitors of Enzymes  
in Drug Metabolism and Transport**

Dissertation

zur Erlangung des Grades

des Doktors der Naturwissenschaften

der Naturwissenschaftlich-Technischen Fakultät

der Universität des Saarlandes

von

**Lea Wagmann**

Saarbrücken

2018

Tag des Kolloquiums: 16.11.2018

Dekan: Univ.-Prof. Dr. Guido Kickelbick

Berichterstatter: Univ.-Prof. Dr. Dr. h.c. Hans H. Maurer

Univ.-Prof. Dr. Claus-Michael Lehr

Vorsitz: Univ.-Prof. Dr. Andriy Luzhetskyy

Akad. Mitarbeiter: Priv.-Doz. Dr. Martin Frotscher





## **VORWORT**

Die nachfolgende Arbeit entstand unter der Anleitung von Herrn Univ.-Prof. Dr. Dr. h.c. Hans H. Maurer in der Abteilung für Experimentelle und Klinische Toxikologie der Fachrichtung Experimentelle und Klinische Pharmakologie und Toxikologie der Universität des Saarlandes in Homburg (Saar) in der Zeit von Januar 2015 bis Juli 2018.

## **DANKSAGUNG**

Mein besonderer Dank gilt:

Herrn Professor Hans H. Maurer für die herzliche Aufnahme in seinen Arbeitskreis, die Vergabe dieses interessanten und anspruchsvollen Dissertationsthemas, die Möglichkeit, selbstständig zu arbeiten, das wissenschaftliche Denken zu erlernen und aktiv an nationalen und internationalen Fachkongressen teilzunehmen, sowie besonders für die ausgezeichnete fachliche Betreuung und sein stets offenes Ohr,

Herrn Professor Claus-Michael Lehr für die Übernahme des Koreferats,

Herrn Professor Markus R. Meyer für seine herausragende wissenschaftliche Expertise und dafür, dass er diese stets nutze, um mir neue Denkansätze oder Lösungswege aufzuzeigen, seine unermüdliche Unterstützung, und nicht zuletzt seine freundschaftliche Verbundenheit,

meinen Kolleginnen und Kollegen für das angenehme Arbeitsklima, die gute Zusammenarbeit und den Zusammenhalt, auch in Zeiten anstrengender Routinedienste oder nahender Deadlines, und die fachbezogenen, aber auch die

nicht fachbezogenen Unterhaltungen, welche Freundschaften entstehen ließen, die die Promotionszeit überdauern werden,

Herrn Armin A. Weber für seine ständige Einsatzbereitschaft, sowie Rat und Tat in technischen Fragestellungen,

Frau Gabriele Ulrich und Herrn Carsten Schröder für gewissenhaft ausgeführte Laborarbeiten, Betreuung der Messgeräte und zahlreiche Substanzbestellungen,

den Auszubildenden für ihr fleißiges Mitwirken,

meiner Familie, insbesondere meinen Eltern, die mich jederzeit bedingungslos unterstützt haben und es mir so ermöglichten, meinen eigenen Weg zu gehen,

meinem Verlobten Kim für seine Geduld und sein Verständnis, besonders nach dienstintensiven Nächten, seinen Rückhalt, seine Motivation und besonders seine Liebe,

meinem Patenkind Mia, das mich stets zum Lachen bringt,

und meinen Freunden, die in den letzten Jahren oft auf mich verzichten mussten und mich dennoch nie vergessen haben.

**Für meine Eltern**



**“All we have to decide  
is what to do with the time  
that is given us.”**

**J.R.R. Tolkien - The Lord of the Rings**



# TABLE OF CONTENTS

<b>1. GENERAL PART .....</b>	<b>1</b>
1.1. PSYCHOACTIVE SUBSTANCES ON THE DRUGS OF ABUSE MARKET .....	1
1.2. PHARMACOLOGY OF PSYCHOACTIVE SUBSTANCES.....	2
1.3. DRUG-DRUG INTERACTIONS OF PSYCHOACTIVE SUBSTANCES .....	2
1.4. ENZYMES IN DRUG METABOLISM AND TRANSPORT.....	3
1.4.1. FLAVIN-CONTAINING MONOOXYGENASES.....	4
1.4.2. MONOAMINE OXIDASES.....	5
1.4.3. BREAST CANCER RESISTANCE PROTEIN.....	5
<b>2. AIMS AND SCOPES.....</b>	<b>7</b>
<b>3. PUBLICATIONS OF THE RESULTS .....</b>	<b>9</b>
3.1. WHAT IS THE CONTRIBUTION OF HUMAN FMO3 IN THE N- OXYGENATION OF SELECTED THERAPEUTIC DRUGS AND DRUGS OF ABUSE? <sup>42</sup> (DOI: 10.1016/J.TOXLET.2016.06.013).....	9
3.2. IN VITRO MONOAMINE OXIDASE INHIBITION POTENTIAL OF ALPHA- METHYLTRYPTAMINE ANALOG NEW PSYCHOACTIVE SUBSTANCES FOR ASSESSING POSSIBLE TOXIC RISKS <sup>43</sup> .....	11
(DOI: 10.1016/J.TOXLET.2017.03.007).....	11
3.3. INTERACTIONS OF PHENETHYLAMINE-DERIVED PSYCHOACTIVE SUBSTANCES OF THE 2C-SERIES WITH HUMAN MONOAMINE OXIDASES <sup>44</sup> (DOI: 10.1002/DTA.2494) .....	13
3.4. AN EASY AND FAST ADENOSINE 5'-DIPHOSPHATE QUANTIFICATION PROCEDURE BASED ON HYDROPHILIC INTERACTION LIQUID	

CHROMATOGRAPHY-HIGH RESOLUTION TANDEM MASS  
SPECTROMETRY FOR DETERMINATION OF THE IN VITRO ADENOSINE  
5'-TRIPHOSPHATASE ACTIVITY OF THE HUMAN BREAST CANCER  
RESISTANCE PROTEIN ABCG2<sup>45</sup>

(DOI: 10.1016/J.CHROMA.2017.09.034) ..... 15

3.5. INHIBITION AND STIMULATION OF THE HUMAN BREAST CANCER  
RESISTANCE PROTEIN AS IN VITRO PREDICTOR OF DRUG-DRUG-  
INTERACTIONS OF DRUGS OF ABUSE<sup>46</sup>

(DOI: 10.1007/s00204-018-2276-y) ..... 17

<b>4.</b>	<b>DISCUSSION AND CONCLUSIONS</b> .....	<b>19</b>
<b>5.</b>	<b>REFERENCES</b> .....	<b>23</b>
<b>6.</b>	<b>ABBREVIATIONS</b> .....	<b>29</b>
<b>7.</b>	<b>SUMMARY</b> .....	<b>31</b>
<b>8.</b>	<b>ZUSAMMENFASSUNG</b> .....	<b>33</b>

## 1. GENERAL PART

### 1.1. PSYCHOACTIVE SUBSTANCES ON THE DRUGS OF ABUSE MARKET

In recent years, the spectrum of psychoactive substances available on the drugs of abuse (DOA) market has widened considerably with the persistence of traditional drugs such as cannabis, amphetamine, 3,4-methylenedioxymethamphetamine (MDMA), cocaine, or heroin, and the emergence of more and more new psychoactive substances (NPS) every year.<sup>1</sup> NPS initially circumvent existing legislation and are usually offered as alternative to controlled DOA with similar chemical structures and expected pharmacological effects.<sup>2</sup> In Europe, most of the emerging NPS belong to the categories stimulant phenethylamines or cathinones, synthetic cannabinoid receptor agonists, and opioids.<sup>3</sup> NPS are easily available via specialized online shops labeled for example as 'legal highs', 'bath salts', or 'research chemicals', but they are also sold by drug dealers on the street.<sup>4</sup> As soon as a certain NPS becomes illegal due to law changes, it is usually replaced by derivatives and the 'cat and mouse game' starts over again.<sup>4</sup> By the end of 2017, more than 670 NPS were notified to the European Union Early Warning System for NPS of the European Monitoring Center of Drugs and Drug Addiction and continuously monitored afterwards.<sup>3</sup> Even though NPS are initially not controlled and easily available, reports about potentially harmful effects or fatalities are frequently published.<sup>1,5-7</sup> One troubling aspect is the high variability of the active ingredient content in NPS products what makes the prediction of a proper dose almost impossible.<sup>1,7</sup> In addition, NPS are often used as adulterants in DOA products or sold under the name of other NPS or controlled drugs.<sup>1,7</sup> Due to their high number, the analytical detection of NPS represents a significant challenge

to forensic and clinical toxicologists.<sup>2,5</sup> In contrast to therapeutic drugs, DOA are marketed and consumed without (pre)clinical studies and their pharmacology and toxicity is completely unknown potentially exposing users to serious health risks.<sup>1,8</sup>

### **1.2. PHARMACOLOGY OF PSYCHOACTIVE SUBSTANCES**

Pharmacology and toxicology are sciences of the use and effects of xenobiotics (drugs or non-drugs, respectively) and can be subdivided into two fields. On the one hand, the pharmacodynamics/toxicodynamics deals with the interaction of pharmacologically active substances with target sites in living systems and the biochemical and physiological consequences leading to therapeutic or adverse effects.<sup>9</sup> On the other, the pharmacokinetics/toxicokinetics summarizes the processes of the uptake of these substances by the body, the biotransformation they undergo, the distribution of the substances and their metabolites in the tissues, and the elimination of the substances and their metabolites from the body over a period of time.<sup>9</sup> Both fields have to be investigated during drug development before a new drug candidate is approved. This is not the case for DOA, which should not be considered as therapeutic drugs being potentially harmful compounds. Therefore, the terms toxicodynamics and toxicokinetics are preferred in this context.<sup>8</sup> However, their toxicology is unknown before they are marketed and consumed.

### **1.3. DRUG-DRUG INTERACTIONS OF PSYCHOACTIVE SUBSTANCES**

A drug-drug interaction (DDI) occurs if a compound influences the pharmacodynamic and/or pharmacokinetic properties of another compound. According to the European Medicines Agency, the compound affected by the DDI is called victim drug and the

---

other one, which affects the properties of the victim drug, is called perpetrator drug.<sup>10</sup> Evaluating the DDI potential of an investigational new drug involves the identification of the principal routes of the drug's elimination, estimation of the contribution of enzymes and transporters to the drug's disposition, and the characterization of the effect of the drug on enzymes and transporters.<sup>11</sup> It is usually investigated during drug development using *in vitro* experiments followed by *in vivo* studies.<sup>10</sup> The DDI potential of psychoactive substances used as therapeutic drugs and its clinical relevance is reviewed in numerous publications.<sup>12-16</sup> Unfortunately, DOA do not pass through a comparable drug development process including (pre)clinical studies and tests for safety and harmlessness.<sup>8</sup> Therefore, the risk for the occurrence of DDI is elevated, as nothing is known about their toxicodynamics or toxicokinetics. A DOA can act as victim or perpetrator drug and the second compound can either be a therapeutic drug or another DOA. Only limited information about DDI of DOA is available. Lindsey et al. summarized the clinical literature on interactions between traditional DOA such as cannabis, amphetamine, MDMA, cocaine, or heroin and prescription therapies.<sup>17</sup> Kumar et al. described interactions between antiretroviral drugs and common DOA such as cannabis, methamphetamine, or cocaine.<sup>18</sup> In both cases, decreased therapeutic efficacy or increased DOA-mediated toxicity were reported, which was mainly ascribed to common metabolic pathways of the involved compounds and further experimental and clinical data was claimed.<sup>17,18</sup>

### **1.4. ENZYMES IN DRUG METABOLISM AND TRANSPORT**

Drugs are required to reach their target structures in a sufficient quantity to cause effects. Therefore, the therapeutic efficacy is determined by its pharmacokinetics and thus by the enzymes involved in its metabolism and membrane transport. Metabolic

---

enzymes catalyze chemical transformations of drugs aiming to increase their hydrophilicity and thus excreatability.<sup>9</sup> These transformations can be subdivided in phase I reactions being enzymatic alterations of the drug in preparation for phase II reactions, a conjugation with endogenous molecules producing more water-soluble derivatives.<sup>9</sup> Usually metabolic alterations lead to inactivation, but bioactivation was also described forming therapeutically active and/or toxic metabolites.<sup>19-21</sup> Today, it is generally recognized that the impact of drug transporters on clinically relevant drug disposition and DDI is equal to that of metabolizing enzymes.<sup>22</sup> Transporters are proteins found in cell membranes, which facilitates the transport of a compound across the membrane.<sup>9</sup> The drug can either be transported into the cell (uptake) or out of it (efflux). Membrane transporters can be grouped in uptake transporters from the solute carrier superfamily and the adenosine 5'-triphosphate (ATP)-dependent efflux pumps from the ATP-binding cassette (ABC) superfamily.<sup>23</sup> Membrane transporters are crucial factors in a drug's disposition and excretion.<sup>23</sup>

### **1.4.1. FLAVIN-CONTAINING MONOOXYGENASES**

Flavin-containing monooxygenases (FMO) form part of the oxidative phase I metabolism just like cytochrome P450 (CYP) enzymes. FMO oxygenate nucleophilic heteroatom containing drugs and generally convert them into harmless, polar, readily excreted metabolites. However, bioactivation by FMO was described in some cases.<sup>20</sup> In contrast to the intensively studied CYP enzymes, FMO have long been disregarded in metabolism studies.<sup>20,24</sup> In addition, experimental conditions were frequently chosen to optimize CYP activity rather than those for other oxidative enzymes leading to underestimation of non-CYP reactions.<sup>20</sup> Consequently, only scarce information concerning the role of FMO in the metabolism of therapeutic drugs

or DOA in particular is available. Solely the *N*-oxygenation of amphetamine and methamphetamine catalyzed by FMO3, the major FMO isoform in the adult human liver, was described forming potentially toxic hydroxylamines.<sup>25</sup>

#### **1.4.2. MONOAMINE OXIDASES**

Monoamine oxidases (MAO) are flavin-containing enzymes of the mitochondrial outer-membrane. Two human isoforms exist, MAO-A and B. MAO, which catalyze the oxidative deamination of endogenous compounds or xenobiotics under formation of an aldehyde, ammonia, and hydrogen peroxide.<sup>26-28</sup> Neurotransmitters such as dopamine, noradrenalin, and serotonin (5-HT) are prominent MAO substrates. Dopamine and noradrenalin are metabolized in a comparable extent by both isoforms, while 5-HT has a higher affinity to MAO-A.<sup>29</sup> Both isoforms are targets of therapeutic drugs being selective and unselective as well as reversible and irreversible MAO inhibitors.<sup>27</sup> By inhibiting MAO, the breakdown of monoamine neurotransmitters is prevented leading to increased concentrations and potential monoaminergic toxicity in intoxication cases.<sup>28</sup> Serotonergic and adrenergic side effects such as tachycardia, hyperthermia, rhabdomyolysis, and agitated delirium were reported.<sup>30</sup> Especially if combined with other serotonergic agents, the occurrence of a potentially life-threatening 5-HT syndrome is likely.<sup>31</sup> MAO inhibition potential was only investigated for a small number of DOA so far.<sup>32-34</sup>

#### **1.4.3. BREAST CANCER RESISTANCE PROTEIN**

The breast cancer resistance protein (BCRP) is an efflux transporter of the ABC superfamily and has been characterized as an important part of the human body's

---

self-defense system.<sup>35</sup> Similar to the P-glycoprotein, the BCRP is primarily present in sites important for drug disposition such as the gastrointestinal tract, liver, kidney, or brain endothelium and has a role in limiting oral bioavailability and transport across the blood–brain barrier.<sup>23</sup> After oral co-administration of a BCRP inhibitor, significantly elevated plasma concentrations of BCRP substrates were described.<sup>36,37</sup> Substrates of the BCRP are highly diverse.<sup>23,38</sup> For their translocation across cellular membranes, ATP is required and hydrolyzed by the BCRP ATPase under formation of adenosine 5'-diphosphate (ADP) and inorganic phosphate.<sup>39</sup> Only few DOA were investigated for their influence on the BCRP yet. However, BCRP inhibition was described for the plant cannabinoids cannabinal, cannabidiol, and delta 9-tetrahydrocannabinol and the alkaloid ibogaine, demonstrating that DOA have to be considered.<sup>40,41</sup>

## 2. AIMS AND SCOPES

As already described, little or nothing is known about the toxicokinetics of DOA before they are marketed. To expand the knowledge surrounding interactions between DOA and metabolic enzymes or transport proteins, the aims of the presented studies were as follows:

- Identification of FMO3 substrates amongst eight structurally different DOA using in vitro incubations and liquid chromatography (LC)-ion trap (IT)-tandem mass spectrometry (MS/MS) analyses
- Elucidation of the contribution of FMO3 and various CYP enzymes to the in vivo hepatic net clearance of the *N*-oxygenated DOA calculated by application of an extended relative activity factor approach
- Development and validation of a MAO inhibition assay based on in vitro incubations of recombinant MAO and hydrophilic interaction liquid chromatography (HILIC)-high resolution (HR) MS/MS analysis
- Investigation of the in vitro inhibition potential of alpha-methyltryptamine (AMT) and 13 ring-substituted analogs on recombinant human MAO-A or B during an initial inhibition screening procedure
- Investigation of the in vitro inhibition potential of 17 phenethylamines, consisting of 12 classic 2C-series drugs and five FLY analogs, on recombinant human MAO-A or B during an initial inhibition screening procedure

- Determination of the DOA concentration that reduced the MAO activity by 50% (IC<sub>50</sub> values)
- Development and validation of an ADP quantification procedure by HILIC-HRMS/MS to assess the BCRP ATPase activity
- Investigation of the influence of 13 structurally different DOA on the BCRP ATPase activity and modeling of enzyme kinetics in case of stimulation or determination of IC<sub>50</sub> values in case of inhibition

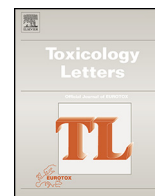
### **3. PUBLICATIONS OF THE RESULTS**

The results of the studies were published in the following papers:

#### **3.1. WHAT IS THE CONTRIBUTION OF HUMAN FMO3 IN THE *N*-OXYGENATION OF SELECTED THERAPEUTIC DRUGS AND DRUGS OF ABUSE?<sup>42</sup>**

**(DOI: 10.1016/j.toxlet.2016.06.013)**





# What is the contribution of human FMO3 in the *N*-oxygenation of selected therapeutic drugs and drugs of abuse?



Lea Wagmann<sup>a</sup>, Markus R. Meyer<sup>a,b</sup>, Hans H. Maurer<sup>a,\*</sup>

<sup>a</sup> Department of Experimental and Clinical Toxicology, Saarland University, Homburg, Germany

<sup>b</sup> Department of Clinical Pharmacology and Pharmacoepidemiology, Heidelberg University Hospital, Heidelberg, Germany

## HIGHLIGHTS

- Single enzyme incubations best suited for FMO3 substrate identification.
- Integration of FMO3 in the relative activity factor (RAF) approach possible.
- Participation of FMO3 and CYPs in the *N*-oxygenation of therapeutics and DOAs.
- Different contributions of FMO3 to the hepatic clearances of the *N*-oxygenated DOAs.

## ARTICLE INFO

### Article history:

Received 3 May 2016

Received in revised form 12 June 2016

Accepted 13 June 2016

Available online 15 June 2016

### Keywords:

FMO3

CYPs

Drugs of abuse

Relative activity factor approach

Hepatic clearance

## ABSTRACT

Little is known about the role of flavin-containing monooxygenases (FMOs) in the metabolism of xenobiotics. FMO3 is the isoform in adult human liver with the highest impact on drug metabolism. The aim of the presented study was to elucidate the contribution of human FMO3 to the *N*-oxygenation of selected therapeutic drugs and drugs of abuse (DOAs). Its contribution to the *in vivo* hepatic net clearance of the *N*-oxygenation products was calculated by application of an extended relative activity factor (RAF) approach to differentiate from contribution of cytochrome P450 (CYP) isoforms. FMO3 and CYP substrates were identified using pooled human liver microsomes after heat inactivation and chemical inhibition, or single enzyme incubations. Kinetic parameters were subsequently determined using recombinant human enzymes and mass spectrometric analysis via authentic reference standards or simple peak areas of the products divided by those of the internal standard. FMO3 was identified as enzyme mainly responsible for the formation of *N,N*-diallyltryptamine *N*-oxide and methamphetamine hydroxylamine (>80% contribution for both). A contribution of 50 and 30% was calculated for the formation of *N,N*-dimethyltryptamine *N*-oxide and methoxypiperamide *N*-oxide, respectively. However, FMO3 contributed with less than 5% to the formation of 3-bromomethcathinone hydroxylamine, amitriptyline *N*-oxide, and clozapine *N*-oxide. There was no significant difference in the contributions when using calibrations with reference metabolite standards or peak area ratio calculations. The successful application of a modified RAF approach including FMO3 proved the importance of FMO3 in the *N*-oxygenation of DOAs in human metabolism.

© 2016 Elsevier Ireland Ltd. All rights reserved.

## 1. Introduction

Monooxygenases are responsible for the major part of the human phase I metabolism and convert xenobiotics to more hydrophilic compounds usually leading to inactivation (Cashman, 2005; Zollner et al., 2010). These monooxygenases can be grouped

into different enzyme families such as the cytochrome P450 monooxygenases (CYPs) and the flavin-containing monooxygenases (FMOs) (Torres Pazmino et al., 2010). CYPs catalyze oxygenation mainly of carbon but also of nitrogen and sulfur. FMOs usually oxygenate soft nucleophiles, in particular nitrogen, sulfur, phosphorous, and selenium atoms. Both microsomal systems have in common, that they transform a wide range of heteroatom-containing substrates (Cashman, 2005; Cruciani et al., 2014).

\* Corresponding author.

E-mail address: [hans.maurer@uks.eu](mailto:hans.maurer@uks.eu) (H.H. Maurer).

In comparison to the extensively studied CYPs, FMOs have long been neglected in metabolism investigations. In addition, experimental conditions were usually chosen to optimize CYP activity rather than the activity of other oxidative enzymes leading to underestimation of non-CYP reactions (Strolin et al., 2006). Recently, Fan et al. asked for further investigations that dissect the relative contribution of FMOs compared to CYPs (Fan et al., 2016). Hence, only limited information about interactions of FMO with therapeutic drugs and drugs of abuse (DOAs) in particular is available. Only the oxygenation of amphetamine and methamphetamine by human FMO was described so far, leading to reactive metabolites (Cashman et al., 1999; Szoko et al., 2004). Cashman et al. reported that amphetamine and methamphetamine were *N*-oxygenated by FMO3, the major FMO isoform in the adult human liver. The formed hydroxylamines were also identified as FMO3 substrates leading to *N,N*-dihydroxylation followed by conversion to phenylpropanone oxime and phenylpropanone, respectively. Particularly the first step may pose a significant toxicological threat due to the potential toxic nature of free hydroxylamine (Cashman et al., 1999).

Therefore, the aim of the presented study was to elucidate the contribution of FMO3 to the human, hepatic metabolism of 12 selected, structurally different therapeutic drugs and eight DOAs. Its contribution to the *in vivo* hepatic net clearance of the *N*-oxygenation products should be calculated by application of an extended relative activity factor (RAF) approach (Crespi and Miller, 1999; Venkatakrishnan et al., 2001) to differentiate from contribution of CYP isoforms. Finally, possible differences in the contributions should be assessed by using calibrations with reference metabolite standards or peak area ratio (PAR) calculations.

## 2. Materials and methods

### 2.1. Chemicals and enzymes

*N,N*-Dimethyltryptamine (DMT) was obtained from THC Pharm (Frankfurt, Germany), methadone from Lipomed (Weil am Rhein, Germany), trimipramine-*d*<sub>3</sub> and norclozapine-*d*<sub>8</sub> from Promochem (Wesel, Germany), *R,S*-methamphetamine, 1-aminobenzotriazole (ABT), isocitrate (IC), isocitrate dehydrogenase (IDH), superoxide dismutase (SOD), potassium dihydrogenphosphate (KH<sub>2</sub>PO<sub>4</sub>), and dipotassium hydrogenphosphate (K<sub>2</sub>HPO<sub>4</sub>) from Sigma-Aldrich (Taufkirchen, Germany). All other used drugs (of abuse) were

supplied by commercial suppliers (e.g. Fluka, Neu Ulm, Germany; LG Chemicals, Teddington, UK; Lipomed, Weil am Rhein, Germany; Promochem, Wesel, Germany) or by the manufacturers of the marketed drugs. NADP<sup>+</sup> was from Biomol (Hamburg, Germany), formic acid (MS grade) from Fluka (Neu-Ulm, Germany), acetonitrile, methanol (both LC-MS grade), and all other chemicals from VWR (Darmstadt, Germany). Methanolic stock solutions (1 mg/mL) of the studied compounds were used. The chemical structures of all tested DOAs are depicted in Fig. 1.

The baculovirus-infected insect cell microsomes (Supersomes) containing human complementary DNA-expressed FMO3 (5 mg protein/mL), CYP1A2, CYP2A6, CYP2B6, CYP2C8, CYP2C9, CYP2C19, CYP2D6, CYP3A4 (1 nmol/mL), or CYP2E1, CYP3A5 (2 nmol/mL), and pooled human liver microsomes (pHLM, 20 mg microsomal protein/mL, 330 pmol total CYP/mg protein) were obtained from Corning (Amsterdam, The Netherlands). After delivery, the microsomes were thawed at 37 °C, aliquoted, snap-frozen in liquid nitrogen, and stored at –80 °C until use.

### 2.2. pHLM incubations

Incubations were performed at 37 °C for 30 min with 25 μM of the substrate, regenerating system, and 1 mg protein/mL pHLM according to Michely et al. (2015). Incubations with pHLM were done without pretreatment, after preincubation with the chemical inhibitors ABT (2 mM) for CYPs or methimazole (200 μM) for FMOs, or after preheating. Heat-treated pHLM were prepared by heating at 55 °C for 1 min in absence of NADP<sup>+</sup> in accordance to Ring et al. (1999) or at 45 °C for 5 min in absence of NADP<sup>+</sup> and cooling on ice for 15 min in accordance to Taniguchi-Takizawa et al. (2015). In addition, blank incubations with buffer instead of enzymes were performed. As described before (Michely et al., 2015), besides enzymes and substrate, the incubation mixtures (final volume 50 μL) contained 90 mM phosphate buffer (pH 7.4), 5 mM Mg<sup>2+</sup>, 5 mM IC, 1.2 mM NADP<sup>+</sup>, 0.5 U/mL IDH, and 200 U/mL SOD. Reactions were initiated by addition of the substrate and stopped with 50 μL of ice-cold acetonitrile, containing 5 μM internal standard. Trimipramine-*d*<sub>3</sub> was used as internal standard for incubations with all analytes, except for amitriptyline, where norclozapine-*d*<sub>8</sub> was used. The solution was centrifuged for 5 min at 14,000g, 70 μL of the supernatant phase was transferred to an autosampler vial and 10 μL injected onto the liquid chromatography (LC)-ion trap (IT)-mass spectrometry (MS) system described below. The amounts of formed metabolites in untreated and

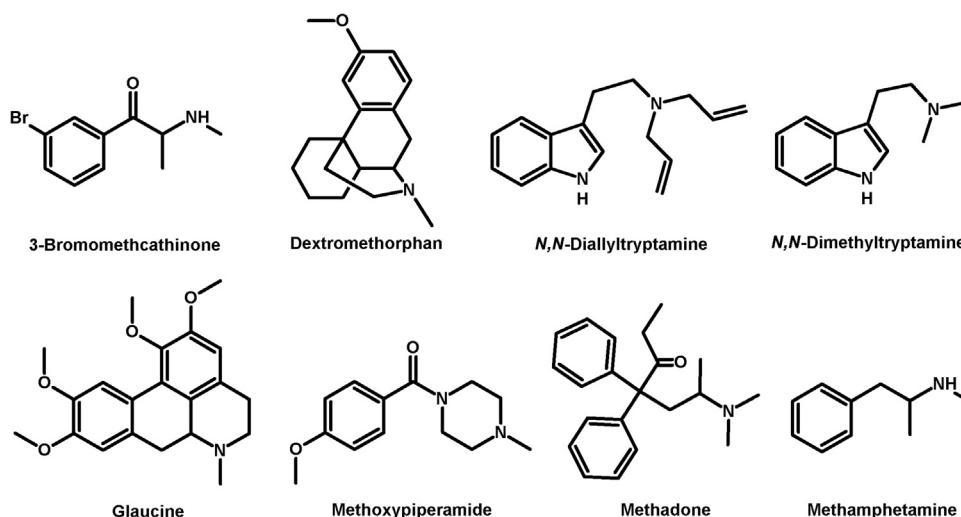


Fig. 1. Chemical structures of tested drugs of abuse in alphabetic order.

pretreated incubations were compared by calculating the PAR of the metabolites and the internal standard. All incubations were performed in duplicate ( $n = 2$ ).

### 2.3. Monoxygenases activity screening

Incubation mixtures contained 25  $\mu\text{M}$  of the test substrate and FMO3 (0.25 mg protein/mL), CYP1A2, CYP2A6, CYP2B6, CYP2C8, CYP2C9, CYP2C19, CYP2D6, CYP2E1, CYP3A4, CYP3A5 (50 pmol/mL, each), or pHLM (1 mg protein/mL). For incubations with CYP2A6 or CYP2C9, phosphate buffer was replaced with 45 or 90 mM Tris buffer, respectively, according to the Gentest manual. Incubations were conducted as described in Section 2.2.

### 2.4. Kinetic studies

The kinetic constants of *N*-oxygenation reactions were derived from incubations with FMO3, single CYPs, or pHLM. Incubation time and enzyme concentration were always set in the linear range of metabolite formation. Substrate concentrations were chosen to allow modeling of enzyme kinetics and were usually between 1 and 2000  $\mu\text{M}$ . The concentration of organic solvent was always  $\leq 2\%$  (Chauret et al., 1998). All incubations were performed in triplicate ( $n = 3$ ). Kinetic constants were calculated via two ways: (a) quantification of the formed products by calibration using the corresponding reference standards (CRS, different concentrations between 0.001 and 1  $\mu\text{M}$ , non-linear regression, either no weighting or weighted ( $1/x^2$ , where  $x$  is the CRS concentration), depending on investigated substrate and enzyme), (b) the peak areas of the products divided by those of the internal standard amitriptyline *N*-oxide (used for clozapine kinetics) or clozapine *N*-oxide (used for kinetics of all other analytes), respectively. These PARs were used instead of concentrations for calculating the enzyme kinetic constants.

Enzyme kinetic constants were estimated by nonlinear curve fitting using GraphPad Prism 5.00 software (GraphPad Software, San Diego, USA). The Michaelis-Menten equation (Eq. (1)) was used to calculate apparent  $K_m$  and  $V_{\max}$  values for single-enzyme systems and pHLM.

$$V = \frac{V_{\max} \times [S]}{K_m + [S]} \quad (1)$$

### 2.5. Calculation of relative activity factors, contributions, and percentages of net clearance

The RAF approach (Crespi and Miller, 1999; Stormer et al., 2000) was based on the hypothesis that the human liver microsomal rates of a biotransformation mediated by multiple CYP isoforms could be mathematically reconstructed from the rates of the biotransformation catalyzed by individual recombinant CYPs (Venkatakrisnan et al., 2001). It was used for the in vitro-in vivo scaling of pharmacokinetic clearance from in vitro intrinsic clearance measurements in heterologous expression systems (Venkatakrisnan et al., 2001).

The turnover rates (TR) of FMO3 (probe substrate (PS) methyl *p*-tolyl sulfide), CYP1A2 (PS phenacetin), CYP2B6 (PS 7-ethoxy-4-trifluoromethylcoumarin), CYP2C8 (PS paclitaxel), CYP2C19 (PS *S*-mephenytoin), CYP2D6 (PS bufuralol), CYP2E1 (PS chlorzoxazone), and CYP3A4 (PS testosterone) in insect cell microsomes (ICM) and pHLM were taken from the supplier's data sheets. The RAFs were calculated according to Eq. (2).

$$\text{RAF}_{\text{enzyme}} = \frac{\text{TR}_{\text{PS in pHLM}}}{\text{TR}_{\text{PS in ICM}}} \quad (2)$$

The enzyme velocities  $V_{\text{enzyme}}$  (see Eq. (1)) for the respective metabolic reactions were calculated at different substrate concentrations and multiplied by the corresponding RAF leading to a value, which was defined as 'contribution' (Eq. (3)). The  $K_m$  and  $V_{\max}$  values (Eq. (1)) were obtained from the incubations with cDNA-expressed enzymes.

$$\text{contribution}_{\text{enzyme}} = \text{RAF}_{\text{enzyme}} \times V_{\text{enzyme}} \quad (3)$$

Based on these corrected activities (contributions) the percentages of net clearance by a particular enzyme at a certain substrate concentration can be calculated using Eq. (4).

$$\text{clearance}_{\text{enzyme}}[\%] = \frac{\text{contribution}_{\text{enzyme}}}{\sum \text{contribution}_{\text{enzyme}}} \times 100 \quad (4)$$

### 2.6. Apparatus and LC-conditions

All samples were analyzed using a ThermoFisher Scientific (TF, Dreieich, Germany) LXQ linear IT-MS, coupled to a TF Accela ultra high performance LC (UHPLC) system consisting of a degasser, a quaternary pump, and an autosampler. Gradient elution was performed on a TF Hypersil GOLD C18 column (100  $\times$  2.1 mm, 1.9  $\mu\text{m}$ ). The mobile phase consisted of 10 mM aqueous ammonium formate plus 0.1% formic acid (pH 3.4, eluent A) and acetonitrile plus 0.1% formic acid (eluent B). The flow rate was set to 0.6 mL/min and the following gradient was used: 0–7.5 min to 5% A, 7.5–10.0 min hold 5% A, 10.0–11.5 min to 98% A, 11.5–15.0 min hold 98% A. For separation of amitriptyline and its *N*-oxide, the flow rate was set to 0.5 mL/min and the gradient was programmed as follows: 0–1.0 min 98% A, 1.0–3.0 min to 90% A, 3.0–5.0 min to 85% A, 5.0–7.5 min to 80% A, 7.5–10.0 min to 75% A, 10.0–11.5 min to 70% A, 11.5–13.0 min to 65% A, 13.0–14.5 min to 50% A, 14.5–16.0 min to 40% A, 16.0–19.0 min to 10% A, 19.0–21.0 hold 10% A, as previously described in (Wissenbach et al., 2011b). Analysis was performed in full-scan mode ( $m/z$  100–800) or in a targeted acquisition mode with inclusion list, where  $\text{MS}^2$  spectra of given precursor ions were recorded. The injection volume for all samples was 10  $\mu\text{L}$  each. The MS was equipped with a heated electrospray ionization II source, other conditions were as follows: positive ionization mode; sheath gas, nitrogen at flow rate of 34 arbitrary units (AU); auxiliary gas, nitrogen at flow rate of 11 AU; vaporizer temperature, 250  $^{\circ}\text{C}$ ; source voltage, 3.00 kV; ion transfer capillary temperature, 300  $^{\circ}\text{C}$ ; capillary voltage, 31 V; tube lens voltage, 110 V; automatic gain control was set to 15,000 ions for full scan and 5000 ions for  $\text{MS}^n$ , as already described in (Wissenbach et al., 2011a). Wissenbach et al. described 0.01, 0.1, or 1.0 mg/L as limits of detection determined for several DOAs (Wissenbach et al., 2011a).

### 2.7. Data analysis

TF Xcalibur Qual Browser software version 2.2 SP1.48 was used for calculation of the peak areas for assessment of the relative amount of metabolites formed during incubation and GraphPad Prism 5.00 for statistical evaluations. T-test conditions were unpaired and one-tailed (\*\*\*,  $P < 0.001$ , \*\*,  $P < 0.01$ , \*,  $P < 0.1$ ).

## 3. Results

### 3.1. Identification of FMO substrates by heat inactivation or chemical inhibition

Incubations of 12 therapeutic drugs using untreated pHLM or preheated pHLM (55  $^{\circ}\text{C}$ , 1 min) were conducted. The unchanged drugs, *N*-oxides, and nor metabolites were analyzed by LC-IT-MS.

Ten out of 12 substrates formed the corresponding *N*-oxides and nor metabolites in incubations with untreated pHLM. For venlafaxine, only the nor metabolite and for ranitidine, no metabolites could be detected. Untreated pHLM incubations were used as control and the amount of metabolite formed, minus metabolite formation in blank samples, was defined as 100%. In comparison to metabolite formation in untreated pHLM incubations, heat-treated (55 °C) pHLM incubations showed a reduced formation for both metabolites each between 60 and 100% as shown in Fig. 2a. The lowest reduction was observed for the metabolites of doxepin, followed by those of amitriptyline, citalopram, prothipendyl, zolpidem, and zopiclone. For clozapine, diphenhydramine, doxylamine, and imipramine, *N*-oxygenation could not be observed.

Results of incubations with amitriptyline, clozapine, imipramine, and zopiclone with pHLM, preheated at 45 °C for 5 min, are shown in Fig. 2b. Here again a reduction of the formation rates of both metabolites was observed, although less pronounced than after preincubation of pHLM at 55 °C. The reduction was between

30 and 50%, except for imipramine *N*-oxide formation that was reduced by 80%. Additionally, these four therapeutic drugs were incubated with recombinant FMO3 under conditions as described in Section 2.3. In these incubations, nor metabolites were not formed at all.

Furthermore, amitriptyline, clozapine, imipramine, and zopiclone were incubated using pHLM preincubated with ABT or methimazole. Results are shown in Fig. 3. After preincubation with ABT (Fig. 3a), formation of the *N*-oxides of amitriptyline and clozapine was reduced by about 80%, while the *N*-oxygenation of imipramine remained unchanged and that of zopiclone was almost entirely prevented. In each case, an almost complete disappearance of the nor metabolites could be observed. After preincubation with methimazole (Fig. 3b), formation rates of both metabolites were affected and reduced between 70 and 90%. Incubations with recombinant FMO3, preincubated with ABT and regenerating system for 30 min were performed, under conditions as already described in Sections 2.2 and 2.3. There was no difference in the *N*-oxide formation between incubations with and without ABT preincubation.

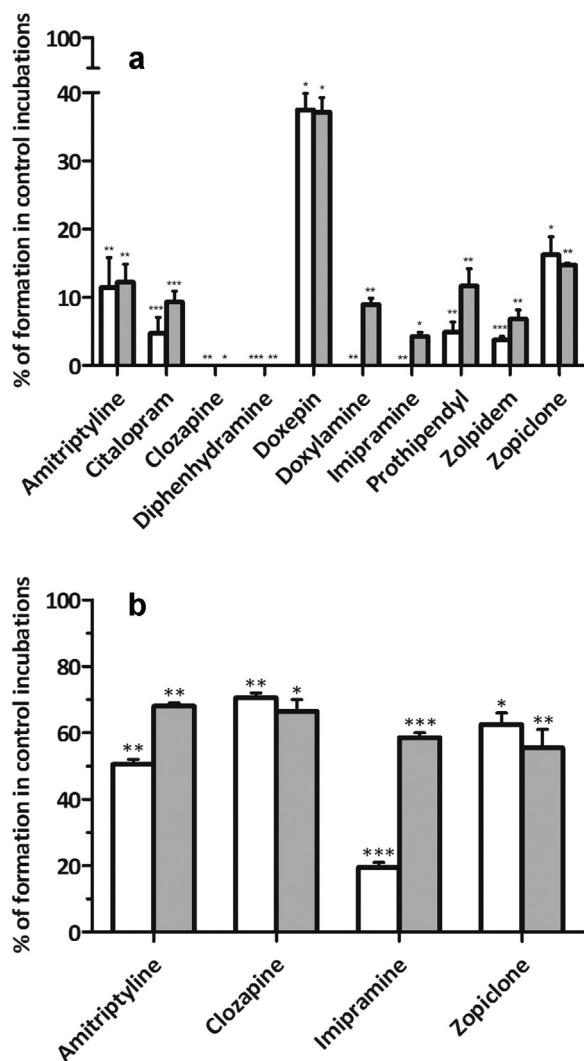


**Fig. 2.** Effect of heat treatment of pHLM (a: 55 °C, 1 min; b: 45 °C, 5 min) on the formation of *N*-oxide (open bars) and nor metabolite (shaded bars) of therapeutic drugs. Data represent formation rates relative to formation in control incubations with untreated pHLM. Values are expressed as mean and were tested for significance ( $n=2$ ; \*\*\*,  $P < 0.001$  for formation in incubations with heat-treated pHLM versus formation in control incubations).

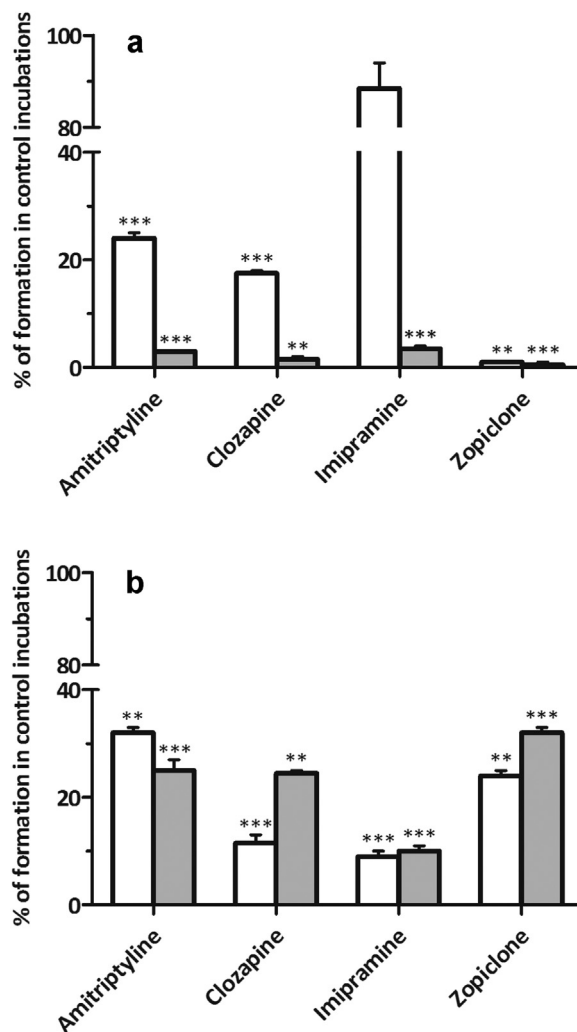


**Fig. 3.** Effect of preincubation with ABT (a) or methimazole (b) of pHLM on the formation of *N*-oxide (open bars) and nor metabolite (shaded bars) of four therapeutic drugs. Data represent formation rates relative to formation in control incubations with untreated pHLM. Values are expressed as mean and were tested for significance ( $n=2$ ; \*\*\*,  $P < 0.001$  for formation in incubations with pHLM preincubated with ABT or methimazole versus formation in control incubations).

### 3.2. Identification of enzymes involved in the N-oxygenation

A monoxygenases activity screening using FMO3, ten CYP isoforms, or pHLM was conducted. The unchanged drugs, N-oxygenation products, and main metabolites (usually nor and mono hydroxy metabolites) were analyzed by LC-IT-MS. The

corresponding N-oxygenation product was detected in all incubations with pHLM, except for methamphetamine. While the highest amount of zopiclone N-oxide was detected in incubations with CYP3A4, FMO3 showed no activity. Low amounts of imipramine N-oxide were found in incubations with FMO3 and also CYP1A2, CYP2B6, CYP2C19, and CYP2D6. N-Oxide formation of

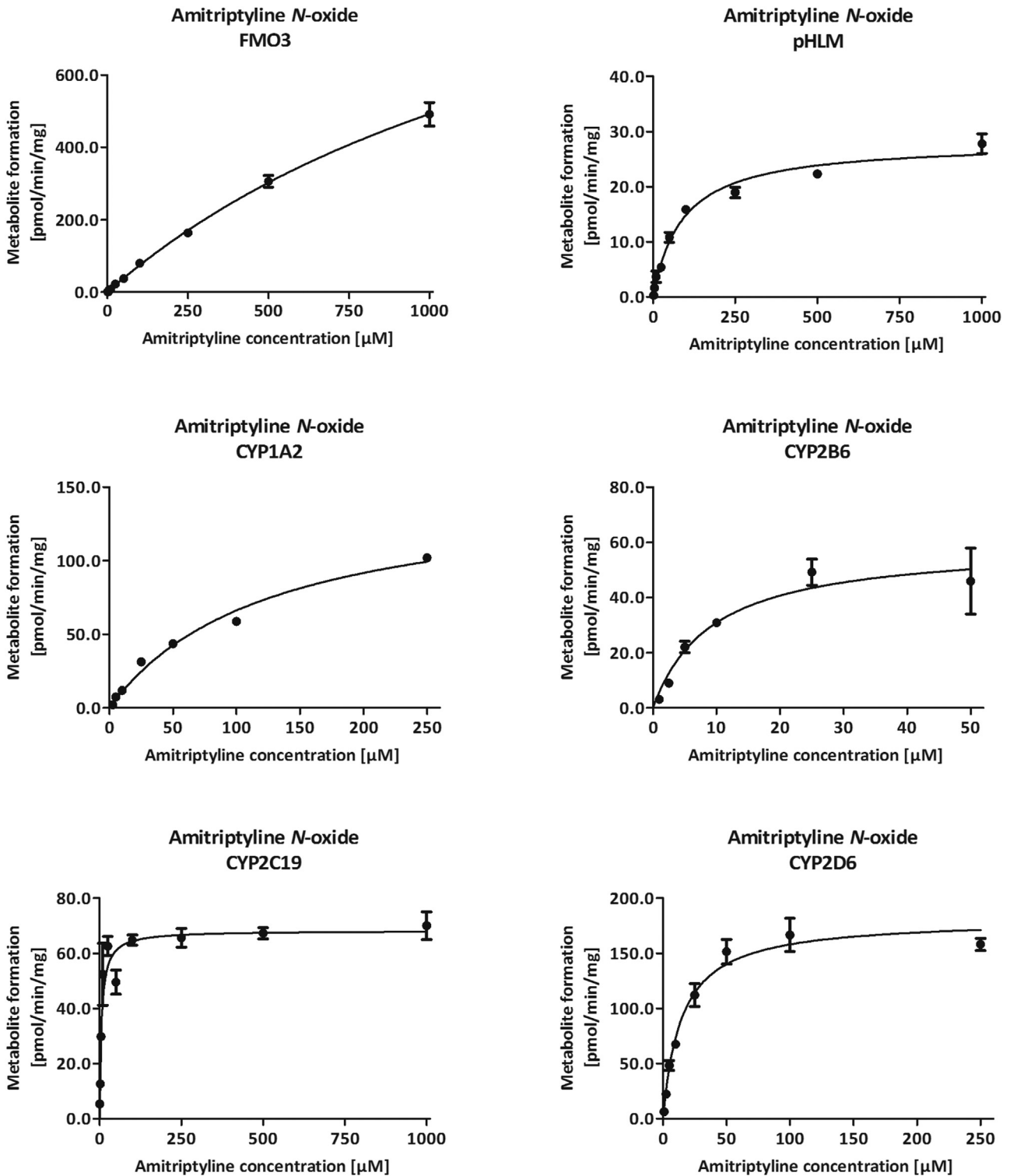


**Fig. 4.** Kinetics of FMO3, pHLM, and single CYP of the corresponding N-oxygenations calculated using corresponding reference standards (CRS) or peak area ratios (PAR). Data points represent means and ranges of triplicate incubations.

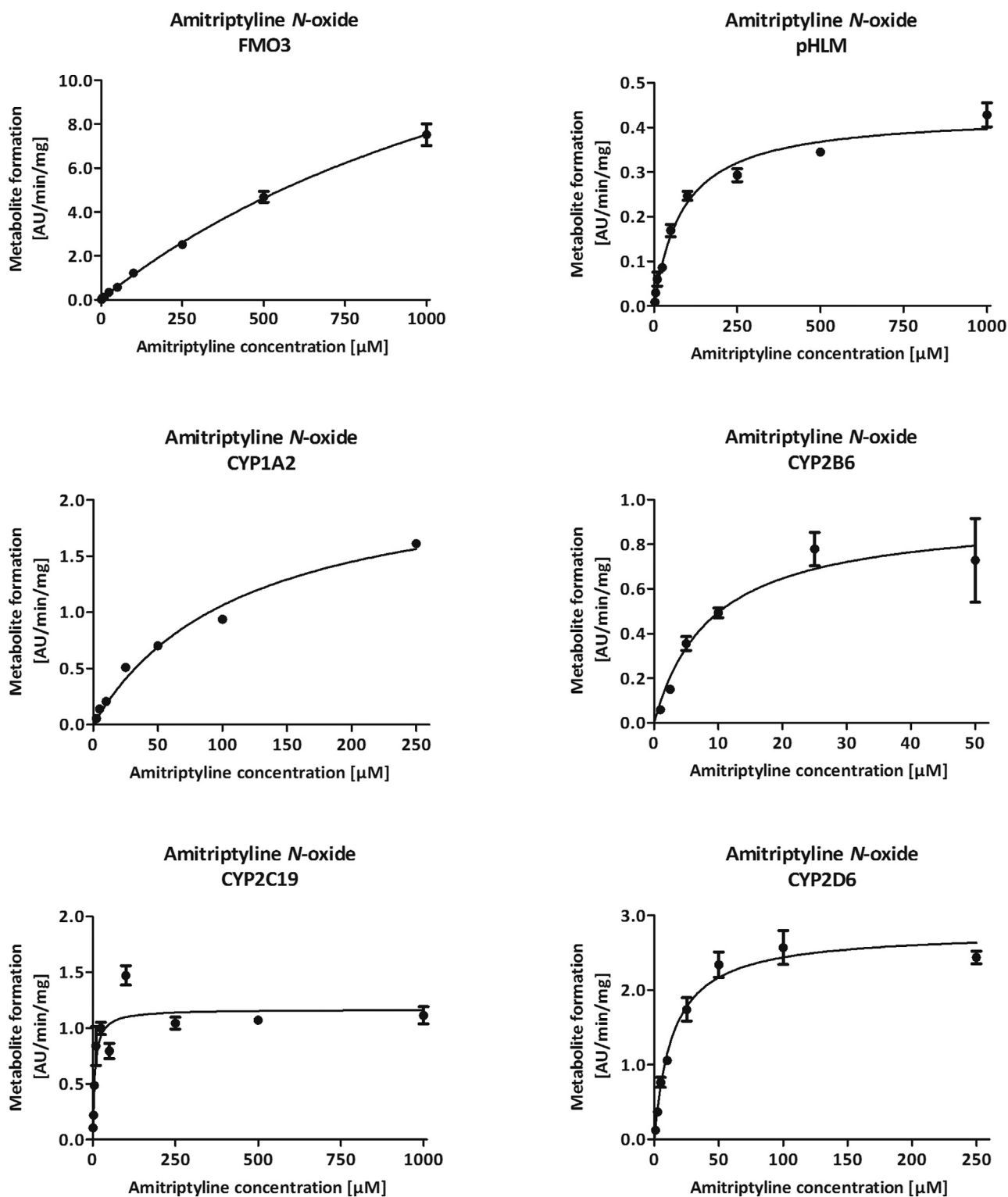


Fig. 4. (Continued)

amitriptyline and clozapine was observed for FMO3 and various CYP isoforms.

*N*-Oxygenation of the DOAs 3-bromomethcathinone (3-BMC), *N,N*-diallyltryptamine (DALT), DMT, methoxypiperamide (MeOP), and methamphetamine was catalyzed by FMO3 and some CYPs, while *N*-oxygenation of dextromethorphan, glaucine, and methadone was not catalyzed by FMO3 but by CYPs.

### 3.3. Kinetic studies, calculation of contributions, and hepatic clearances using a modified RAF approach

The kinetics for all *N*-oxygenations is depicted in Fig. 4 and followed classic Michaelis-Menten kinetics. The corresponding Michaelis-Menten constants are summarized in Table 1. If product inhibition was observed, high concentrations were excluded for

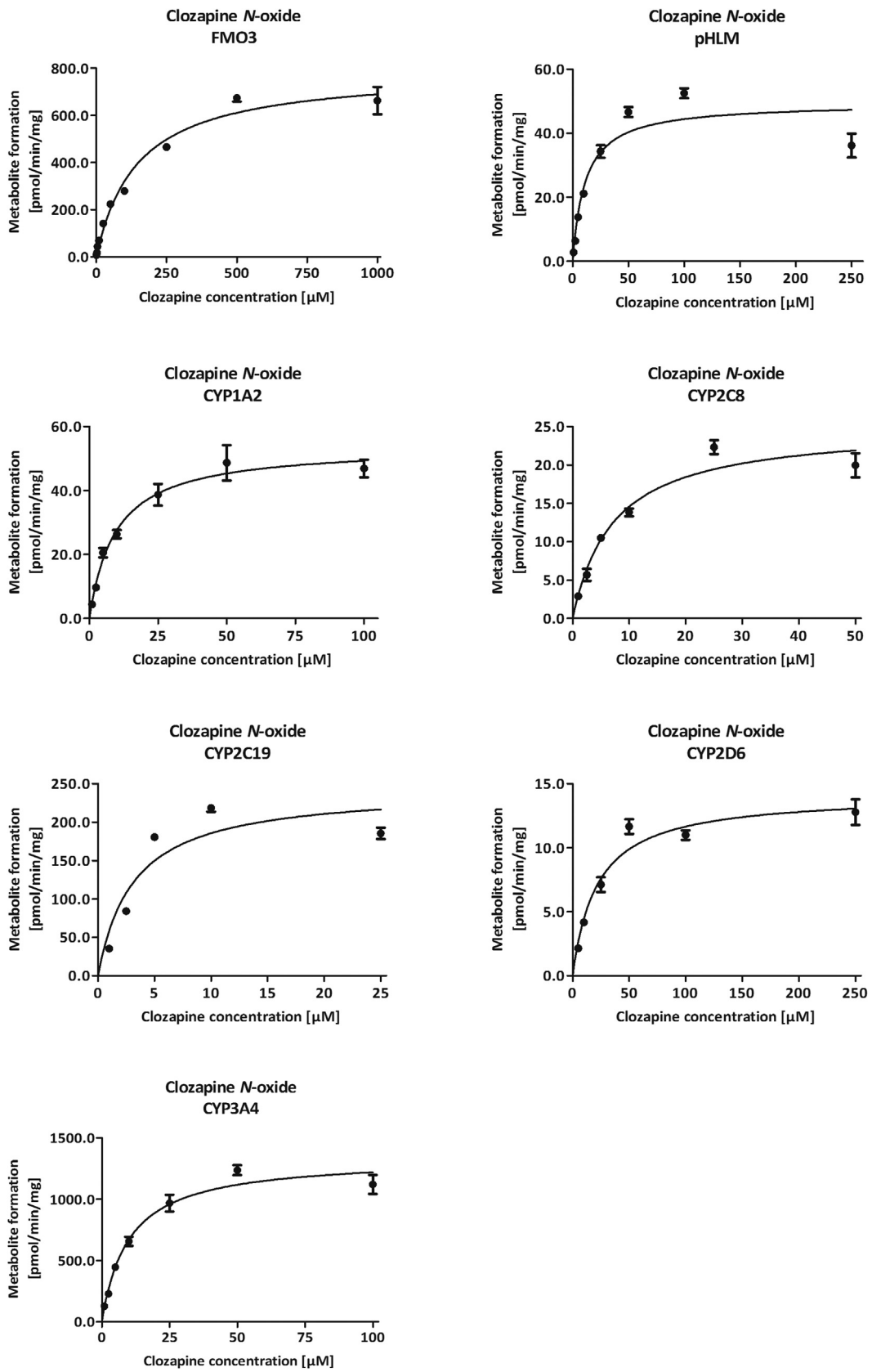


Fig. 4. (Continued)

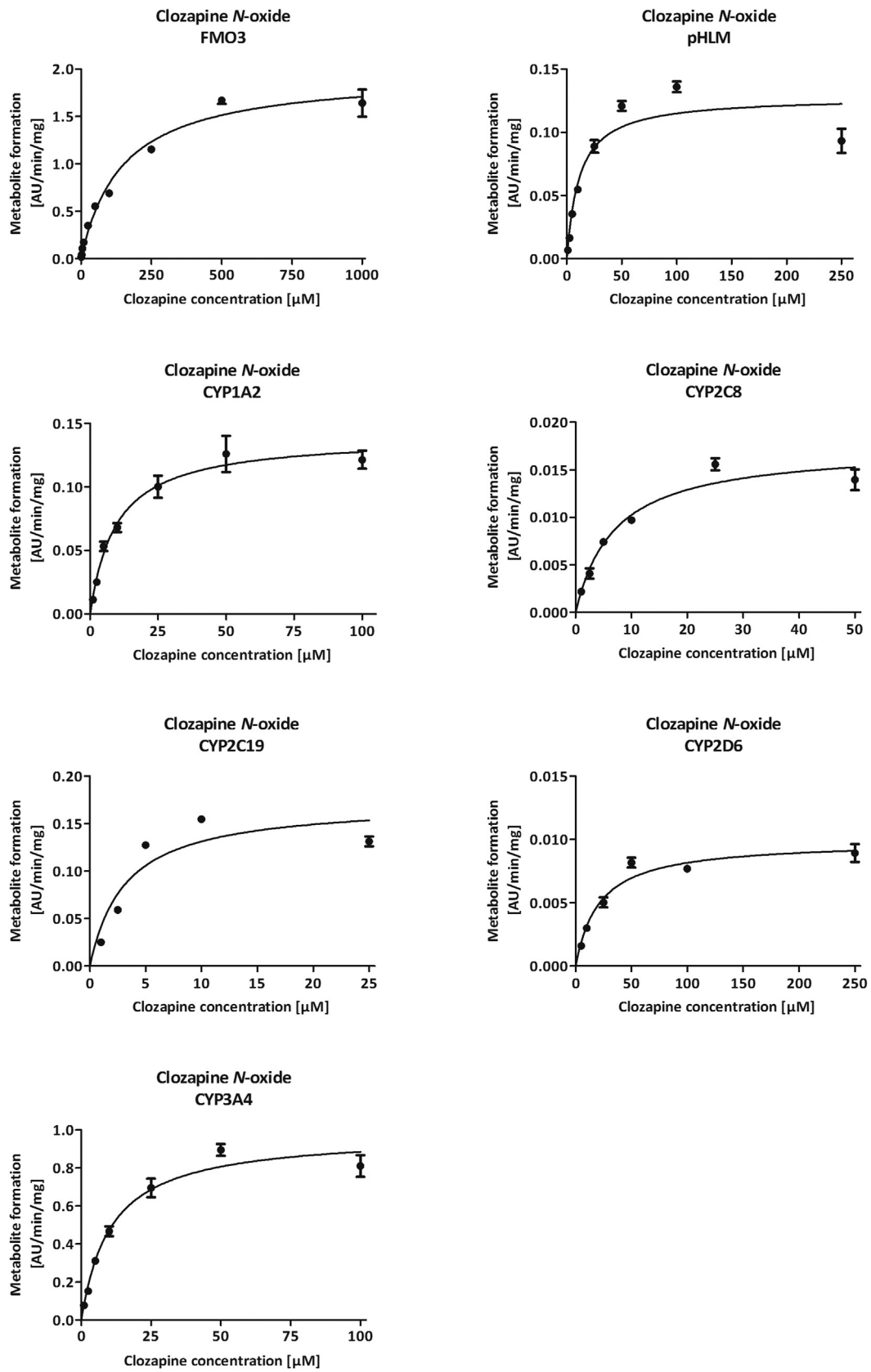


Fig. 4. (Continued)

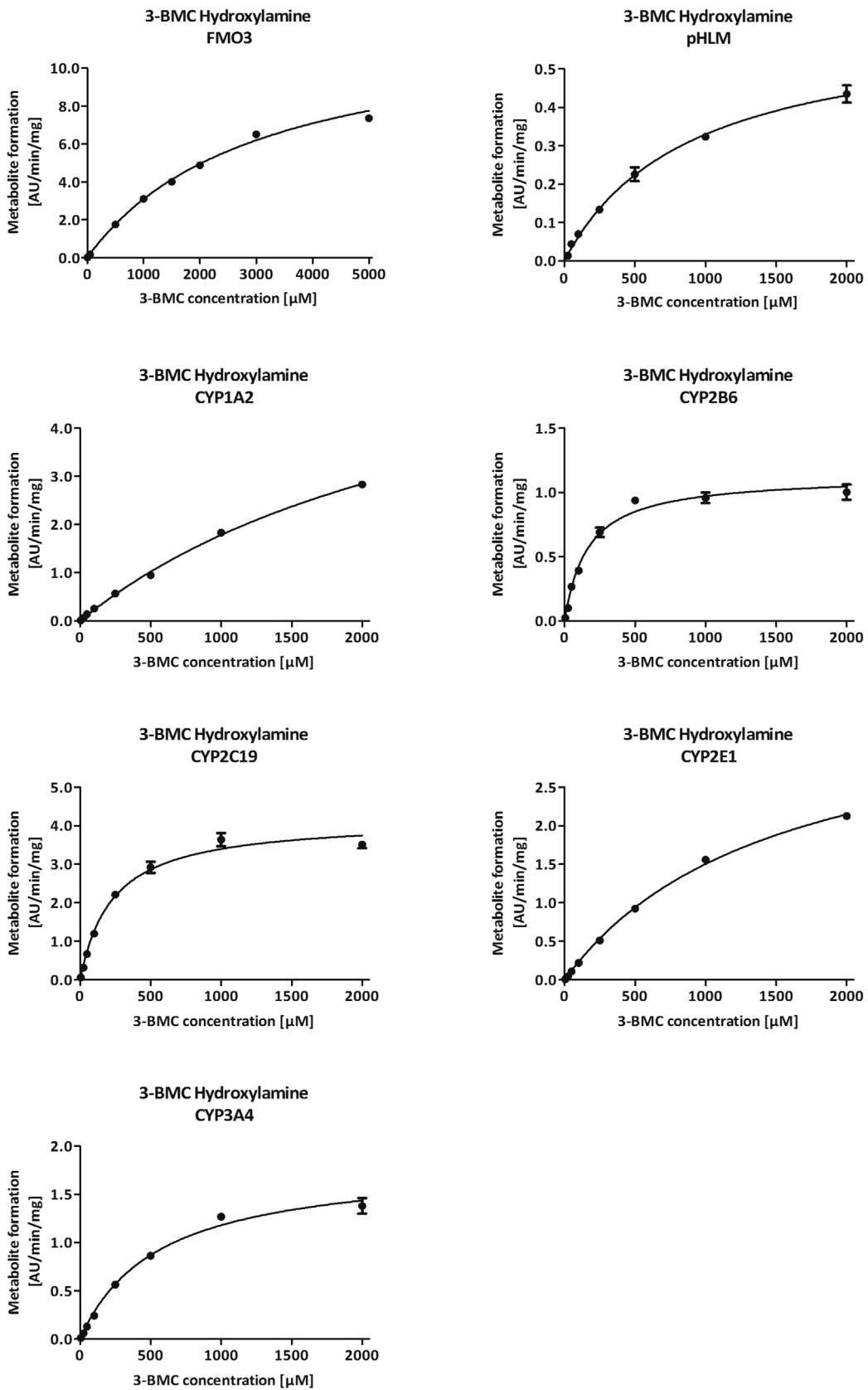


Fig. 4. (Continued)

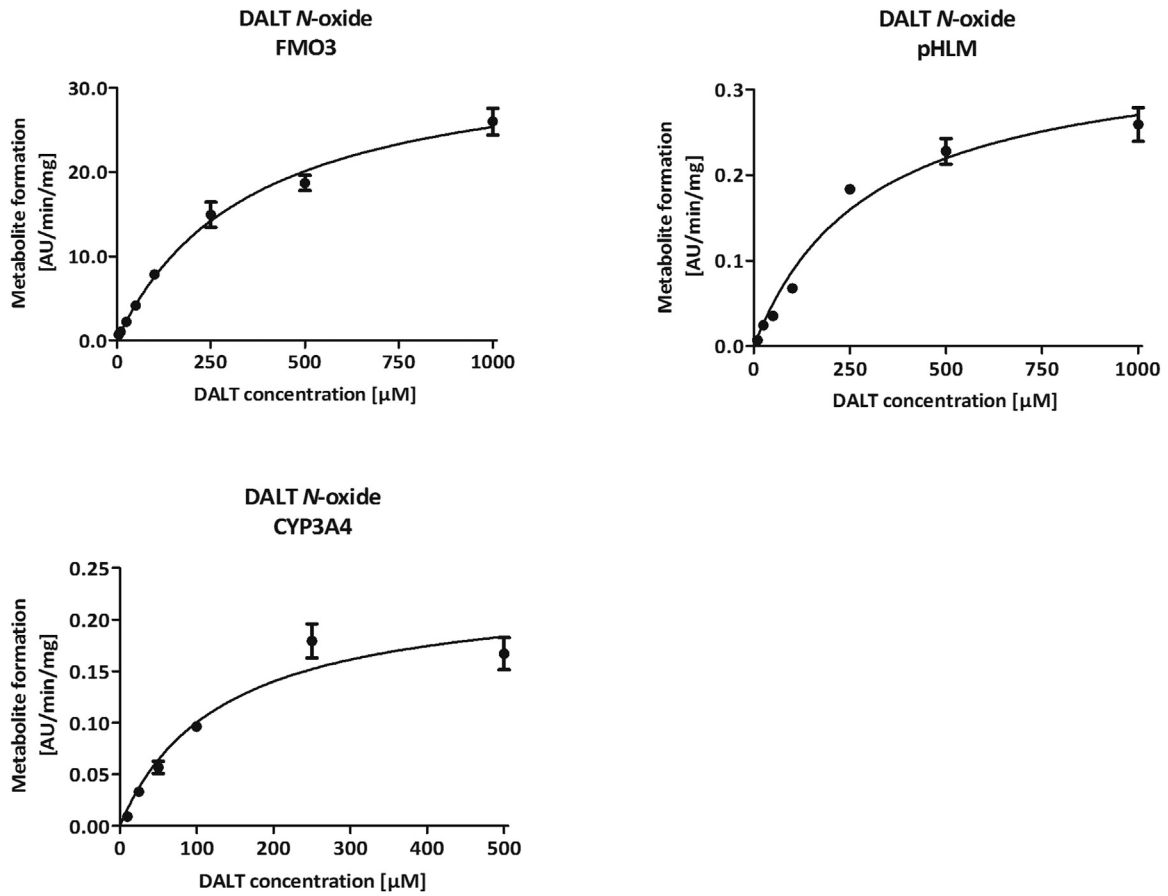


Fig. 4. (Continued)

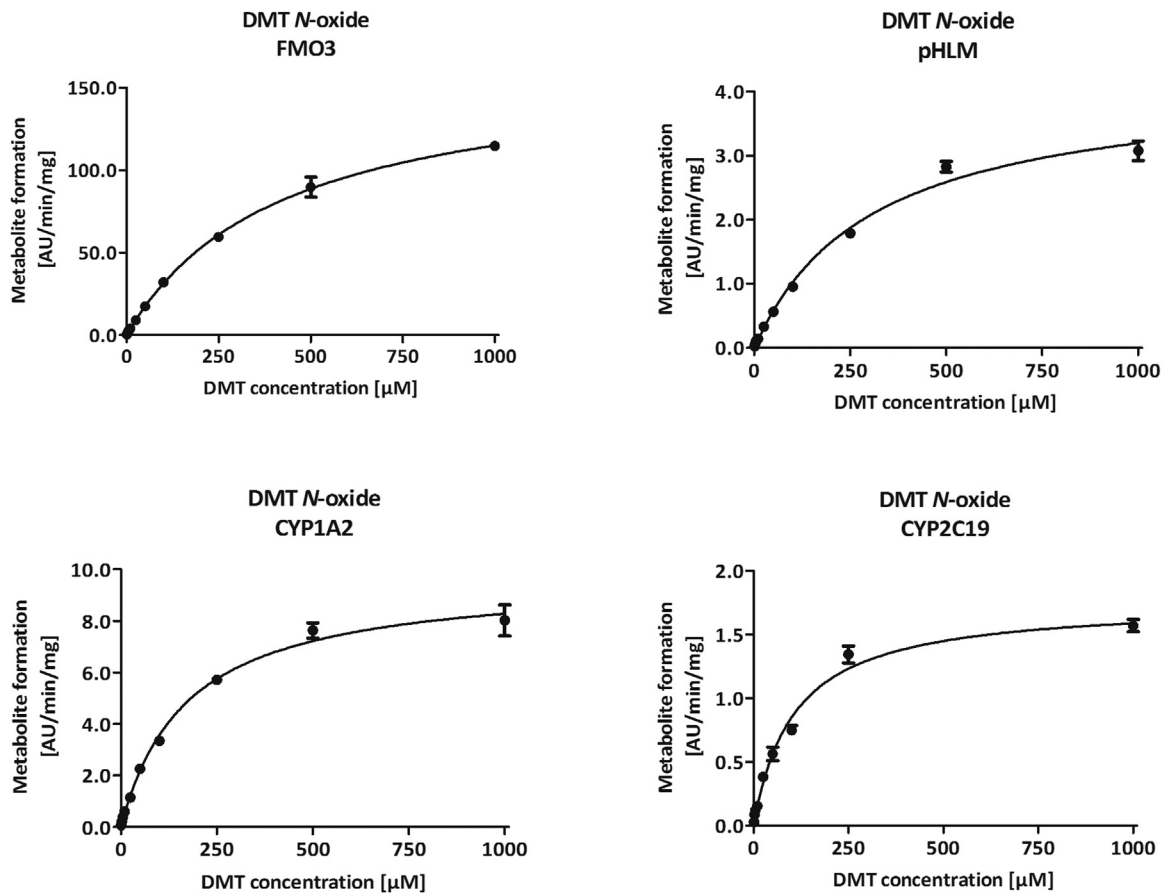


Fig. 4. (Continued)

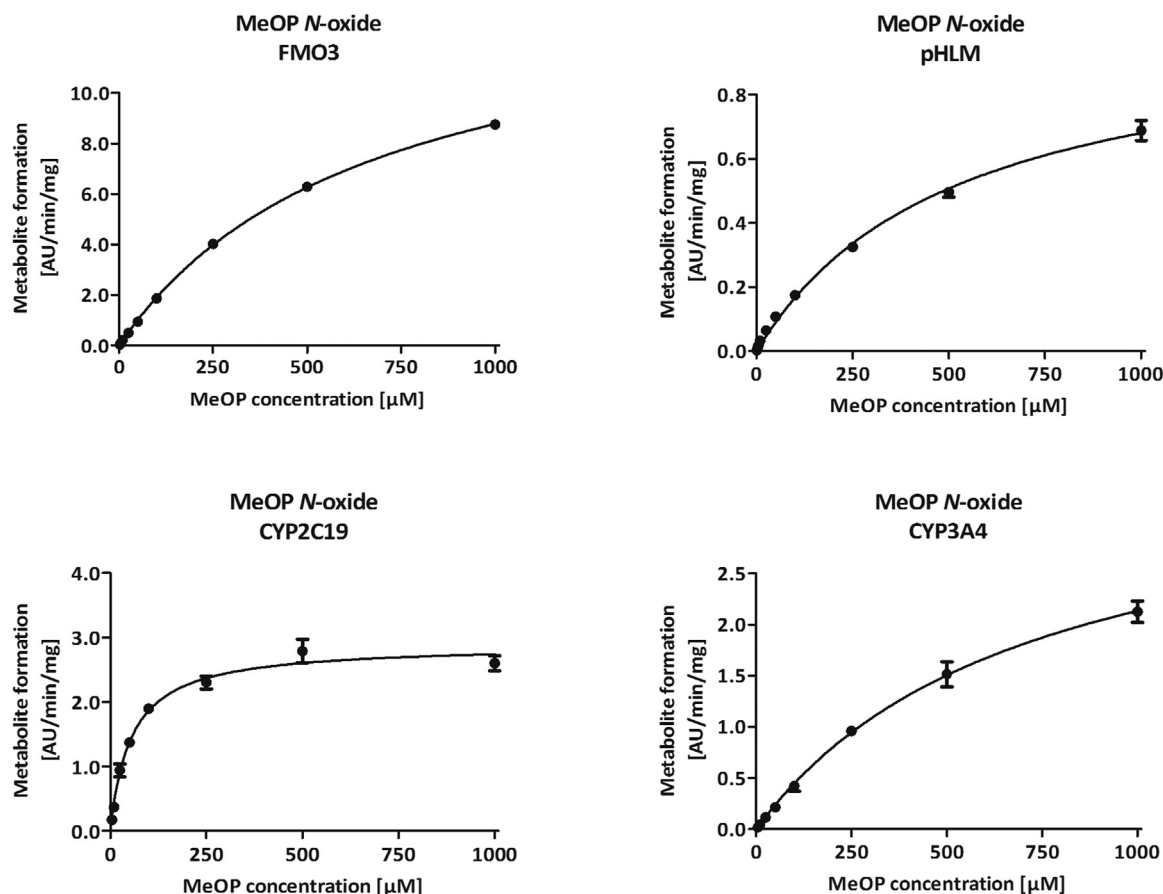


Fig. 4. (Continued)

calculations of  $K_m$  and  $V_{max}$  values. In general, CYPs showed higher affinity, represented by lower  $K_m$  values, in comparison to higher  $K_m$  values for FMO3. As pHLM contained all tested individual enzymes, resulting  $K_m$  values were between CYP and FMO3 values. FMO3 showed the highest turnover rates ( $V_{max}$ ), followed by pHLM and CYPs. Calculations using CRS and PAR resulted in similar  $K_m$  values, while  $V_{max}$  values obtained by different methods could not be compared due to different units (pmol/min/mg for CRS and AU/min/mg for PAR). The RAFs for used recombinant enzymes were calculated according to Eq. (2). Turnover rates for appropriate probe substrates were taken from the supplier's data sheets. Applying the RAF approach, the contribution and in vivo hepatic net clearance was calculated with  $K_m$  and  $V_{max}$  values determined by CRS or PAR. The results for the hepatic net clearance of amitriptyline *N*-oxide at different amitriptyline concentrations are given in Fig. 5. The results for the hepatic net clearance of the *N*-oxygenation products of clozapine and five DOAs at a substrate concentration of 0.1 μM are given in Fig. 6. Results for all tested therapeutic drugs and DOAs at different substrate concentrations are given in Table 2. Concerning amitriptyline and clozapine, FMO3 played only a minor role in the hepatic *N*-oxide clearance, while various CYPs were responsible for the major part of the *N*-oxide formation. In case of amitriptyline *N*-oxide formation, contribution showed almost equal distribution among CYP1A2, CYP2B6, and CYP2D6, while CYP3A4 was predominantly responsible for clozapine *N*-oxide formation. *N*-Oxygenation of 3-BMC showed a similar profile as amitriptyline, concerning a distribution among various CYPs and a low contribution of FMO3. For DALT and methamphetamine, only FMO3 and a single CYP isoform (CYP3A4 or CYP2D6, respectively) were involved in the *N*-oxygenation,

whereby FMO3 played the predominant role with contributions > 80% to the hepatic clearances. For DMT and MeOP *N*-oxygenation, contribution was distributed more equally between FMO3 (50 and about 30%, respectively) and two CYP isoforms.

The results of incubations of the five DOAs using pHLM pretreated with the CYP inhibitor ABT are summarized in Fig. 7. Formation of the nor metabolites was significantly reduced by 80% for DALT or DMT and by 90% for MeOP or methamphetamine in comparison to the formation in control incubations. There was no nor 3-BMC detectable after preincubation with ABT. Residual formation of 3-BMC hydroxylamine was also reduced by 90%, of methamphetamine hydroxylamine by 50%, of MeOP *N*-oxide by 30%, and of DALT *N*-oxide and DMT *N*-oxide by 10% in comparison to formation in control incubations, respectively.

#### 4. Discussion

##### 4.1. Identification of FMO substrates by heat inactivation or chemical inhibition

FMOs and CYPs are both known to catalyze *N*-oxygenation (Cashman and Zhang, 2006), while CYPs, but not FMOs, catalyze nor metabolite formation via *N*-dealkylation, too. Thermal inactivation was supposed to be a suitable approach for elucidating the FMO activity. In the absence of NADPH, FMO3 was thermally labile and about 60–80% of enzyme activity was lost after heat treatment (50–60 °C) for as short as 1 min (Cashman, 2008). No details about the mechanism behind this observation were given by the authors. Amitriptyline, clozapine, diphenhydramine, imipramine, prothipendyl, and ranitidine were already described

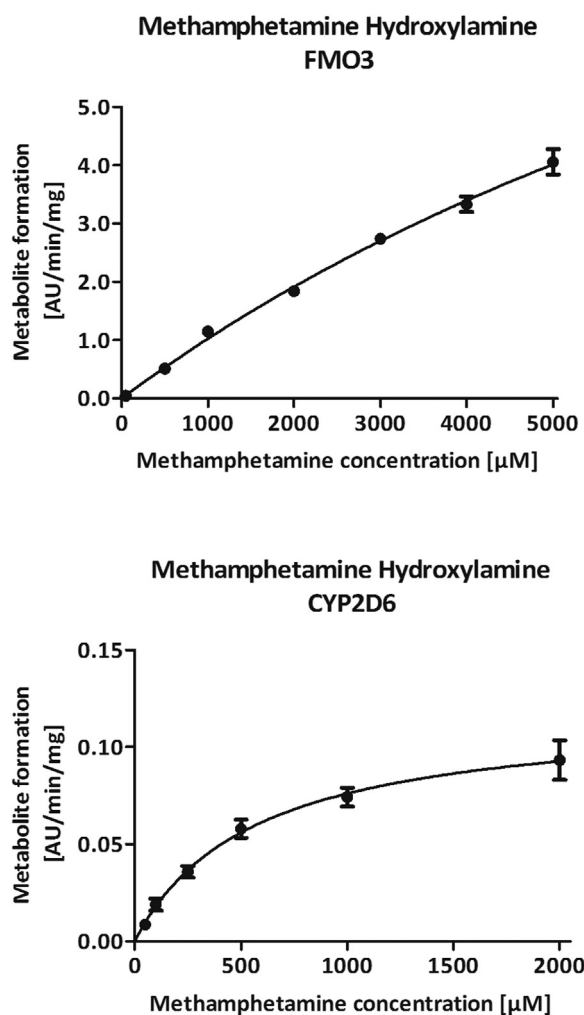


Fig. 4. (Continued)

as substrates of FMO isoforms of different species (Krueger and Williams, 2005). In the present study, out of 12 tested substrates, known for *N*-oxygenation and *N*-dealkylation of their tertiary amine group, 11 showed formation of nor metabolites and 10 of *N*-oxides after incubations with untreated pHLM. Only ranitidine was neither *N*-oxygenated nor *N*-demethylated under the chosen incubation conditions. Furthermore, data obtained by heat-treated pHLM incubations could not be used to determine the role of FMOs in the formation of *N*-oxides, because the nor metabolite formation was also reduced even though CYPs should catalyze this reaction. A possible explanation would be the sensitivity of both, FMOs and CYPs to the used heat treatment, although FMO should be more sensitive to thermal inactivation under similar conditions (Cashman, 2008). To verify these results, a second heat inactivation protocol was tested for selected drugs using milder conditions (45 °C, 5 min) according to Taniguchi-Takizawa et al. (2015). For further experiments, amitriptyline, clozapine, and imipramine were chosen as known substrates of FMO and zopiclone showing highest *N*-oxide formation rate in the pHLM incubations. Again, both metabolic reactions were reduced by a comparable extent and significantly in comparison to untreated pHLM concerning amitriptyline, clozapine, and zopiclone. The formation of the imipramine *N*-oxide was reduced to a greater extent than that of the nor metabolite. Incubations with recombinant FMO3 confirmed the assumption that FMO3 was not involved in the nor metabolite formation, which supported the conclusion that CYPs were also thermally unstable.

As heat inactivation did not allow assessing the FMO contribution to *N*-oxide formations, chemical inhibitors were used to get further information. The first strategy was the inactivation of microsomal CYPs using preincubations with ABT, a known mechanism-based, non-specific CYP inhibitor. Although non-specific, ABT showed different inhibitor potencies towards the CYP isoforms (Emoto et al., 2003). The following CYP isoform-specific reactions were used to test for sufficient ABT inhibition: 4-hydroxylation of bupropion for CYP2B6, *N*-deethylation of amodiaquine for CYP2C8, 5-hydroxylation of omeprazole for CYP2C19, and *O*-demethylation of dextromethorphan for CYP2D6 (U.S. Department of Health and Human Services et al., 2006). Incubations were conducted as described by Dinger et al. (Dinger et al., 2014). The formation of 4-hydroxy bupropion, *N*-deethyl amodiaquine, 5-hydroxy omeprazole, and *O*-demethyl dextromethorphan in pHLM preincubated with ABT was compared with the

**Table 1**  
Determined Michaelis-Menten values (percentage errors in brackets) for each formed metabolite by corresponding enzymes (FMO3, pHLM, CYPs), calculated using corresponding reference standards (CRS) or peak area ratios (PAR). All  $K_m$  values were given in  $\mu\text{M}$ ,  $V_{\text{max}}$  (CRS) in  $\text{pmol}/\text{min}/\text{mg}$  and  $V_{\text{max}}$  (PAR) in  $\text{AU}/\text{min}/\text{mg}$ . ND: not determined due to insufficient activity.

Formed metabolite	Determined via	Michaelis-Menten values, $K_m/V_{\text{max}}$								
		FMO3	pHLM	CYP1A2	CYP2B6	CYP2C8	CYP2C19	CYP2D6	CYP2E1	CYP3A4
Amitriptyline <i>N</i> -oxide	CRS	1689 (20)/ 1323 (14)	90 (13)/ 28 (4)	125 (13)/ 149 (6)	9.3 (37)/ 60 (13)	ND	6.0 (20)/ 68 (4)	15 (15)/ 181 (4)	ND	ND
	PAR	1671 (20)/ 20 (14)	86 (13)/ 0.43 (4)	115 (13)/ 2.3 (6)	8.9 (36)/ 0.93 (13)	ND	6.4 (27)/ 1.2 (5)	14 (15)/ 2.8 (4)	ND	ND
Clozapine <i>N</i> -oxide	CRS	147 (13)/ 790 (4)	11 (23)/ 49 (6)	9.5 (17)/ 54 (5)	ND	7.2 (19)/ 25 (6)	3.1 (32)/ 244 (10)	22 (15)/ 14 (5)	ND	10 (14)/ 1341 (4)
	PAR	147 (13)/ 2.0 (4)	11 (24)/ 0.13 (6)	9.6 (18)/ 0.14 (5)	ND	7.0 (19)/ 0.02 (5)	3.2 (31)/ 0.17 (12)	21 (18)/ 0.01 (5)	ND	11 (15)/ 1.0 (4)
3-BMC hydroxylamine	PAR	3022 (8)/ 12 (5)	893 (11)/ 0.62 (5)	2927 (11)/ 7.0 (7)	165 (11)/ 1.1 (3)	ND	229 (10)/ 4.2 (3)	ND	1498 (7)/ 3.8 (4)	552 (11)/ 1.8 (4)
	PAR	355 (14)/ 34 (6)	300 (18)/ 0.35 (7)	ND	ND	ND	ND	ND	ND	131 (26)/ 0.23 (10)
DMT <i>N</i> -oxide	PAR	421 (7)/ 164 (3)	307 (10)/ 4.2 (4)	172 (9)/ 9.7 (3)	ND	ND	107 (9)/ 1.8 (3)	ND	ND	ND
	PAR	671 (4)/ 15 (2)	517 (9)/ 1.0 (4)	ND	ND	ND	55 (8)/ 2.9 (2)	ND	ND	717 (9)/ 3.7 (5)
Methamphetamine hydroxylamine	PAR	13483 (29)/ 15 (22)	ND	ND	ND	ND	ND	558 (20)/ 0.12 (8)	ND	ND

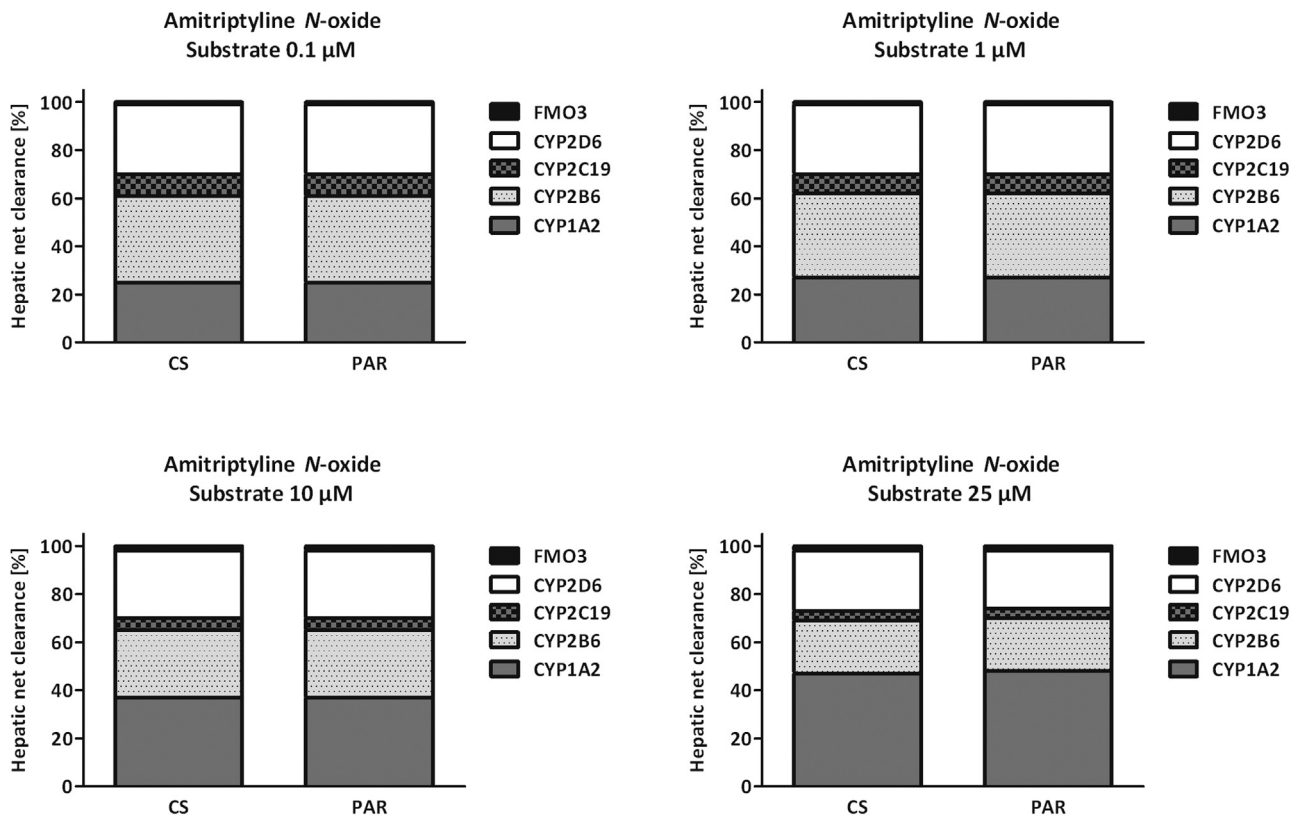


**Fig. 5.** Estimated in vivo hepatic net clearance of amitriptyline *N*-oxide calculated using corresponding reference standards (CRS) or peak area ratios (PAR) for different substrate concentrations.

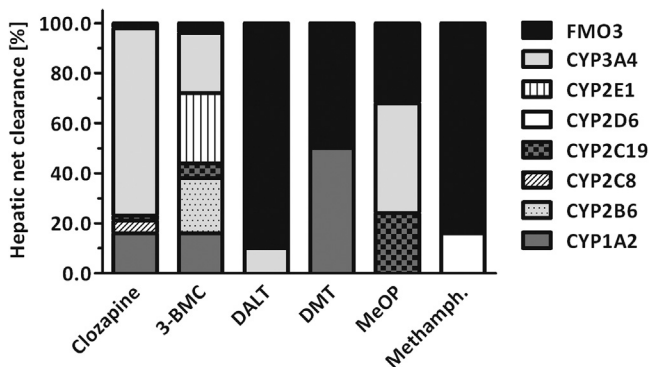


**Fig. 6.** Estimated in vivo hepatic net clearance of the *N*-oxygenation products of clozapine and different drugs of abuse using PAR at a substrate concentration of 0.1  $\mu$ M.

formation in incubations with untreated pHLM. Formation of these metabolites was almost entirely suppressed after treatment with ABT (remained formation between 0 and 6%). The almost complete disappearance of the nor metabolites of amitriptyline, clozapine, imipramine, and zopiclone was in line with these findings (Fig. 3a). As ABT did not inactivate FMOs (Mathews et al., 1985), the remaining *N*-oxide formation should be catalyzed by FMOs. Results of incubations with recombinant FMO3 and ABT were in line with findings of Mathews et al. and allowed the conclusion that the zopiclone *N*-oxide was exclusively formed by CYPs. The unaffected imipramine *N*-oxide formation indicated the predominant role of FMOs in this reaction. For amitriptyline and clozapine *N*-oxygenation, FMOs and also CYPs seemed to be involved.

On the other hand, FMO inactivation should be possible by methimazole (Hamman et al., 2000). However, not only the formation of the *N*-oxides but also of the nor metabolites was significantly reduced. Hence, methimazole seemed to inhibit CYPs as well. These findings are in line with Guo et al. (Guo et al., 1997),

**Table 2**

Calculated in vivo hepatic net clearance [%] of the *N*-oxygenation products for the used enzymes (FMO3, CYPs) at different substrate concentrations (0.1/1/10/25  $\mu$ M), calculated using corresponding reference standards (CRS) or peak area ratios (PAR).

Formed metabolite	Determined via	Hepatic net clearance at a substrate concentration of 0.1/1/10/25 $\mu$ M [%]							
		FMO3	CYP1A2	CYP2B6	CYP2C8	CYP2C19	CYP2D6	CYP2E1	CYP3A4
Amitriptyline <i>N</i> -oxide	CRS	1/1/2/2	25/27/37/47	36/35/28/22		9/8/5/4	29/29/28/25		
	PAR	1/1/2/2	25/27/37/48	36/35/28/22		9/8/5/4	29/29/28/24		
Clozapine <i>N</i> -oxide	CRS	1/1/1/2	5/5/5/5		5/5/5/4	3/2/1/1	<1/<1/<1/<1		86/87/88/88
	PAR	2/2/3/5	16/16/16/15		5/5/4/4	2/2/2/1	<1/<1/<1/<1		75/75/75/75
3-BMC hydroxylamine	PAR	4/4/4/4	16/16/17/17	22/21/21/20		6/6/5/5		28/29/29/30	24/24/24/24
DALT <i>N</i> -oxide	PAR	90/90/91/91							10/10/9/9
DMT <i>N</i> -oxide	PAR	49/49/50/51	50/50/49/48			1/1/1/1			
MeOP <i>N</i> -oxide	PAR	32/32/33/34				24/24/21/18			44/44/46/48
Methamphetamine hydroxylamine	PAR	84/84/85/85					16/16/15/15		

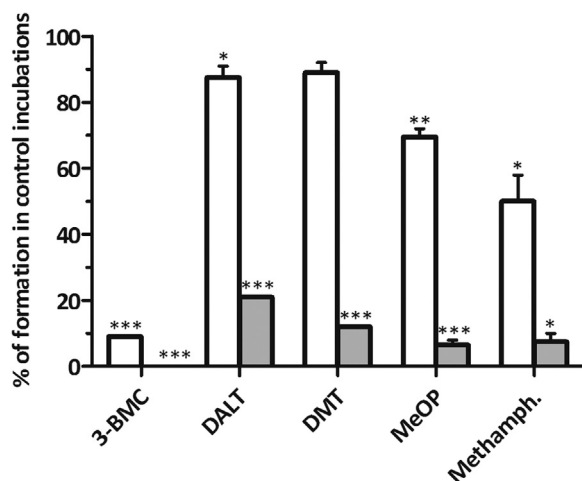


**Fig. 7.** Effect of ABT preincubation of pHLM on the formation of *N*-oxygenation products (open bars) and nor metabolites (shaded bars) of five drugs of abuse. Data represent formation rates relative to formation in control incubations with untreated pHLM. Data are expressed as mean and were tested for significance ( $n = 2$ ; \*\*\*,  $P < 0.001$  for formation in incubations with pHLM preincubated with ABT versus formation in control incubations).

who already described methimazole as CYP inhibitor, but are in contrast to Taniguchi-Takizawa et al., who reported that methimazole had only little influence on the benzyldamine *N*-demethylation (Taniguchi-Takizawa et al., 2015). This again underlined the inconsistency in protocols concerning FMO3 incubation. However, as heat inactivation and chemical inhibition protocols were initially intended to identify FMO substrates and as the results obtained by both methods were not unambiguous, single enzyme incubations were finally chosen to identify enzymes involved in the *N*-oxygenation of the selected DOAs.

#### 4.2. Identification of enzymes involved in the *N*-oxygenation

The aim was to identify all involved enzymes in the *N*-oxygenation of four therapeutic drugs and eight DOAs. Therefore, the established CYP initial activity screening approach (Caspar et al., 2015; Meyer et al., 2013c; Meyer et al., 2014) was extended for FMO3. Five functional forms of FMO in humans are known with controversial data concerning their role in drug metabolism. In 2006, Cashman and Zhang identified FMO5 as most abundant FMO in the adult liver (Cashman and Zhang, 2006), followed by FMO3 and very little amounts of FMO1, 2, and 4. Other authors described FMO3 as major isoform, including the most recent work by Chen et al. (Cashman, 1995; Chen et al., 2016; Overby et al., 1997). However, FMO5 is distinctly different from the other isoforms and does not catalyze the oxygenation of common FMO substrates (Cashman and Zhang, 2006). Hence, FMO3 represents the major enzyme involved in the human hepatic FMO-catalyzed metabolism and was therefore selected for further *in vitro* studies. For identification of the monooxygenases catalyzing the initial metabolic steps, FMO3 and the ten major human hepatic CYPs (Strolin et al., 2007) were incubated under conditions allowing a statement on the qualitative involvement of a particular enzyme. Incubations with pHLM were conducted as positive control. All expected *N*-oxygenation products could be detected, except for methamphetamine, probably due to methamphetamine hydroxylamine levels below the detection limit.

Again, the monooxygenases activity screening showed zopiclone to be no substrate of FMO3. This further underlined the assumption that heat treatment and preincubation with methimazole had a negative influence on the activity of CYPs. Findings

were also in line with the ABT inhibition results, where metabolite formation was almost totally reduced after ABT preincubation.

The amount of amitriptyline and imipramine *N*-oxide formed by FMO3 was very low. Both drugs were already described as substrates of FMO1 (Krueger and Williams, 2005; Phillips and Shephard, 2008). The small formation rates were in accordance to findings by Lemoine et al. They reported that human kidney preparations but not HLM catalyzed the *N*-oxygenation of imipramine and assumed the existence of different FMO isoforms (Lemoine et al., 1990), while more recent works identified FMO1 as most prevalent FMO in the adult kidney (Cashman and Zhang, 2006). The detection of small amounts of the imipramine *N*-oxide in incubations with FMO3 in the present work might be due to more sensitive detection methods. Nevertheless, imipramine *N*-oxide formation was not negatively affected by treatment of pHLM with ABT in contrast to nor metabolite formation, even if the *N*-oxide was not exclusively formed by FMO3. Maybe the FMO activity increased after inhibition of CYPs. Not only imipramine, but also amitriptyline could be identified as FMO3 substrate. Breyer-Pfaff and Bull et al. described amitriptyline and imipramine as substrates of non-human FMOs (Breyer-Pfaff, 2004; Bull et al., 1999), while Venkatakrisnan et al. referred to amitriptyline *N*-oxygenation as minor pathway in humans (Venkatakrisnan et al., 2001). As the current results of the monooxygenases activity screening showed, the *N*-oxides of amitriptyline and clozapine were formed by FMO3 and CYPs, which confirmed the decreased formation after pretreatment of pHLM with ABT. For clozapine, the obtained results were in line with previous findings (Wang et al., 2015).

Furthermore, eight DOAs were investigated using the monooxygenases activity screening. These DOAs were chosen because of their different chemical structures containing amine groups (see Fig. 1) and/or their known metabolic *N*-oxygenation (Cashman et al., 1999; Meyer et al., 2013b; Meyer et al., 2015; Meyer et al., 2012; Michely et al., 2015; Riba et al., 2012). Methamphetamine was already identified as substrate of human FMO3 (Cashman et al., 1999). 3-BMC, DALT, dextromethorphan, DMT, glaucine, MeOP, and methadone have not been tested for *N*-oxygenation by FMO3. The *N*-oxide formation of dextromethorphan, glaucine, and methadone was not catalyzed by human FMO3 most probably due to sterical hindrance. Methamphetamine, 3-BMC, DALT, DMT, and MeOP were identified to be FMO3 substrates. However, *N*-oxygenation was not exclusively catalyzed by FMO3, but also by different CYP isoforms.

#### 4.3. Kinetic studies, calculation of contributions, and hepatic clearances using a modified RAF approach

Chen et al. described the mean protein amount of FMO3 to be 46 pmol/mg in HLM (Chen et al., 2016), which corresponded to CYP1A2 levels (42 pmol/mg HLM protein) (Shimada et al., 1994). The RAF approach was described as tool to transfer recombinant enzyme kinetic data to human liver activity (Stormer et al., 2000). Activity data provided by the manufacturer were used to calculate the RAF within this study (Stormer et al., 2000).

The two therapeutic drugs amitriptyline and clozapine and their corresponding *N*-oxides were used to compare the hepatic net clearances calculated via CRS or PAR. As already described by Meyer et al., missing analytical standards for absolute quantification of formed metabolites might be a bottleneck in the assessment of kinetic data (Meyer et al., 2013a). The use of simple PAR of formed metabolite and internal standard was an alternative to calculate the contribution of enzymes to the hepatic clearance (Meyer et al., 2013a). As shown in Table 2, there was no significant difference in contributions calculated via CRS and PAR for amitriptyline and clozapine. Hence, relative  $V_{max}$  values were a

useful tool for comparison of velocities of different enzymes catalyzing the same reaction and for assessing their contributions to the hepatic clearance. In conclusion, neither CRS nor PAR had substantial impact on the estimation of *in vivo* hepatic net clearance. This was in line with previous findings (Meyer et al., 2013a).

Results for amitriptyline and clozapine indicated that FMO3 only played a minor role in their hepatic clearance as only 1–8% of amitriptyline and clozapine were excreted as *N*-oxide (Santagostino et al., 1974; Schaber et al., 1998). However, as the amitriptyline *N*-oxide was formed immediately after administration and disappeared soon, the *N*-oxygenation was discussed as ‘emergency’ route of metabolism for high drug levels (Santagostino et al., 1974). This assumption was consistent with the findings presented here of high FMO3  $K_m$  and  $V_{max}$  values, indicating a fast metabolism of high drug levels.

*N*-Oxygenation after CYP inhibition in pHLM was about 20% and thus higher than expected. Possible explanations were that either FMO3 worked more efficiently if CYPs were inhibited or the involved CYPs were not completely inhibited by ABT. However, these results confirmed the low contribution of FMO3 calculated via the RAF approach. RAF calculations were also done for different substrate concentrations (0.1–25  $\mu$ M) to cover different concentration ranges but only minor changes in calculated *in vivo* enzyme contributions were observed. Dextromethorphan, glaucine, and methadone were not metabolized by FMO3 and no further investigations were conducted, as the hepatic clearance of their *N*-oxides was expected to be only CYP-mediated.

Concerning the five DOAs identified as FMO3 substrates, only PAR could be used for calculating *in vivo* contribution. 3-BMC hydroxylamine was predominantly formed by CYP isoforms, while the formation of all other *N*-oxides was mainly FMO3-dependent. In order to confirm these calculations, pHLM incubations after ABT inhibition were performed and nor metabolites were monitored to verify successful CYP inhibition. 3-BMC hydroxylamine formation was significantly reduced after CYP inhibition but *N*-oxygenation of the other DOAs was not influenced by ABT inhibition and remained at more than 50% of formation in control incubations. These data fitted well with the higher contributions of FMO3 calculated using the RAF approach. FMO3 contribution did not change with increasing substrate concentrations calculated based on reported DMT and methamphetamine plasma concentrations (Huestis and Cone, 2007; Oliveira et al., 2012).

As FMO3 and different CYP isoforms (one in case of DALT and methamphetamine, two for DMT and MeOP, up to five for 3-BMC) were involved in the hepatic clearance of the *N*-oxygenation products of all investigated DOAs, a clinically relevant interaction with single inhibitors should not be expected. In addition, further metabolic steps were described to contribute to the total hepatic clearance (Cashman et al., 1999; Meyer et al., 2013b; Meyer et al., 2015; Meyer et al., 2012; Michely et al., 2015; Riba et al., 2012). Finally, FMO3 was not expected to be induced or inhibited by other substances (Cashman and Zhang, 2006) as described for CYPs.

## 5. Conclusions

Only single enzyme incubations were suitable for unambiguous identification of FMO3 substrates as heat inactivation and chemical inhibition provided contradictory results. Kinetic parameters of the *N*-oxygenation reactions were determined using the involved, recombinant enzymes. Finally, FMO3 was included for the first time in the RAF approach and its contribution to the human, hepatic clearance could be calculated. FMO3 was identified as enzyme mainly responsible for the formation of DALT *N*-oxide and methamphetamine hydroxylamine (>80% contribution for both). A contribution of 50 and 30% was calculated for the formation of

DMT *N*-oxide and MeOP *N*-oxide, respectively. However, FMO3 contributed with less than 5% to the formation of 3-BMC hydroxylamine, amitriptyline *N*-oxide, and clozapine *N*-oxide. There was no significant difference in the contributions when using calibrations with reference metabolite standards or peak area ratio calculations. As the application of the RAF approach containing FMO3 was not described in literature so far, the importance of FMO3 in the *N*-oxygenation of DOAs in human metabolism was shown for the first time here.

## Conflict of interest

The authors declared no conflict of interest.

## Acknowledgements

The authors like to thank Achim T. Caspar, Julia Dinger, Andreas G. Helfer, Julian A. Michely, Lilian H.J. Richter, and Armin A. Weber for their support and fruitful discussion.

## References

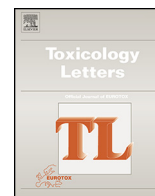
- Breyer-Pfaff, U., 2004. The metabolic fate of amitriptyline: nortriptyline and amitriptylinoxide in man. *Drug Metab. Rev.* 36, 723–746.
- Bull, S., Catalani, P., Garle, M., Coecke, S., Clothier, R., 1999. Imipramine for cytochrome P450 activity determination: a multiple-species metabolic probe. *Toxicol. In Vitro* 13, 537–541.
- Cashman, J.R., Zhang, J., 2006. Human flavin-containing monooxygenases. *Annu. Rev. Pharmacol. Toxicol.* 46, 65–100.
- Cashman, J.R., Xiong, Y.N., Xu, L., Janowsky, A., 1999. *N*-oxygenation of amphetamine and methamphetamine by the human flavin-containing monooxygenase (form 3): role in bioactivation and detoxication. *J. Pharmacol. Exp. Ther.* 288, 1251–1260.
- Cashman, J.R., 1995. Structural and catalytic properties of the mammalian flavin-containing monooxygenase. *Chem. Res. Toxicol.* 8, 166–181.
- Cashman, J.R., 2005. Some distinctions between flavin-containing and cytochrome P450 monooxygenases. *Biochem. Biophys. Res. Commun.* 338, 599–604.
- Cashman, J.R., 2008. Role of flavin-containing monooxygenase in drug development. *Expert. Opin. Drug Metab. Toxicol.* 4, 1507–1521.
- Caspar, A.T., Helfer, A.G., Michely, J.A., Auwaerter, V., Brandt, S.D., Meyer, M.R., Maurer, H.H., 2015. Studies on the metabolism and toxicological detection of the new psychoactive designer drug 2-(4-iodo-2,5-dimethoxyphenyl)-N-[(2-methoxyphenyl)methyl]ethanamine (25I-NBOMe) in human and rat urine using GC–MS LC–MSn, and LC–HR–MS/MS. *Anal. Bioanal. Chem.* 407, 6697–6719.
- Chauret, N., Gauthier, A., Nicoll-Griffith, D.A., 1998. Effect of common organic solvents on *in vitro* cytochrome P450-mediated metabolic activities in human liver microsomes. *Drug Metab. Dispos.* 26, 1–4.
- Chen, Y., Zane, N.R., Thakker, D.R., Wang, M.Z., 2016. Quantification of flavin-containing monooxygenases 1, 3 and 5 in human liver microsomes by UPLC–MRM-based targeted quantitative proteomics and its application to the study of ontogeny. *Drug Metab. Dispos.* (Epub ahead of print).
- Crespi, C.L., Miller, V.P., 1999. The use of heterologously expressed drug metabolizing enzymes-state of the art and prospects for the future. *Pharmacol. Ther.* 84, 121–131.
- Cruciani, G., Valeri, A., Goracci, L., Pellegrino, R.M., Buonerba, F., Baroni, M., 2014. Flavin monooxygenase metabolism: why medicinal chemists should matter. *J. Med. Chem.* 57, 6183–6196.
- Dinger, J., Meyer, M.R., Maurer, H.H., 2014. Development of an *in vitro* cytochrome P450 cocktail inhibition assay for assessing the inhibition risk of drugs of abuse. *Toxicol. Lett.* 230, 28–35.
- Emoto, C., Murase, S., Sawada, Y., Jones, B.C., Iwasaki, K., 2003. *In vitro* inhibitory effect of 1-aminobenzotriazole on drug oxidations catalyzed by human cytochrome P450 enzymes: a comparison with SKF-525A and ketoconazole. *Drug Metab. Pharmacokin.* 18, 287–295.
- Fan, P.W., Zhang, D., Driscoll, J.P., Halladay, J.S., Khojasteh, C., 2016. Going beyond common drug metabolizing enzymes: case studies of biotransformation involving aldehyde oxidase, gamma-glutamyl transpeptidase, cathepsin B, flavin-containing monooxygenase, and ADP-ribosyltransferase. *Drug Metab. Dispos.* (Epub ahead of print).
- Guo, Z., Raeissi, S., White, R.B., Stevens, J.C., 1997. Orphenadrine and methimazole inhibit multiple cytochrome P450 enzymes in human liver microsomes. *Drug Metab. Dispos.* 25, 390–393.
- Hamman, M.A., Haehner-Daniels, B.D., Wrighton, S.A., Rettie, A.E., Hall, S.D., 2000. Stereoselective sulfoxidation of sulindac sulfide by flavin-containing monooxygenases: comparison of human liver and kidney microsomes and mammalian enzymes. *Biochem. Pharmacol.* 60, 7–17.
- Huestis, M.A., Cone, E.J., 2007. Methamphetamine disposition in oral fluid plasma, and urine. *Ann. N. Y. Acad. Sci.* 1098, 104–121.

- Krueger, S.K., Williams, D.E., 2005. Mammalian flavin-containing monooxygenases: structure/function: genetic polymorphisms and role in drug metabolism. *Pharmacol. Ther.* 106, 357–387.
- Lemoine, A., Johann, M., Cresteil, T., 1990. Evidence for the presence of distinct flavin-containing monooxygenases in human tissues. *Arch. Biochem. Biophys.* 276, 336–342.
- Mathews, J.M., Dostal, L.A., Bend, J.R., 1985. Inactivation of rabbit pulmonary cytochrome P-450 in microsomes and isolated perfused lungs by the suicide substrate 1-aminobenzotriazole. *J. Pharmacol. Exp. Ther.* 235, 186–190.
- Meyer, M.R., Vollmar, C., Schwaninger, A.E., Maurer, H.H., 2012. New cathinone-derived designer drugs 3-bromomethcathinone and 3-fluoromethcathinone: studies on their metabolism in rat urine and human liver microsomes using GC-MS and LC-high-resolution MS and their detectability in urine. *J. Mass Spectrom.* 47, 253–262.
- Meyer, G.M.J., Meyer, M.R., Wink, C.S.D., Zapp, J., Maurer, H.H., 2013a. Studies on the in vivo contribution of human cytochrome P450s to the hepatic metabolism of glaucine, a new drug of abuse. *Biochem. Pharmacol.* 86, 1497–1506.
- Meyer, G.M.J., Meyer, M.R., Wissenbach, D.K., Maurer, H.H., 2013b. Studies on the metabolism and toxicological detection of glaucine, an isoquinoline alkaloid from *Glauclium flavum* (Papaveraceae), in rat urine using GC-MS, LC-MS<sup>n</sup> and LC-high-resolution MS<sup>n</sup>. *J. Mass Spectrom.* 48, 24–41.
- Meyer, M.R., Bach, M., Welter, J., Bovens, M., Turcant, A., Maurer, H.H., 2013c. Ketamine-derived designer drug methoxetamine: metabolism including isoenzyme kinetics and toxicological detectability using GC-MS and LC-(HR-) MSn. *Anal. Bioanal. Chem.* 405, 6307–6321.
- Meyer, M.R., Lindauer, C., Welter, J., Maurer, H.H., 2014. Dimethocaine, a synthetic cocaine derivative: studies on its in vivo metabolism and its detectability in urine by LC-HR-MS<sup>n</sup> and GC-MS using a rat model. *Anal. Bioanal. Chem.* 406, 1845–1854.
- Meyer, M.R., Holderbaum, A., Kavanagh, P., Maurer, H.H., 2015. Low and high resolution MS for studies on the metabolism and toxicological detection of the new psychoactive substance methoxypiperamide (MeOP). *J. Mass Spectrom.* 50, 1163–1174.
- Michely, J.A., Helfer, A.G., Brandt, S.D., Meyer, M.R., Maurer, H.H., 2015. Metabolism of the new psychoactive substances N,N-diallyltryptamine (DALT) and 5-methoxy-DALT and their detectability in urine by GC-MS LC-MSn, and LC-HR-MS/MS. *Anal. Bioanal. Chem.* 407, 7831–7842.
- Oliveira, C.D., Okai, G.G., da Costa, J.L., de Almeida, R.M., Oliveira-Silva, D., Yonamine, M., 2012. Determination of dimethyltryptamine and beta-carbolines (ayahuasca alkaloids) in plasma samples by LC-MS/MS. *Bioanalysis* 4, 1731–1738.
- Overby, L.H., Carver, G.C., Philpot, R.M., 1997. Quantitation and kinetic properties of hepatic microsomal and recombinant flavin-containing monooxygenases 3 and 5 from humans. *Chem. Biol. Interact.* 106, 29–45.
- Phillips, I.R., Shephard, E.A., 2008. Flavin-containing monooxygenases: mutations: disease and drug response. *Trends Pharmacol. Sci.* 29, 294–301.
- Riba, J., McIlhenny, E.H., Valle, M., Bouso, J.C., Barker, S.A., 2012. Metabolism and disposition of N,N-dimethyltryptamine and harmala alkaloids after oral administration of ayahuasca. *Drug Test. Anal.* 4, 610–616.
- Ring, B.J., Wrighton, S.A., Aldridge, S.L., Hansen, K., Haehner, B., Shipley, L.A., 1999. Flavin-containing monooxygenase-mediated N-oxidation of the M(1)-muscarinic agonist xanomeline. *Drug Metab. Dispos.* 27, 1099–1103.
- Santagostino, G., Facino, R.M., Pirillo, D., 1974. Urinary excretion of amitriptyline N-oxide in humans. *J. Pharm. Sci.* 63, 1690–1692.
- Schaber, G., Stevens, I., Gaertner, H.J., Dietz, K., Breyer-Pfaff, U., 1998. Pharmacokinetics of clozapine and its metabolites in psychiatric patients: plasma protein binding and renal clearance. *Br. J. Clin. Pharmacol.* 46, 453–459.
- Shimada, T., Yamazaki, H., Mimura, M., Inui, Y., Guengerich, F.P., 1994. Interindividual variations in human liver cytochrome P-450 enzymes involved in the oxidation of drugs, carcinogens and toxic chemicals: studies with liver microsomes of 30 Japanese and 30 Caucasians. *J. Pharmacol. Exp. Ther.* 270, 414–423.
- Stormer, E., von Moltke, L.L., Greenblatt, D.J., 2000. Scaling drug biotransformation data from cDNA-expressed cytochrome P-450 to human liver: a comparison of relative activity factors and human liver abundance in studies of mirtazapine metabolism. *J. Pharmacol. Exp. Ther.* 295, 793–801.
- Strolin, B.M., Whomsley, R., Baltes, E., 2006. Involvement of enzymes other than CYPs in the oxidative metabolism of xenobiotics. *Expert. Opin. Drug Metab. Toxicol.* 2, 895–921.
- Strolin, B.M., Tipton, K.F., Whomsley, R., 2007. Amine oxidases and monooxygenases in the in vivo metabolism of xenobiotic amines in humans: has the involvement of amine oxidases been neglected? *Fundam. Clin. Pharmacol.* 21, 467–480.
- Szoko, E., Tabi, T., Borbas, T., Dalmadi, B., Tihanyi, K., Magyar, K., 2004. Assessment of the N-oxidation of deprenyl, methamphetamine, and amphetamine enantiomers by chiral capillary electrophoresis: an in vitro metabolism study. *Electrophoresis* 25, 2866–2875.
- Taniguchi-Takizawa, T., Shimizu, M., Kume, T., Yamazaki, H., 2015. Benzydamine N-oxygenation as an index for flavin-containing monooxygenase activity and benzydamine N-demethylation by cytochrome P450 enzymes in liver microsomes from rats dogs, monkeys, and humans. *Drug Metab. Pharmacokinet.* 30, 64–69.
- Torres Pazmino, D.E., Winkler, M., Glieder, A., Fraaije, M.W., 2010. Monooxygenases as biocatalysts: classification, mechanistic aspects and biotechnological applications. *J. Biotechnol.* 146, 9–24.
- U.S. Department of Health and Human Services, Food and Drug Administration, Center for Drug Evaluation and Research (CDER), Center for Biologics Evaluation and Research (CBER) Guidance for Industry: Drug Interaction Studies—Study Design, Data Analysis, and Implications for Dosing and Labeling [Draft]. <http://www.fda.gov/downloads/drugs/guidancecomplianceregulatoryinformation/guidances/ucm292362.pdf>.
- Venkatakrishnan, K., von Moltke, L.L., Greenblatt, D.J., 2001. Application of the relative activity factor approach in scaling from heterologously expressed cytochromes p450 to human liver microsomes: studies on amitriptyline as a model substrate. *J. Pharmacol. Exp. Ther.* 297, 326–337.
- Wang, W., Tian, D.D., Zheng, B., Wang, D., Tan, Q.R., Wang, C.Y., Zhang, Z.J., 2015. Peony-glycyrrhiza decoction, an herbal preparation, inhibits clozapine metabolism via cytochrome P450s, but not flavin-containing monooxygenase in in vitro models. *Drug Metab. Dispos.* 43, 1147–1153.
- Wissenbach, D.K., Meyer, M.R., Remane, D., Philipp, A.A., Weber, A.A., Maurer, H.H., 2011a. Drugs of abuse screening in urine as part of a metabolite-based LC-MS(n) screening concept. *Anal. Bioanal. Chem.* 400, 3481–3489.
- Wissenbach, D.K., Meyer, M.R., Remane, D., Weber, A.A., Maurer, H.H., 2011b. Development of the first metabolite-based LC-MSn urine drug screening procedure—exemplified for antidepressants. *Anal. Bioanal. Chem.* 400, 79–88.
- Zollner, A., Buchheit, D., Meyer, M.R., Maurer, H.H., Peters, F.T., Bureik, M., 2010. Production of human phase 1 and 2 metabolites by whole-cell biotransformation with recombinant microbes. *Bioanalysis* 2, 1277–1290.

**3.2. IN VITRO MONOAMINE OXIDASE INHIBITION POTENTIAL OF ALPHA-METHYLTRYPTAMINE ANALOG NEW PSYCHOACTIVE SUBSTANCES FOR ASSESSING POSSIBLE TOXIC RISKS<sup>43</sup>**

**(DOI: 10.1016/j.toxlet.2017.03.007)**





# In vitro monoamine oxidase inhibition potential of alpha-methyltryptamine analog new psychoactive substances for assessing possible toxic risks



Lea Wagmann<sup>a</sup>, Simon D. Brandt<sup>b</sup>, Pierce V. Kavanagh<sup>c</sup>, Hans H. Maurer<sup>a</sup>, Markus R. Meyer<sup>a,\*</sup>

<sup>a</sup> Department of Experimental and Clinical Toxicology, Institute of Experimental and Clinical Pharmacology and Toxicology, Saarland University, Homburg, Germany

<sup>b</sup> School of Pharmacy and Biomolecular Sciences, Liverpool John Moores University, Liverpool, UK

<sup>c</sup> Department of Pharmacology and Therapeutics, Trinity Centre for Health and Sciences, St. James's Hospital, Dublin, Ireland

## HIGHLIGHTS

- Study provided in vitro data on inhibitory potential of tryptamine-like new psychoactive substances towards human MAO-A/B.
- Compounds were shown to inhibit at least one MAO isoform.
- 7-Me-AMT was identified to have the lowest IC<sub>50</sub> value against MAO-A and to act as competitive inhibitor.
- MAO inhibition by tested NPS was shown to be of possible clinical relevance concerning serotonergic and adrenergic effects.

## ARTICLE INFO

### Article history:

Received 27 January 2017

Received in revised form 8 March 2017

Accepted 10 March 2017

Available online 14 March 2017

### Keywords:

Alpha-methyltryptamine analog new psychoactive substances  
Drugs of abuse  
MAO inhibition  
LC–HR–MS/MS  
IC<sub>50</sub> value

## ABSTRACT

Tryptamines have emerged as new psychoactive substances (NPS), which are distributed and consumed recreationally without preclinical studies or safety tests. Within the alpha-methylated tryptamines, some of the psychoactive effects of the prototypical alpha-methyltryptamine (AMT) have been described decades ago and a contributing factor of its acute toxicity appears to involve the inhibition of monoamine oxidase (MAO). However, detailed information about analogs is scarce. Therefore, thirteen AMT analogs were investigated for their potential to inhibit MAO. An in vitro assay analyzed using hydrophilic interaction liquid chromatography–high resolution–tandem mass spectrometry was developed and validated. The AMT analogs were incubated with recombinant human MAO-A or B and kynuramine, a non-selective MAO substrate to determine the IC<sub>50</sub> values. The known MAO-A inhibitors 5-(2-aminopropyl)indole (5-IT), harmine, harmaline, yohimbine, and the MAO-B inhibitor selegiline were tested for comparison. AMT and all analogs showed MAO-A inhibition properties with IC<sub>50</sub> values between 0.049 and 166 μM, whereas four analogs inhibited also MAO-B with IC<sub>50</sub> values between 82 and 376 μM. 7-Me-AMT provided the lowest IC<sub>50</sub> value against MAO-A comparable to harmine and harmaline and was identified as a competitive MAO-A inhibitor. Furthermore, AMT, 7-Me-AMT, and nine further analogs inhibited MAO activity in human hepatic S9 fraction used as model for the human liver which expresses both isoforms. The obtained results suggested that MAO inhibition induced by alpha-methylated tryptamines might be clinically relevant concerning possible serotonergic and adrenergic effects and interactions with drugs (of abuse) particularly acting as monoamine reuptake inhibitors. However, as in vitro assays have only limited conclusiveness, further studies are needed.

© 2017 Elsevier B.V. All rights reserved.

## 1. Introduction

New psychoactive substances (NPS) are emerging drugs that are mainly consumed as legal and easy available substitutes for

\* Corresponding author.

E-mail address: [markus.meyer@uks.eu](mailto:markus.meyer@uks.eu) (M.R. Meyer).

traditional and controlled drugs of abuse (Brandt et al., 2014; Meyer, 2016). The detection of synthetic tryptamines including alpha-methyltryptamine (AMT) has been frequently reported to the EU Early Warning System coordinated by the European Monitoring Centre for Drugs and Drug Addiction (EMCDDA) and continuously monitored as part of the EMCDDA's toxicovigilance system (EMCDDA, 2015). AMT ( $\alpha$ -MT, 3-IT, IT-290) has been investigated in the 1960s as a potential antidepressant and its popularity as a drug of abuse came to light in the 1990s due to its hallucinogenic and stimulant properties (Araujo et al., 2015). In late 2011, an isomer of AMT, 5-(2-aminopropyl)indole (5-IT, 5-API), appeared on the European drug market (EMCDDA, 2014). After intake of AMT or 5-IT, symptoms related to monoaminergic toxicity were described, such as restlessness, agitation, disorientation, shivering, sweating, mydriasis, vomiting, tachycardia, or hyperthermia (EMCDDA, 2015; Shulgin and Shulgin, 1997). Both were also involved in several fatalities (Boland et al., 2005; Elliott and Evans, 2014). A key factor involved in the occurrence of clinical features included the inhibition of monoamine oxidase (MAO) enzymes, followed by increased monoamine levels inducing a serotonin syndrome (Boyer and Shannon, 2005; EMCDDA, 2014). In 1968, AMT, 5-IT, and four positional isomers were identified as inhibitors of guinea pig MAO (Cerletti et al., 1968). More recently, 5-IT was confirmed as highly selective and potent inhibitor of recombinant human MAO-A (Herraiz and Brandt, 2014).

Furthermore, tryptamines were identified in NPS products combining different NPS groups (UNODC, 2016). Thus, the risk of encountering monoaminergic (side) effects and drug–drug interactions is very likely although the extent to which this might occur is difficult to predict, given that systematic data are not available. In contrast to authorized medicines, NPS are marketed and consumed without preclinical or clinical studies. Procedures employed for various substrates, mostly therapeutic drugs, have been described for in vitro monitoring of MAO activity (Tipton et al., 2006). Examples of drugs of abuse tested for human MAO inhibition activity include MDMA and its metabolites, and 5-IT (Herraiz and Brandt, 2014; Steuer et al., 2016).

Therefore, the aim of the present study was to develop a MAO inhibition assay based on hydrophilic interaction liquid chromatography–high resolution–tandem mass spectrometry (HILIC–HR–MS/MS), to investigate the in vitro inhibition potential of AMT and 13 ring-substituted analogs (Fig. 1) on recombinant human MAO-A or B, and to determine their  $IC_{50}$  values.

## 2. Materials and methods

### 2.1. Chemicals and enzymes

Harmine was obtained from THC Pharm (Frankfurt, Germany), amphetamine- $d_5$  and AMT succinate from LGC Standards (Wesel,

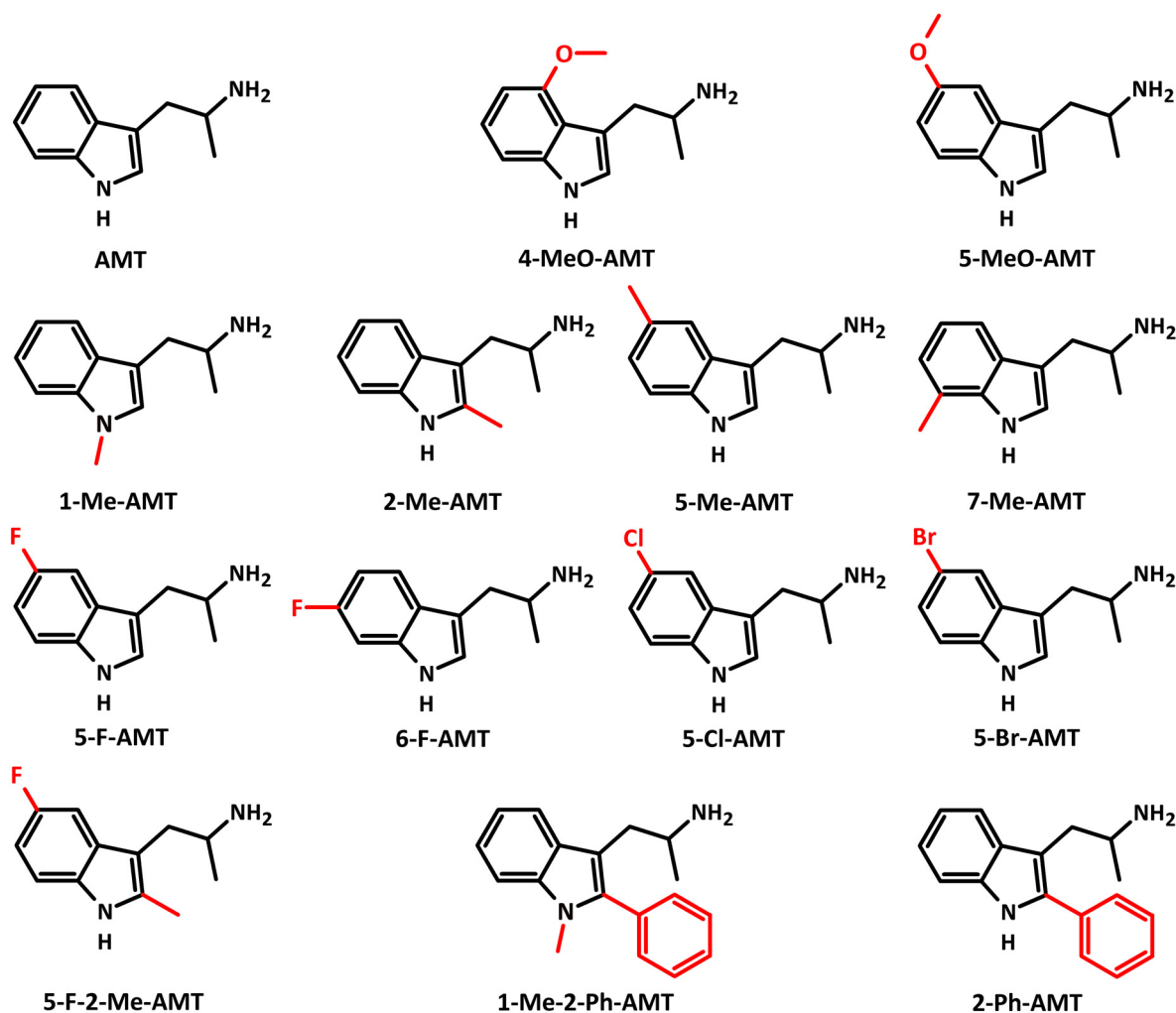


**Fig. 1.** Chemical structures of tested alpha-methyltryptamines. Structural variations in comparison to AMT were given in red (For interpretation of the reference to color in this figure legend, the reader is referred to the web version of the article).

Germany), harmaline, yohimbine, selegiline, kynuramine (KYN), 4-hydroxyquinoline (4-OHC), ammonium acetate, potassium dihydrogenphosphate, and dipotassium hydrogenphosphate from Sigma-Aldrich (Taufkirchen, Germany), formic acid (MS grade) from Fluka (Neu-Ulm, Germany), acetonitrile, methanol (both LC-MS grade), and all other chemicals from VWR (Darmstadt, Germany). 5-IT was synthesized (Scott et al., 2014) and kindly provided by the Department of Pharmacology and Therapeutics, Trinity Centre for Health Sciences, St James's Hospital, Dublin 8, Ireland, before it was scheduled. All non-scheduled AMT analogs were prepared following procedures published previously (Young, 1958). Details can also be found in (Brandt et al., 2004).

The baculovirus-infected insect cell microsomes (Supersomes) containing human complementary DNA-expressed MAO-A or MAO-B (5 mg protein/mL), wild-type Supersomes as negative control without MAO activity (MAO control, 5 mg protein/mL), and pooled human liver S9 (20 mg protein/mL) were obtained from Corning (Amsterdam, The Netherlands). After delivery, enzyme preparations were thawed at 37 °C, aliquoted, snap-frozen in liquid nitrogen, and stored at –80 °C until use.

## 2.2. HILIC–HR-MS/MS apparatus

A Thermo Fisher Scientific (TF, Dreieich, Germany) Dionex UltiMate 3000 Rapid Separation (RS) UHPLC system with a quaternary UltiMate 3000 RS pump and an UltiMate 3000 RS autosampler was used and controlled by the TF Chromeleon software version 6.80. It was coupled to a TF Q-Exactive Plus equipped with a heated electrospray ionization II source (HESI-II). The gradient elution was performed on a Macherey-Nagel (Düren, Germany) HILIC Nucleodur column (125 × 3 mm, 3 μm) using aqueous ammonium acetate (25 mM, eluent A) and acetonitrile containing 0.1% (v/v) formic acid (eluent B). The flow rate was set to 500 μL/min and the gradient was programmed as follows: 0–0.5 min hold 80% B, curve 5; 0.5–3.8 min to 50% B, curve 5; 3.8–3.9 min to 40% B, curve 5; 3.9–5 min hold 40% B, curve 5; 5–5.1 min to 80% B, curve 5; and 5.1–6 min hold 80% B, curve 5. Chromatography was performed at 60 °C maintained by a Dionex UltiMate 3000 RS analytical column heater. The injection volume for all samples was 1 μL. HESI-II conditions were already described before (Richter et al., 2016): sheath gas, 53 arbitrary units (AU); auxiliary gas, 14 AU; sweep gas, 3 AU; spray voltage, 3.50 kV; heater temperature, 438 °C; ion transfer capillary temperature, 269 °C; and S-lens RF level, 60.0. Mass calibration was done prior to analysis according to the manufacturer's recommendations using external mass calibration. For evaluating the chromatographic separation, a full scan experiment was used with the following scan parameters: polarity, positive; micro scan, 1; resolution, 35,000; automatic gain control (AGC) target, 3e6; maximum injection time (IT), 200 ms; and scan range, 50–750. The final quantification was performed using a targeted single ion monitoring (t-SIM) and a subsequent data-dependent MS<sup>2</sup> (dd-MS<sup>2</sup>) mode with an inclusion list containing the exact masses of positively charged KYN (*m/z* 165.1022), 4-OHC (*m/z* 146.0600), and the internal standard (IS) amphetamine-*d*<sub>5</sub> (*m/z* 141.1434). The settings for the t-SIM mode were as follows: micro scan, 1;

resolution, 35,000; AGC target, 5e4; maximum IT, 100 ms; and isolation window, 4 *m/z*. The settings for the dd-MS<sup>2</sup> mode were as follows: micro scan, 1; resolution, 35,000; AGC target, 2e5; maximum IT, 100 ms; isolation window, 4 *m/z*; and dynamic exclusion, 4 s. TF Xcalibur Qual Browser 2.2 software was used for data handling. The settings for automated peak integration were as follows: peak detection algorithm, ICIS; area noise factor, 5; and peak noise factor, 300. GraphPad QuickCalcs (GraphPad Software, San Diego, USA) was used for outlier detection (<http://graphpad.com/quickcalcs/grubbs1>), while GraphPad Prism 5.00 (GraphPad Software) was used for statistical evaluation.

## 2.3. Preparation of stock solutions

Stock solutions of the MAO substrate KYN (6.25 mM) or its metabolite 4-OHC (0.1 mM) were prepared in water. Stock solutions of harmine, harmaline, 5-IT, selegiline, AMT (5 mM, respectively), or yohimbine (3 mM) were used in methanol. Stock solutions of the AMT analogs (5 mM, respectively) were prepared in DMSO. Afterwards, they were diluted 1:5 (v/v) with methanol, gently evaporated under nitrogen, and resolved in water/methanol (9:1, v/v). To obtain the solutions for incubation, the stock solutions were diluted in phosphate buffer. The organic solvent content in the final incubation mixtures was always below 2.5% (Chauret et al., 1998). Stock solutions were aliquoted and stored at –20 °C.

## 2.4. Method validation

The method for quantification of 4-OHC was validated in accordance to the “Guideline on bioanalytical method validation” published by the European Medicines Agency (EMA, 2011). For validation, 30 μL samples containing 1 μg/mL MAO control in phosphate buffer were used. If needed, 10 μL of the phosphate buffer were replaced by appropriate amounts of the calibration or quality control (QC) stock solution. These samples were diluted with the same volume of acetonitrile with or without IS. Briefly, the method was tested for selectivity (using ten blank samples without IS), carry-over (using a blank sample without IS following the high QC), lower limit of quantification (LLOQ) defined as lowest calibration standard, within-run accuracy and precision (analyzed in a single run five samples per level at four concentration levels: LLOQ QC, low QC, medium QC, and high QC), between-run accuracy and precision (analyzed in three different runs on two different days six samples per level at four concentration levels: LLOQ QC, low QC, medium QC, and high QC), matrix effect (using six samples with matrix and six samples without matrix at two concentration levels: low QC and high QC), and stability of processed samples in the autosampler. The calibration consisted of six concentration points (50, 200, 400, 600, 800, and 1000 nM) equally distributed over the whole range. The concentrations of LLOQ QC, low QC, medium QC, and high QC were as follows: 50, 100, 500, and 900 nM. Instead of MAO-A or B, MAO control was used for sample preparation. For quantification, the ratios of 4-OHC versus IS were used. The analytical runs consisted of a blank sample without IS, a blank sample with IS, calibration standards, three levels of QC

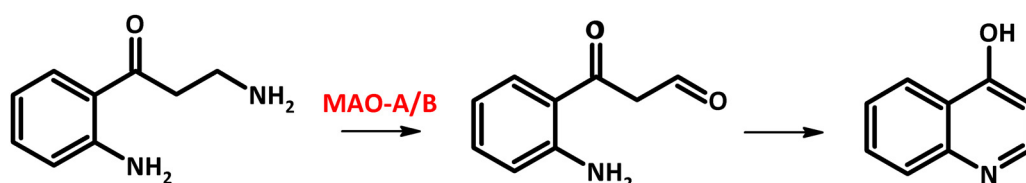


Fig. 2. Deamination of kynuramine catalyzed by MAO-A or MAO-B providing an aldehyde, followed by non-enzymatic condensation to 4-hydroxyquinoline.

samples (low, medium, and high) in duplicate, and the study samples. All calculations were done using GraphPad Prism 5.00.

### 2.5. Determination of $K_m$ values

KYN deamination is depicted in Fig. 2. The kinetic constants were derived from incubations with MAO-A, MAO-B, or S9. Incubations were performed at 37 °C for 20 min using 1 µg/mL MAO-A or MAO-B, respectively, or 100 µg/mL S9, and the MAO substrate KYN at concentrations of 0.1, 0.5, 1, 5, 10, 25, 50, 100, 150, 200, 250, and 500 µM. In addition, blank incubations with 1 µg/mL MAO control were prepared as negative control. Besides enzyme preparations and substrate, the incubation mixtures (final volume 30 µL) contained 100 mM phosphate buffer. Reactions were initiated by addition of the ice-cold enzyme preparation and stopped with 30 µL of ice-cold acetonitrile, containing 10 µM amphetamine- $d_5$  as IS. The solution was centrifuged for 2 min at 10,000g, 50 µL of the supernatant were transferred to an autosampler vial, and injected onto the HILIC–HR-MS/MS apparatus for analysis. Enzyme kinetic constants were estimated by non-linear curve fitting using GraphPad Prism 5.00 after validated quantification of the formed metabolite 4-OHC via six-point calibration. The Michaelis–Menten equation (Eq. (1)) was used to calculate apparent  $K_m$  and  $V_{max}$  values for MAO-A, MAO-B, or S9, where  $v$  is the initial reaction velocity,  $S$  the substrate concentration,  $V_{max}$  the maximal reaction velocity, and  $K_m$  the substrate concentration at half  $V_{max}$ .

$$v = \frac{V_{max} \times S}{K_m + S} \quad (1)$$

### 2.6. Initial inhibition screening and determination of $IC_{50}$ values and inhibition constants

#### 2.6.1. Initial inhibition screening

For inhibition studies, 10 µL of the phosphate buffer was replaced by appropriate amounts of the potential inhibitor solution. KYN was used in concentrations comparable to its  $K_m$  value. All other incubation conditions were the same as described above. To test for inhibition capability, MAO-A or B was incubated with 10 µM of the potential inhibitor in triplicate ( $n=3$ ). In addition to these samples, control samples without inhibitor, positive control samples with model inhibitors (10 µM 5-IT for MAO-A or 10 µM selegiline for MAO-B), blank samples without MAO activity, and interfering samples were also prepared in triplicates. For preparation of the interfering samples, control samples without inhibitor were incubated and the reaction was terminated with ice-cold acetonitrile containing the IS and the potential inhibitors. The 4-OHC formation in test samples was then compared to metabolite formation in control samples. For statistical analysis of data, a one-way ANOVA followed by Dunnett's multiple comparison test (significance level,  $P < 0.001$ , 99.9% confidence intervals) by GraphPad Prism 5.00 was used.

#### 2.6.2. Determination of $IC_{50}$ values

Inhibitors were incubated at least at ten different concentrations (0.00004, 0.0002, 0.0006, 0.002, 0.01, 0.04, 0.2, 0.6, 2.5, 10, 40, 160, 640, 2560 µM), depending on their expected inhibition strengths after initial inhibition screening. All other incubation conditions were the same as described above. Control samples were also prepared as described above. The  $IC_{50}$  values were calculated by plotting the metabolite formation (relative to the control samples) over the logarithm of the inhibitor concentration using GraphPad Prism 5.00.

**Table 1**

Test compounds, reference plasma concentrations, and  $IC_{50}$  values (percentage errors in brackets) of AMT-type new psychoactive substances (NPS) and known MAO inhibitors. Plasma concentrations in µM were calculated from the published data (in mg/L or µg/L). Probable clinically relevant  $IC_{50}$  values for AMT-type NPS are given in bold. PM: post-mortem cases.

Test compounds	Reference plasma concentrations		$IC_{50}$ values, µM	
	µg/L	µM	MAO-A	MAO-B
AMT-type NPS				
AMT	440 (Ferec et al., 2015)	2.5	<b>0.38</b> (8)	
	160–1300 (PM) (Elliott and Evans, 2014)	0.9–7.5		
4-MeO-AMT	*	0.8–6.4	1.4 (11)	
5-MeO-AMT	*	0.8–6.4	31 (4)	
1-Me-AMT	*	0.9–6.9	51 (3)	
2-Me-AMT	*	0.9–6.9	11 (7)	
5-Me-AMT	*	0.9–6.9	1.5 (13)	
7-Me-AMT	*	0.9–6.9	<b>0.049</b> (2)	
5-F-AMT	*	0.8–6.8	<b>0.45</b> (23)	376 (1)
6-F-AMT	*	0.8–6.8	1.8 (19)	126 (2)
5-Cl-AMT	*	0.8–6.2	<b>0.25</b> (7)	82 (2)
5-Br-AMT	*	0.6–5.2	1.3 (7)	
5-F-2-Me-AMT	*	0.8–6.3	4.1 (7)	223 (3)
1-Me-2-Ph-AMT	*	0.6–4.9	166 (2)	
2-Ph-AMT	*	0.6–5.2	3.7 (18)	
Known inhibitors				
5-IT	15–590 (Backberg et al., 2014)	0.1–3.4	0.20 (1)	
	700–5100 (PM) (EMCDDA, 2014)	4.0–29		
Selegiline	0.3–1.5 (Barrett et al., 1996)	0.002–0.01		0.017 (2)
Harmine	36–222 (Baselt, 2008)	0.2–1.0	0.006 (2)	
	1.0–15.6 (Oliveira et al., 2012)	0.005–0.07		
Harmaline	2.7–15.7 (Oliveira et al., 2012)	0.01–0.07	0.011 (2)	
Yohimbine	3.7–171 (Baselt, 2008)	0.01–0.5	6.0 (7)	

\*No plasma concentrations reported, thus concentrations estimated according to the structure-related compound AMT.

### 2.6.3. Determination of inhibition constants ( $K_i$ values)

For experimental determination, four concentration levels of the test inhibitor were incubated with KYN at five different concentrations (0.5, 5, 25, 100, and 500  $\mu\text{M}$ ). Inhibitor concentration levels depended on the previously determined  $\text{IC}_{50}$  value. For selegiline and 7-Me-AMT, inhibitor concentration levels were 0, 0.01, 0.05, and 0.1  $\mu\text{M}$ , for 5-IT, 0, 0.1, 0.5, and 1  $\mu\text{M}$ . All other incubation conditions were the same as described above. 7-Me-AMT and 5-IT were incubated with MAO-A, whereas MAO-B was

used in the case of selegiline. The inhibition constants ( $K_i$  values) were calculated using GraphPad Prism 5.00. Michaelis–Menten plots were transferred to Lineweaver–Burk plots ( $1/V$  versus  $1/S$ ), and fit factors for different inhibition models were compared to determine the most probable inhibition mode. If competitive inhibition was identified as most probable inhibition model, the equation of Cheng and Prusoff (Eq. (2)) (Cheng and Prusoff, 1973)

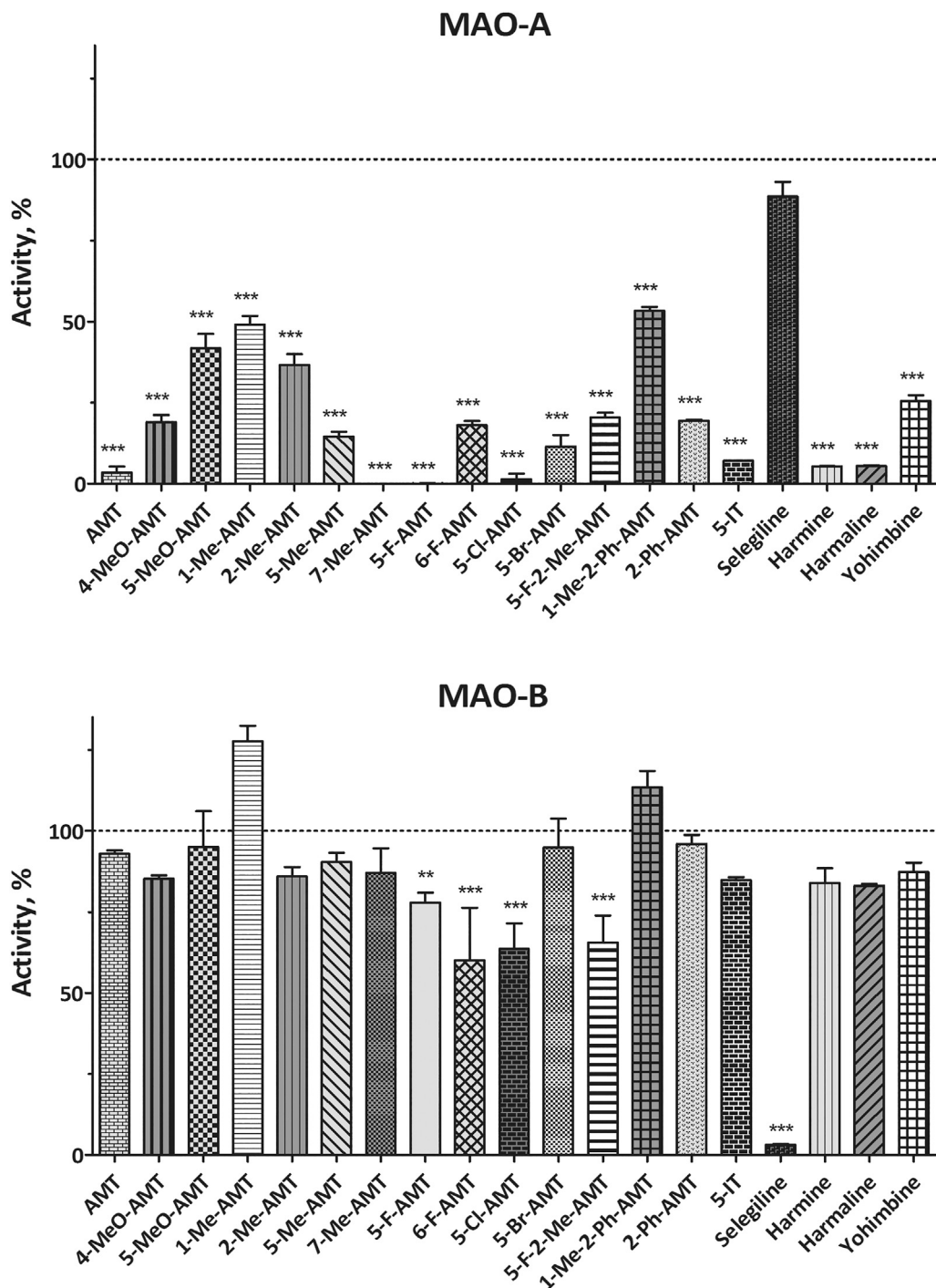


**Fig. 3.** Initial inhibition screening results using 10  $\mu\text{M}$  each of the inhibitor. Percentage of activity represented the percentage of metabolite formation in relation to control incubations without inhibitor (100%). Values are expressed as mean and were tested for significance ( $n=3$ , \*\*\*,  $P < 0.001$ , \*\*,  $P < 0.01$ , \*,  $P < 0.1$  for 4-hydroxyquinoline formation in incubations with the test inhibitor versus 4-hydroxyquinoline formation in control incubations).

was additionally used to calculate  $K_i$  from  $IC_{50}$  and  $K_m$  values.

$$IC_{50} = K_i \times \left( 1 + \frac{S}{K_m} \right) \quad (2)$$

### 2.7. MAO inhibition in S9 fraction

Three concentration levels of the inhibitors were incubated with KYN at concentrations at its  $K_m$  value. Inhibitor concentration level one was the lowest concentration and chosen based on plasma concentrations reported after intake (Table 1). Concentration levels two and three were calculated to be ten and one hundred times concentration level one, respectively. For selegiline, inhibitor concentration levels were 0.005, 0.05, and 0.5  $\mu\text{M}$ ; for harmine, harmaline, and yohimbine, 0.1, 1, and 10  $\mu\text{M}$  inhibitor were chosen, and for all other compounds, 1, 10, and 100  $\mu\text{M}$ . All other incubation conditions were the same as described above. In addition, control samples without inhibitor and blank samples were prepared. All incubations were performed in triplicate ( $n=3$ ). For evaluation, the metabolite formation in test samples was compared to metabolite formation in control samples. For statistical analysis of the data, a one-way ANOVA followed by Dunnett's multiple comparison test (significance level,  $P < 0.05$ , 95% confidence intervals) by GraphPad Prism 5.00 was used.

## 3. Results

### 3.1. Method validation

The analytical procedure was based on HILIC–HR-MS/MS in t-SIM mode with a subsequent dd-MS<sup>2</sup> mode. The method was successfully validated in accordance to the criteria of the (EMA, 2011). The method was selective at LLOQ levels, with a response of interfering components less than 20% or 5% compared to the response of the analyte at the LLOQ and the response of the IS, respectively. No carry-over problems could be observed and the LLOQ for 4-OHC was defined as 50 nM. The mean for within-run and between-run accuracies ranged from 3% to 19% but were within 20% of the nominal values for the LLOQ QC and within 15% for the low, medium, and high QC samples. The mean within-run and between-run precisions ranged from 1% to 13%. Precisions were within 20% for the LLOQ QC and within 15% for the low, medium, and high QC samples. The coefficients of variation (CVs) of matrix factors were 9% and 11% for the analytes and the IS at low QC level and 3% and 7% at high QC level. The CVs of IS-normalized matrix factor were 14% for low and 9% at high QC level and thus not greater than 15%. Processed samples showed sufficient stability in

the autosampler for at least 10 h, corresponding to the maximum duration of the analytical runs.

### 3.2. Determination of $K_m$ values

The kinetics for KYN deamination using MAO-A, MAO-B, or S9 followed classic Michaelis–Menten behavior. Calculated  $K_m$  values were  $43 \pm 5 \mu\text{M}$ ,  $23 \pm 4 \mu\text{M}$ , and  $34 \pm 2 \mu\text{M}$  for MAO-A, MAO-B, and S9, respectively.  $V_{max}$  values were  $75 \pm 2 \text{ nmol/min/mg}$ ,  $56 \pm 2 \text{ nmol/min/mg}$ , and  $7 \pm 0.1 \text{ nmol/min/mg}$  for MAO-A, MAO-B, and S9, respectively.  $R^2$  values were 0.9910, 0.9760, and 0.9980, respectively.

### 3.3. Initial inhibition screening results

The results are summarized in Fig. 3. All test tryptamines showed significant inhibition of MAO-A resulting in residual activities below 50%. MAO-B was additionally inhibited by 5-F-AMT, 6-F-AMT, 5-Cl-AMT, and 5-F-2-Me-AMT, resulting in residual activities between 60 and 80%. Harmine, harmaline, and yohimbine also showed inhibition of MAO-A in this assay. Whereas harmine and harmaline inhibited MAO-A activity almost completely, yohimbine inhibition resulted in residual activities of about 25%. No analytical interferences could be detected for all incubation sets and the positive control samples showed almost complete inhibition of MAO-A or B with residual activities of about 5%.

### 3.4. Determination of $IC_{50}$ values

All results are given in Table 1.  $IC_{50}$  values of AMT and its analogs for MAO-A inhibition were between 0.049 (7-Me-AMT) and 166  $\mu\text{M}$  (1-Me-2-Ph-AMT), for MAO-B inhibition,  $IC_{50}$  values of 5-Cl-AMT, 6-F-AMT, 5-F-2-Me-AMT, and 5-F-AMT were 82, 126, 223, and 376  $\mu\text{M}$ , respectively. The known MAO-A inhibitors harmine, harmaline, 5-IT, and yohimbine resulted in  $IC_{50}$  values of 0.006, 0.011, 0.20, and 6.0  $\mu\text{M}$ , respectively, while the  $IC_{50}$  value of selegiline towards MAO-B was 0.017  $\mu\text{M}$ .

### 3.5. Determination of $K_i$ values

Michaelis–Menten and Lineweaver–Burk plots after incubation of 7-Me-AMT are given in Fig. 4. The  $K_i$  value was 0.026  $\mu\text{M}$ . A competitive inhibition model was preferred, which was in line with the visual inspection of the intersection in the Lineweaver–Burk plot.  $K_i$  value calculated from  $IC_{50}$  and  $K_m$  values was 0.025  $\mu\text{M}$ . For 5-IT and selegiline, experimentally determined  $K_i$  values were 0.18 and 0.011  $\mu\text{M}$ , respectively. Calculated  $K_i$  values

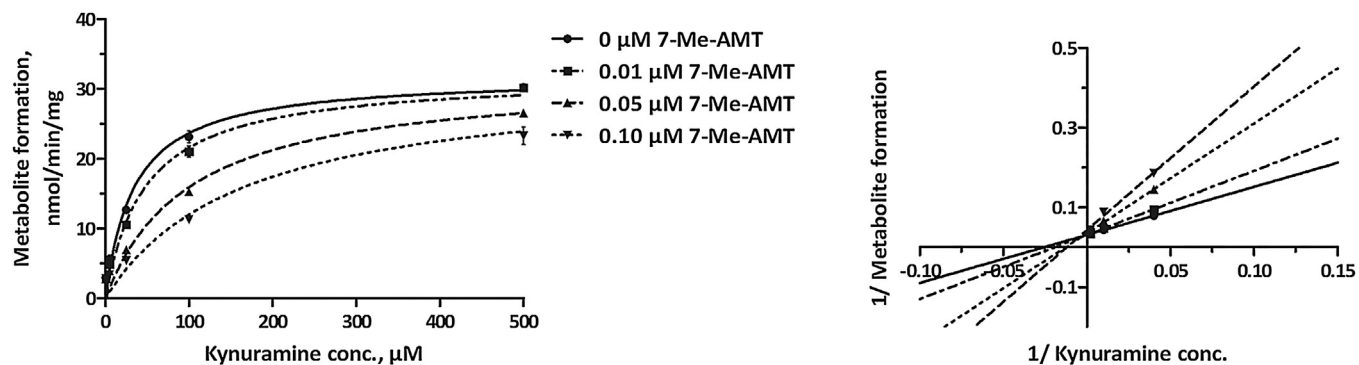


Fig. 4. Michaelis–Menten plot (left part) of the deamination of kynuramine in absence or presence of three given concentrations of 7-Me-AMT for determination of the inhibition constant. Data points represent means and ranges (error bars) of duplicate measurements. Transformation of data to a Lineweaver–Burk plot (right part) for determination of the inhibition mode.

were 0.10 and 0.009  $\mu\text{M}$ , respectively. Visual inspection and software based evaluation preferred competitive inhibition model for both compounds.

### 3.6. MAO inhibition in S9 fraction

Results are summarized in Fig. 5. 7-Me-AMT exerted significant inhibition of KYN deamination by MAO in S9 for all concentration levels. AMT, 5-Cl-AMT, and 5-Br-AMT inhibited MAO activity when incubated at concentration levels two or three. 4-MeO-AMT, 2-Me-AMT, 5-Me-AMT, 5-F-AMT, 6-F-AMT, 5-F-2-Me-AMT, and 2-Ph-AMT showed significant inhibition only when incubated in concentration level three. 5-MeO-AMT, 1-Me-AMT, and 1-Me-2-Ph-AMT showed no MAO inhibition in S9, even at the highest concentration level. Harmine and harmaline showed significant inhibition of MAO-A at all concentration levels, while in case of 5-IT and selegiline concentration levels two or three led to significant inhibition, and for yohimbine only concentration level three.

## 4. Discussion

MAO activity was assessed using KYN, a non-selective substrate for MAO-A and B, which was transformed to the corresponding aldehyde, followed by non-enzymatic condensation to 4-OHC (Fig. 2) (Weissbach et al., 1960). 4-OHC formation was analyzed using HILIC–HR-MS/MS. Although literature described many MAO activity assays (Tipton et al., 2006), Herraiz and Chaparro found that the needed selectivity for analyzing 4-OHC could only be achieved by chromatographic separation before detection (Herraiz and Chaparro, 2006). Since HILIC was shown to provide sufficient retention and separation of small and polar analytes (Steuer et al., 2016), it was anticipated that HILIC separation would be a suitable method in the present study. Due to its high flexibility and sensitivity, HR-MS/MS required comparatively low levels of recombinant MAO enzymes and thus reduction of the total protein content, which can lead to non-specific protein binding of analytes (Baranczewski et al., 2006). The t-SIM mode with a subsequent dd-MS<sup>2</sup> acquisition allowed simultaneous quantification and identification, respectively. The t-SIM provided approximately 50 scans per peak by far sufficient for quantification, whereas the dd-MS<sup>2</sup> provided additional selectivity for further studies without the need

for revalidation. Experimental variability during sample preparation and analysis was corrected by addition of the internal standard amphetamine-*d*<sub>5</sub>, which provided comparable properties to 4-OHC. The whole analytical procedure was successfully validated in accordance with international guidelines (EMA, 2011).

For determination of  $K_i$  values, the substrate concentration should be used below or at its  $K_m$  value. Different  $K_m$  values of KYN deamination by MAO-A or B derived from diverse enzyme sources were published (Herraiz and Brandt, 2014; Naoi and Nagatsu, 1988; Parikh et al., 2002; Ro et al., 2001) and none for S9. Therefore,  $K_m$  values were also determined in this study. The question as to whether the S9 fraction would show MAO activity remained inconsistently answered. As enzymes of the outer mitochondrial membrane, MAO was expected to be removed by centrifugation at 9000g during production of S9 fraction (Lee and Zhu, 2011). However, Salva et al. reported NADPH-independent formation of metabolites even in pooled human liver microsomes, which could be abolished by MAO inhibitors. They ascribed this MAO activity to a contamination with mitochondrial enzymes (Salva et al., 2003). Furthermore, the guidance for industry by the Food and Drug Administration recommended the addition of the MAO inhibitor pargyline to the S9 fraction to identify MAO contribution in the oxidative biotransformation of any given tested drug (FDA, 2006). As 4-OHC formation in S9 was also observed in the present study, the  $K_m$  value of KYN transformation in S9 was determined. Resulting  $K_m$  values for MAO-A and MAO-B were similar, as expected for a non-selective substrate, and comparable to published values (Herraiz and Brandt, 2014; Naoi and Nagatsu, 1988; Parikh et al., 2002; Ro et al., 2001). Initial experiments were conducted to choose incubation time and enzyme concentration (data not shown) to be within the linear range of metabolite formation. Substrate concentrations between 0.1 and 500  $\mu\text{M}$  KYN allowed modeling of enzyme kinetics. Less than 20% of substrate was metabolized in all incubations, except of the lowest substrate concentrations. To avoid non-specific protein binding, the protein concentrations were chosen as low as analytically possible as recommended by (Baranczewski et al., 2006). Blank incubations should be used to consider MAO-independent formation of 4-OHC.

Applicability of the initial inhibition screening procedure to assess the inhibition by either MAO-A or MAO-B was tested using positive control samples containing 5-IT or selegiline, known for

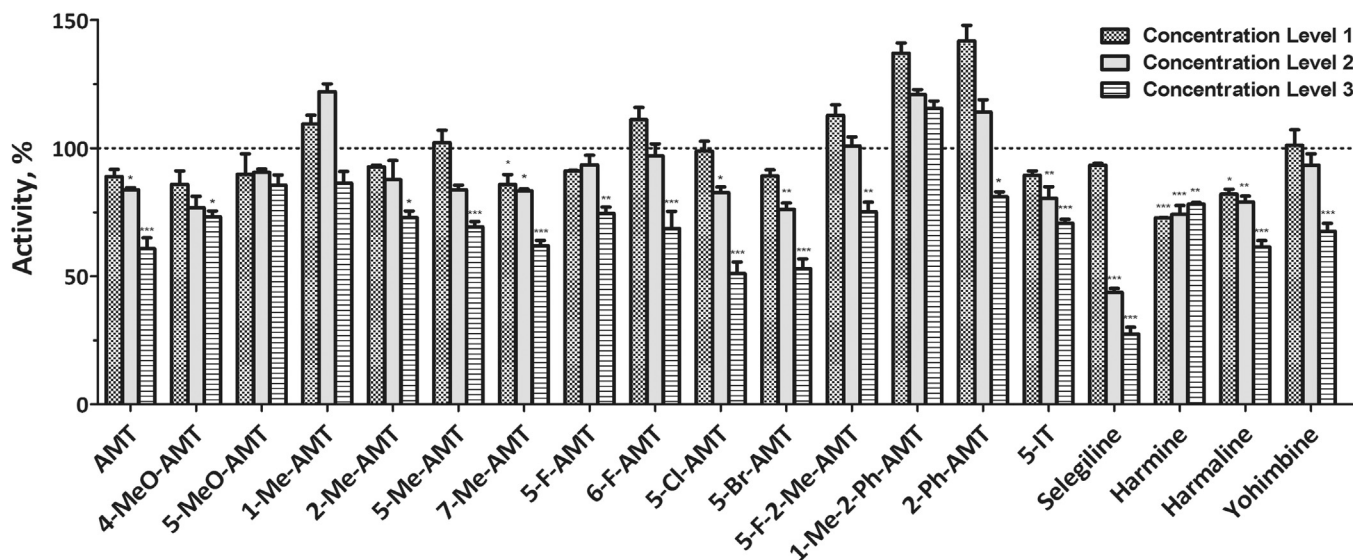


Fig. 5. Inhibition of MAO activity in S9 fraction by different inhibitor concentration levels (level 3 represented highest inhibitor concentration). Percentage of activity represented the percentage of metabolite formation in relation to control incubations without inhibitor (100%). Values are expressed as mean and were tested for significance ( $n = 3$ , \*\*\*,  $P < 0.001$ , \*\*,  $P < 0.01$ , \*,  $P < 0.1$  for 4-hydroxyquinoline formation in incubations with the test inhibitor versus 4-hydroxyquinoline formation in control incubations).

inhibition of MAO-A or B, respectively. A one-way ANOVA followed by Dunnett's multiple comparison test was used to decide whether 4-OHC formation in test samples was statistically significantly different from 4-OHC formation in control samples. Such an initial inhibition screening strategy was already described by Dinger et al. for studying the cytochrome P450 (CYP) inhibition potential of 3,4-methylenedioxy-derived designer drugs (Dinger et al., 2016a). In the present study, a set of blank samples was also analyzed. A lower inhibitor concentration (10  $\mu$ M) in the positive control samples was chosen because plasma concentrations of known MAO inhibitors were expected to be lower than those of CYP inhibitors. No significant inhibition at 10  $\mu$ M was thus considered as weak and probably not clinically relevant. Interfering samples were used to exclude mass spectral ion suppression or enhancement effects, caused by co-eluting analytes (Remane et al., 2010). These samples were mandatory as only KYN, 4-OHC, and the IS were monitored by the analytical method and co-eluting compounds could lead to false positive (in case of ion suppression) or false negative (in case of ion enhancement) results.

In accordance to Cerletti et al. (1968) and Zirkle and Kaiser (1964), AMT was identified as MAO-A inhibitor. All tested analogs also revealed MAO-A inhibition properties, whereas 5-F-AMT, 6-F-AMT, 5-Cl-AMT, and 5-F-2-Me-AMT inhibited MAO-B as well. Furthermore, harmine, harmaline, and yohimbine showed MAO-A inhibition consistent with previous investigations e.g. (Dos Santos et al., 2013). The initial inhibition screening was useful to realize that most tested compounds inhibited only one MAO isoform. Hence, time and costs for further IC<sub>50</sub> determinations could be saved. Consequently, only for compounds showing a statistically significant inhibition in the initial inhibition screening, IC<sub>50</sub> values were determined.

To predict a potential clinical relevance of the MAO inhibition based on IC<sub>50</sub> values, the expected plasma levels of inhibitors (given in Table 1) of inhibitors should be considered. In case of NPS, only scarce information is available, concerning plasma concentrations after intake. The only information source was case reports of fatal or non-fatal intoxications but particularly postmortem data is difficult to interpret, due to postmortem redistribution and unclear cause of death. But also data of non-fatal cases is problematic, as dosage and time of ingestion remain often unclear.

7-Me-AMT showed an IC<sub>50</sub> value against MAO-A activity comparable to the strong inhibitors harmine and harmaline. For 7-Me-AMT, plasma levels were not yet published, but described plasma concentrations for AMT (Elliott and Evans, 2014; Ferec et al., 2015) were much higher than published harmine and harmaline plasma concentrations (Baselt, 2008; Oliveira et al., 2012). For AMT, Shulgin and Shulgin (1997) described oral intake of 15–30 mg or smoking of 5–20 mg as common dosage. These amounts were comparable to oral dosages of 5-IT (Shulgin and Shulgin, 1997). In comparison, 5-MeO-AMT, however, was found to be significantly more potent with an active oral dose in the 1.5–4.5 mg range (Kantor et al., 1980; Shulgin, 1979; Shulgin and Nichols, 1978; Shulgin and Shulgin, 1997). Concerning other AMT analogs, no data about dosage or plasma concentrations are available so far, but similar doses followed by similar plasma concentrations may be expected. Considering assumed plasma levels, clinical relevance of the MAO-A inhibition after intake of 7-Me-AMT could not be excluded. The same should be true for 5-Cl-AMT, AMT, and 5-F-AMT, as their IC<sub>50</sub> values against MAO-A were in the same range as the IC<sub>50</sub> value of 5-IT. Given that the other AMT analogs showed higher IC<sub>50</sub> values against MAO-A, clinical relevance should be unlikely. Comparing the structural properties and IC<sub>50</sub> values, a methylation in the 7-position of the indole ring appeared to result in increased potency whereas compounds with a methylation in position 1, 2, or 5 provided a higher IC<sub>50</sub> value than AMT itself. The two compounds carrying a methyl group in position

1 provided the highest IC<sub>50</sub> values. Therefore, an unchanged position 1 might be essential for the unhindered binding to MAO-A and especially the combination of a methyl group in position 1 with a phenyl group in position 2 reduced the inhibition potential. Furthermore, a methoxy group in the 5-position led to an increased IC<sub>50</sub> value, whereas the methoxy group located at position 4, or insertion of a halogen atom in position 5, had nearly no effect on the IC<sub>50</sub> value, compared to AMT. Concerning MAO-B inhibition, determined IC<sub>50</sub> values of four AMT analogs were hundred to one thousand times higher than the IC<sub>50</sub> value of selegiline but also expected plasma concentrations of the AMT analogs were hundred to thousand times higher than published selegiline plasma concentrations. Additionally, these AMT analogs inhibited both MAO isoforms and thus, clinical relevance could not be excluded.

Furthermore, the K<sub>i</sub> values of 7-Me-AMT, 5-IT, and selegiline were experimentally determined and additionally calculated from the IC<sub>50</sub> values resulting in comparable K<sub>i</sub> values. Both K<sub>i</sub> values for 5-IT were similar to those published by Herraiz and Brandt (2014). In the current study, all three compounds were identified as competitive inhibitors and 7-Me-AMT confirmed as potent MAO-A inhibitor, far stronger than 5-IT.

Moreover, MAO inhibition was tested in human hepatic S9 fraction given that MAO-B is slightly overexpressed in human liver (Nishimura and Naito, 2006; Wang et al., 2013). In contrast to the artificial system of recombinant human MAO expressed in baculovirus-infected insect cells, the S9 fraction represents an in vitro model of the human liver, containing both isoforms in their natural environment and different abundances. The test drugs were used at three different concentration levels. Concentration level one represented expected plasma concentrations, as actual concentrations in the liver were difficult to estimate. Being the main metabolizing organ, a higher concentration than in plasma is more than likely (concentration levels two and three). Obtained results correlated well with the determined IC<sub>50</sub> values. 7-Me-AMT, with the lowest IC<sub>50</sub> value, showed significant inhibition of MAO activity for all concentration levels, while 5-MeO-AMT, 1-Me-AMT, and 1-Me-2-Ph-AMT, with the highest IC<sub>50</sub> values towards MAO-A, showed no inhibition at all. Residual MAO activity towards KYN in presence of the test inhibitor could be explained by inhibition of only one isoform, which means that the effect might be more pronounced for a MAO-A specific substrate such as serotonin or noradrenalin. As tryptamines were often identified in NPS products containing different NPS groups (UNODC, 2016), an intake with substances that increase monoamine levels or inhibit MAO could lead to severe intoxications as described by (Brush et al., 2004). They reported about an adolescent who suffered from a severe intoxication exhibiting hyperthermia, tachycardia, and massive agitation after consumption of the combination of a hallucinogenic tryptamine and the monoamine oxidase inhibitor harmaline (Brush et al., 2004). Therefore, clinical effects due to MAO inhibition by AMT or its analogs could not be excluded for most of the tested compounds.

As controlled human trials for NPS are not feasible due to ethical reasons, in vitro approaches for studying their toxicokinetics have to be used (Caspar et al., 2015; Dinger et al., 2016b; Meyer, 2016; Meyer et al., 2015; Michely et al., 2015; Wagmann et al., 2016). Concerning MAO inhibition by drugs of abuse, only few studies were published. Cerletti et al. identified AMT, 5-IT, and four positional isomers as inhibitors of guinea pig MAO in an assay based on the manometric determination of the oxygen uptake of guinea pig liver homogenates with serotonin as substrate (Cerletti et al., 1968). Herraiz and Brandt confirmed 5-IT as highly selective and potent inhibitor of recombinant human MAO-A by measuring the KYN deamination using high-performance liquid chromatography coupled to diode array detection (Herraiz and Brandt, 2014). Steuer et al. investigated the MAO inhibition potential of MDMA

and its metabolites on the deamination of the neurotransmitters dopamine and serotonin using HILIC-MS/MS. MDMA and MDA were identified as inhibitors of recombinant human MAO-A (Steuer et al., 2016). However, MAO inhibition is not always an effect of the abused drug itself. Users also intentionally consume MAO inhibitors in order to enhance the activity of substances such as *N,N*-dimethyltryptamine (DMT) that otherwise would be metabolically inactivated. Ayahuasca for example, a hallucinogenic beverage, is the combination of DMT and the  $\beta$ -carbolines MAO inhibitors harmine and harmaline (Araujo et al., 2015).

## 5. Conclusion

The presented study was the first to describe the MAO inhibition for a broad range of NPS of the alpha-methylated tryptamine type. The workup and analysis based on HILIC-HR-MS/MS were validated according to international guidelines. Due to its high sensitivity, only minimal amounts of recombinant MAO enzymes were needed, thus, reducing the risk of non-specific protein binding, as well as material costs. All tested AMT analogs inhibited MAO-A activity, whereas four compounds inhibited MAO-B as well. 7-Me-AMT was identified as potent and competitive inhibitor of MAO-A. MAO inhibition by AMT and its analogs are expected to be clinically relevant. Plasma levels of other MAO substrates, for example neurotransmitters or drugs, could increase, especially if these substances were selective MAO-A substrates. Further clinical studies are warranted to facilitate a more complete assessment.

## Conflict of interest

The authors declare that they have no conflict of interest.

## Acknowledgements

The authors like to thank Achim T. Caspar, Julia Dinger, Andreas G. Helfer, Sascha K. Manier, Julian A. Michely, Lilian H. J. Richter, and Armin A. Weber for their support and fruitful discussion.

## References

- Araujo, A.M., Carvalho, F., Bastos Mde, L., Guedes de Pinho, P., Carvalho, M., 2015. The hallucinogenic world of tryptamines: an updated review. *Arch. Toxicol.* 89 (8), 1151–1173.
- Backberg, M., Beck, O., Hulten, P., Rosengren-Holmberg, J., Helander, A., 2014. Intoxications of the new psychoactive substance 5-(2-aminopropyl)indole (5-IT): a case series from the Swedish STRIDA project. *Clin. Toxicol.* 52 (6), 618–624.
- Baranczewski, P., Stanczak, A., Sundberg, K., et al., 2006. Introduction to in vitro estimation of metabolic stability and drug interactions of new chemical entities in drug discovery and development. *Pharmacol. Rep.* 58 (4), 453–472.
- Barrett, J.S., Rohatagi, S., DeWitt, K.E., Morales, R.J., DiSanto, A.R., 1996. The effect of dosing regimen and food on the bioavailability of the extensively metabolized, highly variable drug Eldepryl((R)) (Selegiline hydrochloride). *Am. J. Ther.* 3 (4), 298–313.
- Baselt, R.C., 2008. *Disposition of Toxic Drugs and Chemicals in Man*, 8th ed. Biomedical Publications, Seal Beach, CA.
- Boland, D.M., Andollo, W., Hime, G.W., Hearn, W.L., 2005. Fatality due to acute alpha-methyltryptamine intoxication. *J. Anal. Toxicol.* 29 (5), 394–397.
- Boyer, E.W., Shannon, M., 2005. The serotonin syndrome. *N. Engl. J. Med.* 352 (11), 1112–1120.
- Brandt, S.D., Freeman, S., McGagh, P., Abdul-Halim, N., Alder, J.F., 2004. An analytical perspective on favoured synthetic routes to the psychoactive tryptamines. *J. Pharm. Biomed. Anal.* 36 (4), 675–691.
- Brandt, S.D., King, L.A., Evans-Brown, M., 2014. The new drug phenomenon. *Drug Test. Anal.* 6 (7–8), 587–597.
- Brush, D.E., Bird, S.B., Boyer, E.W., 2004. Monoamine oxidase inhibitor poisoning resulting from Internet misinformation on illicit substances. *J. Toxicol. Clin. Toxicol.* 42 (2), 191–195.
- Caspar, A.T., Helfer, A.G., Michely, J.A., et al., 2015. Studies on the metabolism and toxicological detection of the new psychoactive designer drug 2-(4-iodo-2,5-dimethoxyphenyl)-*N*-[(2-methoxyphenyl)methyl]ethanamine (25I-NBOMe) in human and rat urine using GC-MS, LC-MS(n), and LC-HR-MS/MS. *Anal. Bioanal. Chem.* 407 (22), 6697–6719.
- Cerletti, A., Taeschler, M., Weidmann, H., 1968. Pharmacologic studies on the structure-activity relationship of hydroxyindole alkylamines. *Adv. Pharmacol.* 6 (Pt. B), 233–246.
- Chaufert, N., Gauthier, A., Nicoll-Griffith, D.A., 1998. Effect of common organic solvents on in vitro cytochrome P450-mediated metabolic activities in human liver microsomes. *Drug Metab. Dispos.* 26 (1), 1–4.
- Cheng, Y., Prusoff, W.H., 1973. Relationship between the inhibition constant (K<sub>1</sub>) and the concentration of inhibitor which causes 50 per cent inhibition (I<sub>50</sub>) of an enzymatic reaction. *Biochem. Pharmacol.* 22 (23), 3099–3108.
- Dinger, J., Meyer, M.R., Maurer, H.H., 2016a. In vitro cytochrome P450 inhibition potential of methylenedioxy-derived designer drugs studied with a two-cocktail approach. *Arch. Toxicol.* 90 (2), 305–318.
- Dinger, J., Woods, C., Brandt, S.D., Meyer, M.R., Maurer, H.H., 2016b. Cytochrome P450 inhibition potential of new psychoactive substances of the tryptamine class. *Toxicol. Lett.* 241, 82–94.
- Dos Santos, P.C., Soldi, T.C., Torres, A.R., et al., 2013. Monoamine oxidase inhibition by monoterpene indole alkaloids and fractions obtained from *Psychotria suterella* and *Psychotria lacinata*. *J. Enzyme Inhib. Med. Chem.* 28 (3), 611–618.
- EMA, 2011. *Guideline on Bioanalytical Method Validation*. [http://www.ema.europa.eu/docs/en\\_GB/document\\_library/Scientific\\_guideline/2011/08/WC500109686.pdf](http://www.ema.europa.eu/docs/en_GB/document_library/Scientific_guideline/2011/08/WC500109686.pdf).
- EMCDDA, 2014. *Report on the Risk Assessment of 5-(2-aminopropyl)indole in the Framework of the Council Decision on New Psychoactive Substances*. [http://www.emcdda.europa.eu/attachements.cfm/att\\_222688\\_EN\\_TDAK13002ENN-1.pdf](http://www.emcdda.europa.eu/attachements.cfm/att_222688_EN_TDAK13002ENN-1.pdf).
- EMCDDA, 2015. *New Psychoactive Substances in Europe. An Update from the EU Early Warning System*. [http://www.emcdda.europa.eu/attachements.cfm/att\\_235958\\_EN\\_TD0415135ENN.pdf](http://www.emcdda.europa.eu/attachements.cfm/att_235958_EN_TD0415135ENN.pdf).
- Elliott, S., Evans, J., 2014. A 3-year review of new psychoactive substances in casework. *Forensic Sci. Int.* 243, 55–60.
- FDA, 2006. *Guidance for Industry: Drug Interaction Studies—Study Design, Data Analysis, and Implications for Dosing and Labeling*. <http://www.fda.gov/OHRMS/DOCKETS/98fr/06d-0344-gd10001.pdf>.
- Ferec, S., Leborgne, I., Bruneau, C., et al., 2015. Syndrome sérotoninergique sévère après ingestion d' $\alpha$ -méthyl-tryptamine (AMT). *Toxicol. Anal. Clin.* 27 (2), 25.
- Herraiz, T., Brandt, S.D., 2014. 5-(2-Aminopropyl)indole (5-IT): a psychoactive substance used for recreational purposes is an inhibitor of human monoamine oxidase (MAO). *Drug Test. Anal.* 6 (7–8), 607–613.
- Herraiz, T., Chaparro, C., 2006. Analysis of monoamine oxidase enzymatic activity by reversed-phase high performance liquid chromatography and inhibition by beta-carboline alkaloids occurring in foods and plants. *J. Chromatogr. A* 1120 (1–2), 237–243.
- Kantor, R.E., Dudlettes, S.D., Shulgin, A.T., 1980. 5-Methoxy- $\alpha$ -methyltryptamine ( $\alpha$ , *O*-dimethylserotonin), a hallucinogenic homolog of serotonin. *Biol. Psychiatry* 15 (2), 349–358.
- Lee, M.S., Zhu, M., 2011. *Mass Spectrometry in Drug Metabolism and Disposition*. Wiley, Hoboken, NJ.
- Meyer, M.R., Waggmann, L., Schneider-Daum, N., et al., 2015. P-glycoprotein interactions of novel psychoactive substances—stimulation of ATP consumption and transport across Caco-2 monolayers. *Biochem. Pharmacol.* 94 (3), 220–226.
- Meyer, M.R., 2016. New psychoactive substances: an overview on recent publications on their toxicodynamics and toxicokinetics. *Arch. Toxicol.* 90 (10), 2421–2444.
- Michely, J.A., Helfer, A.G., Brandt, S.D., Meyer, M.R., Maurer, H.H., 2015. Metabolism of the new psychoactive substances *N,N*-diallyltryptamine (DALT) and 5-methoxy-DALT and their detectability in urine by GC-MS, LC-MSn, and LC-HR-MS/MS. *Anal. Bioanal. Chem.* 407 (25), 7831–7842.
- Naoi, M., Nagatsu, T., 1988. Inhibition of type A monoamine oxidase by methylquinolines and structurally related compounds. *J. Neurochem.* 50 (4), 1105–1110.
- Nishimura, M., Naito, S., 2006. Tissue-specific mRNA expression profiles of human phase I metabolizing enzymes except for cytochrome P450 and phase II metabolizing enzymes. *Drug Metab. Pharmacokinet.* 21 (5), 357–374.
- Oliveira, C.D., Okai, G.G., da Costa, J.L., de Almeida, R.M., Oliveira-Silva, D., Yonamine, M., 2012. Determination of dimethyltryptamine and beta-carbolines (ayahuasca alkaloids) in plasma samples by LC-MS/MS. *Bioanalysis* 4 (14), 1731–1738.
- Parikh, S.N., Hanscom, S.R., Gagne, P.V., Crespi, C.L., Patten, C.J., 2002. A fluorescent-based, high-throughput assay for detecting inhibitors of human monoamine oxidase A and B. *Drug Metab. Rev.* 34, 164.
- Remane, D., Meyer, M.R., Wissenbach, D.K., Maurer, H.H., 2010. Ion suppression and enhancement effects of co-eluting analytes in multi-analyte approaches: systematic investigation using ultra-high-performance liquid chromatography/mass spectrometry with atmospheric-pressure chemical ionization or electrospray ionization. *Rapid Commun. Mass Spectrom.* 24 (21), 3103–3108.
- Richter, L.H., Kaminski, Y.R., Noor, F., Meyer, M.R., Maurer, H.H., 2016. Metabolic fate of desomorphine elucidated using rat urine, pooled human liver preparations, and human hepatocyte cultures as well as its detectability using standard urine screening approaches. *Anal. Bioanal. Chem.* 408 (23), 6283–6294.
- Ro, J.S., Lee, S.S., Lee, K.S., Lee, M.K., 2001. Inhibition of type A monoamine oxidase by coptisine in mouse brain. *Life Sci.* 70 (6), 639–645.
- Salva, M., Jansat, J.M., Martinez-Tobed, A., Palacios, J.M., 2003. Identification of the human liver enzymes involved in the metabolism of the antimigraine agent almotriptan. *Drug Metab. Dispos.* 31 (4), 404–411.

- Scott, K.R., Power, J.D., McDermott, S.D., et al., 2014. Identification of (2-aminopropyl)indole positional isomers in forensic samples. *Drug Test. Anal.* 6 (7–8), 598–606.
- Shulgin, A.T., Nichols, D.E., 1978. Characterization of three new psychotomimetics. In: Stillman, R.C., Willette, R.E. (Eds.), *The Psychopharmacology of Hallucinogens*. Pergamon, New York pp. 74–84.
- Shulgin, A.T., Shulgin, A., 1997. *Tihkal, The Continuation*. Transform Press, Berkeley, CA.
- Shulgin, A.T., 1979. Profiles of psychedelic drugs. *J. Psychedelic Drugs* 11 (4), 355.
- Steuer, A.E., Boxler, M.I., Stock, L., Kraemer, T., 2016. Inhibition potential of 3,4-methylenedioxyamphetamine (MDMA) and its metabolites on the in vitro monoamine oxidase (MAO)-catalyzed deamination of the neurotransmitters serotonin and dopamine. *Toxicol. Lett.* 243, 48–55.
- Tipton, K.F., Davey, G., Motherway, M., 2006. Monoamine oxidase assays. *Curr. Protoc. Toxicol.* 21 (Chapter 4, Unit 4).
- UNODC, 2016. *World Drug Report 2016*. . [https://www.unodc.org/doc/wdr2016/WORLD\\_DRUG\\_REPORT\\_2016\\_web.pdf](https://www.unodc.org/doc/wdr2016/WORLD_DRUG_REPORT_2016_web.pdf).
- Wagmann, L., Meyer, M.R., Maurer, H.H., 2016. What is the contribution of human FMO3 in the N-oxygenation of selected therapeutic drugs and drugs of abuse? *Toxicol. Lett.* 258, 55–70.
- Wang, C.C., Billett, E., Borchert, A., Kuhn, H., Ufer, C., 2013. Monoamine oxidases in development. *Cell. Mol. Life Sci.* 70 (4), 599–630.
- Weissbach, H., Smith, T.E., Daly, J.W., Witkop, B., Udenfriend, S., 1960. A rapid spectrophotometric assay of mono-amine oxidase based on the rate of disappearance of kynuramine. *J. Biol. Chem.* 235, 1160–1163.
- Young, E.H.P., 1958. The synthesis of 5-hydroxytryptamine (serotonin) and related tryptamines. *J. Chem. Soc.* 3 (October), 3493–3496.
- Zirkle, C.L., Kaiser, C., 1964. Monoamine oxidase inhibitors (nonhydrazines). In: Gordon, M. (Ed.), *Psychopharmacological Agents*, vol. 1. Academic Press, New York.

**3.3. INTERACTIONS OF PHENETHYLAMINE-DERIVED PSYCHOACTIVE  
SUBSTANCES OF THE 2C-SERIES WITH HUMAN MONOAMINE  
OXIDASES<sup>44</sup>**

**(DOI: 10.1002/dta.2494)**



## RESEARCH ARTICLE

# Interactions of phenethylamine-derived psychoactive substances of the 2C-series with human monoamine oxidases

Lea Wagmann<sup>1</sup> | Simon D. Brandt<sup>2</sup>  | Alexander Stratford<sup>3</sup> | Hans H. Maurer<sup>1</sup>  | Markus R. Meyer<sup>1</sup> 

<sup>1</sup>Department of Experimental and Clinical Toxicology, Institute of Experimental and Clinical Pharmacology and Toxicology, Center for Molecular Signaling (PZMS), Saarland University, Homburg, Germany

<sup>2</sup>School of Pharmacy and Biomolecular Sciences, Liverpool John Moores University, Liverpool, UK

<sup>3</sup>Synex Synthetics BV, Karveelweg 20, 6222 NH, Maastricht, The Netherlands

**Correspondence**

Markus R. Meyer, Department of Experimental and Clinical Toxicology, Institute of Experimental and Clinical Pharmacology and Toxicology, Center for Molecular Signaling (PZMS), Saarland University, Homburg, Germany.  
Email: markus.meyer@uks.eu

**Abstract**

Psychoactive substances of the 2C-series (2Cs) are phenethylamine-derived designer drugs that can induce psychostimulant and hallucinogenic effects. Chemically, the classic 2Cs contain two methoxy groups in positions 2 and 5 of the phenyl ring, whereas substances of the so-called FLY series contain rigidified methoxy groups integrated in a 2,3,6,7-tetrahydrobenzo[1,2-b:4,5-b']difuran core. One of the pharmacological features that has not been investigated in detail is the inhibition of monoamine oxidase (MAO). Inhibition of this enzyme can cause elevated monoamine levels that have been associated with adverse events such as agitation, nausea, vomiting, tachycardia, hypertension, or seizures. The aim of this study was to extend the knowledge surrounding the potential of MAO inhibition for 17 test drugs, which consisted of 12 2Cs (2C-B, 2C-D, 2C-E, 2C-H, 2C-I, 2C-N, 2C-P, 2C-T-2, 2C-T-7, 2C-T-21, bk-2C-B, and bk-2C-I) and five FLY analogs (2C-B-FLY, 2C-E-FLY, 2C-EF-FLY, 2C-I-FLY, and 2C-T-7-FLY). The extent of MAO inhibition was assessed using an established *in vitro* procedure based on heterologously expressed enzymes and analysis by hydrophilic interaction liquid chromatography–high resolution tandem mass spectrometry. Thirteen test drugs showed inhibition potential for MAO-A and 11 showed inhibition of MAO-B. In cases where MAO-A  $IC_{50}$  values were determined, values ranged from 10 to 125  $\mu$ M (7 drugs) and from 1.7 to 180  $\mu$ M for MAO-B (9 drugs). In the absence of detailed clinical information on most test drugs, it is concluded that a pharmacological contribution of MAO inhibition cannot be excluded and that further studies are warranted.

**KEYWORDS**

drugs of abuse, HILIC–HRMS/MS,  $IC_{50}$  value, monoamine oxidase inhibition, phenethylamines

## 1 | INTRODUCTION

Year after year, more and more so-called new psychoactive substances (NPS) enter the drugs of abuse (DOA) market with 803 different substances being reported to the United Nations Office on Drugs and Crime in the period 2009–2017.<sup>1,2</sup> Many NPS show psychoactive effects similar to drugs under international control and are often sold via the Internet.<sup>1</sup> Although NPS are initially not controlled and easily

available, they can pose a significant health risk and reports about adverse effects are frequently available.<sup>3–6</sup> One of the challenges when dealing with this phenomenon is the lack of knowledge concerning pharmacokinetics and toxicity since they are marketed without (pre)clinical safety studies.<sup>7</sup> The 2C-series drugs of abuse (2Cs) are phenethylamine derivatives that commonly exhibit a primary amine functionality separated from the phenyl ring by two carbon atoms. This differs from their amphetamine counterparts that show a

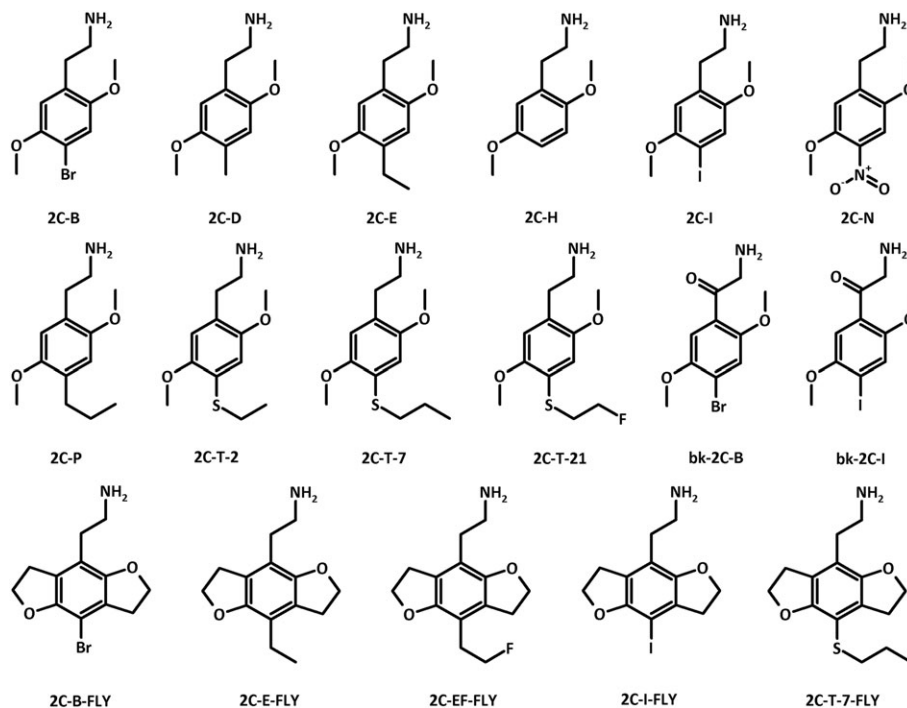


**FIGURE 1** Chemical structures of the investigated test drugs of abuse

methyl group at the alpha-position (3Cs) (Figure 1). Within a 2,5-dimethoxyphenethylamine nucleus, a lipophilic substituent is commonly present in position 4.<sup>8</sup> In the so-called FLY series, the methoxy groups are rigidified into a 2,3,6,7-tetrahydrobenzo[1,2-b:4,5-b']difuran core.<sup>9</sup> A number of 2Cs have shown psychostimulant and hallucinogenic properties and information gathered from casework suggests that intoxicated patients might exhibit either sympathomimetic toxidrome, serotonin (5-HT) toxicity, hallucinogenesis, or combinations thereof.<sup>10</sup> The available information on the pharmacology of 2Cs indicates that the interaction with 5-HT receptor subtypes is one of the pharmacological features linked to these substances.<sup>9,11-14</sup> Partial agonism at alpha-1 adrenergic receptors has also been described for 4-bromo-2,5-dimethoxyphenethylamine (2C-B).<sup>15</sup> In addition, the re-uptake inhibition of the monoamines norepinephrine and 5-HT into rat brain synaptosomes was described for 4-ethyl-2,5-dimethoxyphenethylamine (2C-E) and 4-iodo-2,5-dimethoxyphenethylamine (2C-I).<sup>16</sup> At the same time, monoamine oxidase (MAO) inhibition may also lead to elevated monoamine levels that have been associated with adverse events described in cases of 2C intoxications, which included agitation, nausea, vomiting, tachycardia, hypertension, or seizures.<sup>10,17-19</sup>

The aim of this study was to extend the knowledge surrounding the potential of MAO inhibition (and to determine their  $IC_{50}$  values) for 17 test drugs, which consisted of 12 2Cs and five FLY analogs (Figure 1). A previously published MAO inhibition assay based on heterologously expressed enzymes and hydrophilic interaction liquid chromatography-high resolution tandem mass spectrometry (HILIC-HRMS/MS) was applied for this purpose. MAO activity should be assessed using kynuramine (KYN) as the non-selective substrate, as the formation of the corresponding aldehyde is catalyzed by MAO-A and B and followed by non-enzymatic condensation to the product 4-hydroxyquinoline (4-OHC).

## 2 | EXPERIMENTAL

### 2.1 | Chemicals and enzymes

The baculovirus-infected insect cell microsomes (Supersomes) containing human complementary DNA-expressed MAO-A or MAO-B (5 mg protein/mL) and wild-type Supersomes without MAO activity as negative control (MAO control, 5 mg protein/mL) were obtained from Corning (Amsterdam, Netherlands). After delivery, enzyme preparations were thawed at 37°C, aliquoted, snap-frozen in liquid nitrogen, and stored at -80°C until use.

Amphetamine-d<sub>5</sub> was obtained from LGC Standards (Wesel, Germany); selegiline, KYN, 4-OHC, ammonium acetate, potassium dihydrogenphosphate, and dipotassium hydrogenphosphate from Sigma-Aldrich (Taufkirchen, Germany); formic acid (MS grade) from Fluka (Neu-Ulm, Germany); acetonitrile, methanol (both LC-MS grade), and all other chemicals from VWR (Darmstadt, Germany). 5-(2-Aminopropyl)indole (5-IT) was synthesized<sup>20</sup> and provided by the Department of Pharmacology and Therapeutics, Trinity Centre for Health Sciences, St James's Hospital (Dublin, Ireland). 2C-B tartrate was provided for research purposes before scheduled by Hessisches Landeskriminalamt (Wiesbaden, Germany); 2C-I hydrochloride by Landeskriminalamt Baden-Württemberg (Stuttgart, Germany); 4-ethylthio-2,5-dimethoxyphenethylamine (2C-T-2) hydrochloride by Bundeskriminalamt (Wiesbaden, Germany); and 4-nitro-2,5-dimethoxyphenethylamine (2C-H) and 2,5-dimethoxy-4-nitrophenethylamine (2C-N) by the Department of Forensic Toxicology, Institute of Forensic Research (Krakow, Poland). 5-IT, 2C-B, 2C-I, and 2C-T-2 were provided before they were scheduled. 4-Methyl-2,5-dimethoxyphenethylamine (2C-D) hydrochloride, 2C-E hydrochloride, and 4-propylthio-2,5-dimethoxyphenethylamine (2C-T-7) hydrochloride were purchased from Lipomed AG (Weil am Rhein, Germany);

4-propyl-2,5-dimethoxyphenethylamine (2C-P) hydrochloride from Dejachem (Schwendt, Germany); and 2-(8-bromo-2,3,6,7-tetrahydrobenzo[1,2-b:4,5-b']difuran-4-yl)ethan-1-amine (2C-B-FLY) hydrochloride from Cayman Chemicals (Ann Arbor, MI, USA). 2-Amino-1-(4-bromo-2,5-dimethoxyphenyl)ethan-1-one (bk-2C-B) hydrochloride and 2-amino-1-(4-iodo-2,5-dimethoxyphenyl)ethan-1-one (bk-2C-I) were available from previous work.<sup>21,22</sup> 4-(2-Fluoroethylthio)-2,5-dimethoxyphenethylamine (2C-T-21) hydrochloride was obtained in high purity from a research chemicals supplier. 2-(8-Ethyl-2,3,6,7-tetrahydrobenzo[1,2-b:4,5-b']difuran-4-yl)ethan-1-amine (2C-E-FLY) hydrochloride, 2-[8-(2-fluoroethyl)-2,3,6,7-tetrahydrobenzo[1,2-b:4,5-b']difuran-4-yl]ethan-1-amine (2C-EF-FLY) hydrochloride, 2-(8-iodo-2,3,6,7-tetrahydrobenzo[1,2-b:4,5-b']difuran-4-yl)ethan-1-amine (2C-I-FLY), and 2-[8-propylthio-2,3,6,7-tetrahydrobenzo[1,2-b:4,5-b']difuran-4-yl]ethan-1-amine (2C-T-7-FLY) hydrochloride were provided by Synex Synthetics BV (Maastricht, Netherlands).

Stock solutions were prepared in water (KYN: 6.25 mM, 4-OHC: 0.1 mM) or methanol (5-IT: 5 mM, selegiline: 5 mM, 2Cs and FLYs: 1 mg/mL, each). Stock solutions were aliquoted and stored at -20°C until use. To obtain the working solutions used for the incubations, stock solutions or enzyme preparations were serially diluted using 100 mM phosphate buffer. Prior to the determinations of IC<sub>50</sub> values, 2C stock solutions were gently evaporated under nitrogen and dissolved in water/methanol (9:1, v/v) to keep the organic solvent content in the final incubation mixtures constantly below 1%.<sup>23</sup>

## 2.2 | Initial MAO inhibition screening

Final incubation mixtures had a volume of 30 µL and consisted of 1 µg/mL MAO-A or MAO-B, the non-selective MAO substrate KYN at concentrations comparable to its K<sub>m</sub> value (MAO-A: 43 µM, MAO-B: 23 µM), and 10 µM of one of the potential inhibitors as described before.<sup>24</sup> Reactions were initiated by addition of the ice-cold enzyme dilution, incubated for 20 minutes at 37°C, and stopped with 30 µL of ice-cold acetonitrile containing 10 µM amphetamine-d<sub>5</sub> as internal standard (IS). The mixture was centrifuged for 2 minutes at 10 000 g, 50 µL of the supernatant were transferred to an autosampler vial, and injected onto the HILIC-HRMS/MS apparatus

for analysis. All incubations were performed in triplicate (*n* = 3). In addition to these samples, reference samples without inhibitor, positive control samples with known inhibitors (MAO-A: 5-IT, MAO-B: selegiline, 10 µM, each), blank samples without MAO activity, and interfering samples were also prepared in triplicate. Interfering samples were incubated reference samples without inhibitor and terminated with ice-cold acetonitrile containing the IS and the test drugs each at a concentration of 10 µM. A simplified scheme of the initial inhibition screening procedure is given in Figure 2. The 4-OHC amount, given as the peak area ratio of 4-OHC and the IS, in blank samples without MAO activity was subtracted from the 4-OHC amount detected in all other samples. The 4-OHC amount detected in reference samples without inhibitor was set at 100% MAO activity and compared to all other incubations. For statistical analysis, a one-way ANOVA followed by Dunnett's multiple comparison test (significance level, *P* < 0.001, 99.9% confidence intervals) by GraphPad Prism 5.00 (GraphPad Software, San Diego, CA, USA) was used.

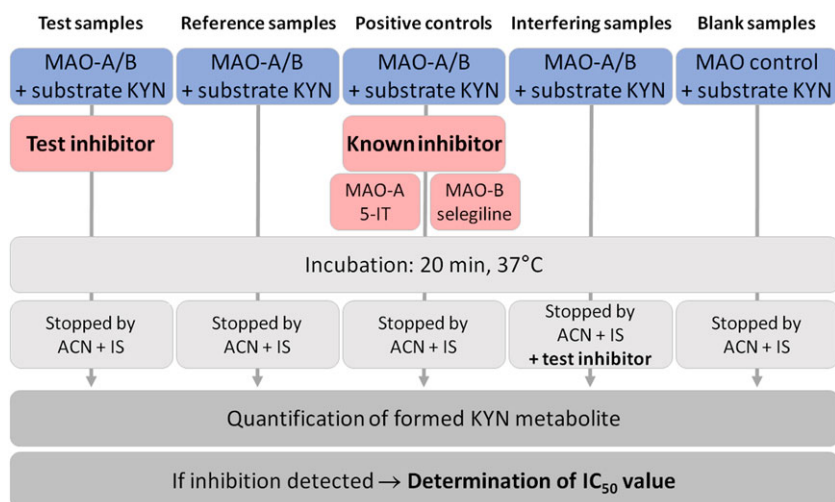
## 2.3 | Determination of IC<sub>50</sub> values

MAO-A or B were incubated with the following 10 inhibitor concentrations: 2, 5, 10, 20, 39, 78, 156, 313, 625, and 1250 µM, with the exception of 2C-H that was used in lower concentrations (0.04, 0.08, 0.15, 0.3, 0.6, 1, 2, 5, 10, and 20 µM). All incubations were performed in duplicate (*n* = 2). All other incubation conditions were the same as described in section 2.2. Reference and blank samples were also prepared as described in section 2.2. The IC<sub>50</sub> values were calculated by plotting the 4-OHC formation expressed as MAO activity (relative to reference samples) over the logarithm of the inhibitor concentration using GraphPad Prism 5.00.

## 2.4 | HILIC-HRMS/MS conditions

Apparatus and conditions were the same as already described.<sup>24</sup> A Thermo Fisher Scientific (TF, Dreieich, Germany) Dionex UltiMate 3000 Rapid Separation (RS) UHPLC system with a quaternary Ulti-Mate 3000 RS pump and an UltiMate 3000 RS autosampler were used and controlled by TF Chromeleon software version 6.80. The chromatographic system was coupled to a TF Q-Exactive Plus equipped

**FIGURE 2** Simplified scheme of the initial monoamine oxidases (MAO) inhibition screening procedure. (ACN: Acetonitrile, IS: Internal standard, 5-IT: 5-(2-aminopropyl) indole, KYN: Kynuramine) [Colour figure can be viewed at [wileyonlinelibrary.com](http://wileyonlinelibrary.com)]



with a heated electrospray ionization II source (HESI-II). The gradient elution was performed on a Macherey-Nagel (Düren, Germany) HILIC Nucleodur column (125 x 3 mm, 3  $\mu$ m) using aqueous ammonium acetate (25 mM, eluent A) and acetonitrile-containing 0.1% (v/v) formic acid (eluent B). The flow rate was set to 500  $\mu$ L/min and the gradient was programmed as follows: 0–0.5 minutes hold 80% B, curve 5; 0.5–3.8 minutes to 50% B, curve 5; 3.8–3.9 minutes to 40% B, curve 5; 3.9–5 minutes hold 40% B, curve 5; 5–5.1 minutes to 80% B, curve 5; and 5.1–6 minute hold 80% B, curve 5. Chromatography was performed at 60°C maintained by a Dionex UltiMate 3000 RS analytical column heater. The injection volume for all samples was 1  $\mu$ L. HESI-II conditions were modified according to Helfer et al. due to improved robustness: sheath gas, 60 arbitrary units (AU); auxiliary gas, 10 AU; spray voltage, 4.00 kV; heater temperature, 320°C; ion transfer capillary temperature, 320°C; and S-lens RF level, 60.0.<sup>25</sup> Mass calibration was performed prior to analysis according to the manufacturer's recommendations using external mass calibration. Quantification was performed using targeted single ion monitoring (t-SIM) and a subsequent data-dependent MS<sup>2</sup> (dd-MS<sup>2</sup>) mode with an inclusion list containing the exact masses of positively charged KYN (m/z 165.1022), 4-OHC (m/z 146.0600), and the IS (m/z 141.1434). The settings for the t-SIM mode were as follows: micro scan, 1; resolution, 35,000; AGC target, 5e<sup>4</sup>; maximum IT, 100 ms; and isolation window, 4 m/z. The settings for the dd-MS<sup>2</sup> mode were as follows: micro scan, 1; resolution, 35 000; AGC target, 2e<sup>5</sup>; maximum IT, 100 ms; isolation window, 4 m/z; and dynamic exclusion, 4 seconds. TF Xcalibur Qual Browser 2.2 software was used for data handling. The settings for automated peak integration were as follows: Peak detection algorithm, ICIS; area noise factor, 5; and peak noise factor, 300. GraphPad QuickCalcs was used for outlier detection (<http://graphpad.com/quickcalcs/grubbs1>), while GraphPad Prism 5.00 was used for statistical evaluation.

### 3 | RESULTS AND DISCUSSION

#### 3.1 | Initial MAO inhibition screening

Formation of 4-OHC was measured using HILIC-HRMS/MS and the complete analytical procedure was already previously successfully validated.<sup>24</sup> The results of the initial MAO inhibition screening of the 2Cs are summarized in Figure 3. Suitable incubation conditions were verified using positive control samples with known inhibitors (Figure 2). 5-IT reduced MAO-A activity by more than 90%, while selegiline almost completely inhibited MAO-B activity, which was in agreement with a previous study.<sup>24</sup> As only 4-OHC, KYN, and the IS were detected by the analytical method, it was mandatory to exclude analytical interferences, such as ion suppression or enhancement caused by potentially co-eluting test drugs. Therefore, MAO activity determined from the interfering samples was compared to that in the reference samples. The test compounds caused no analytical interferences.

For 13 test drugs, MAO-A inhibition was observed to some degree. Seven of these drugs (2C-B, 2C-I, 2C-T-7, 2C-B-FLY, 2C-E-FLY, 2C-I-FLY, and 2C-T-7-FLY) provided a statistically significant reduction of MAO-A activity (\*\*\*,  $P < 0.001$ ). However, none of these drugs was able to reduce the MAO-A activity by more than 50%,

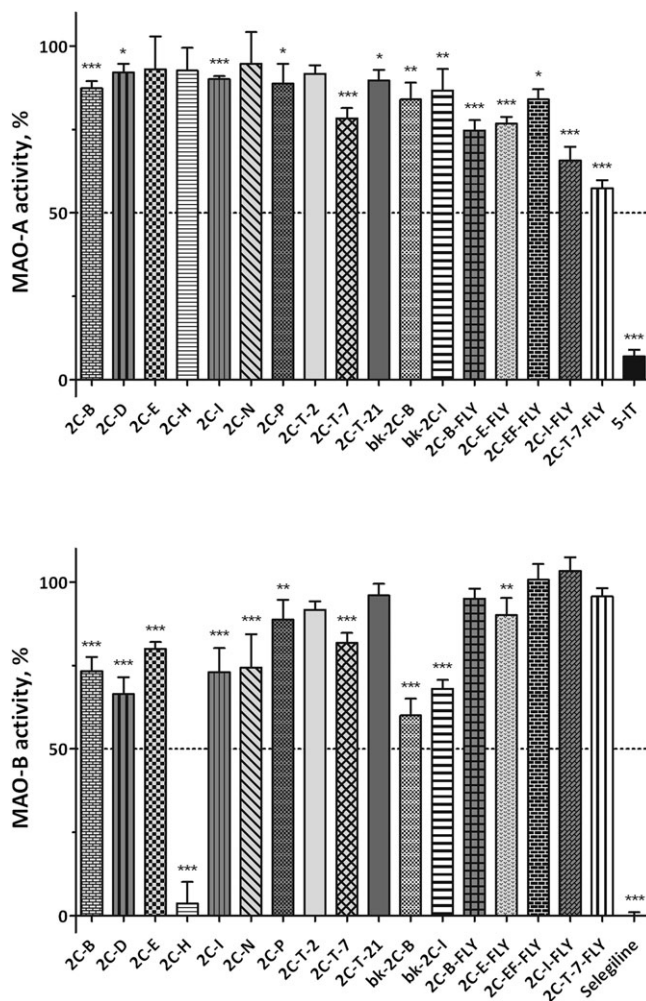


**FIGURE 3** Initial monoamine oxidases (MAO) inhibition screening results using 10  $\mu$ M of each test drug (MAO-A: Top, MAO-B: Bottom). Percentage of MAO activity represented the percentage of 4-hydroxyquinoline (4-OHC) formation in relation to reference incubations without test drug (100%). Values are expressed as mean and were tested for significance ( $n = 3$ , \*\*\*,  $P < 0.001$ , \*\*,  $P < 0.01$ , \*,  $P < 0.1$  for 4-OHC formation in incubations with the inhibitor versus 4-OHC formation in reference incubations)

which meant that IC<sub>50</sub> values could not be determined below 10  $\mu$ M, as this was the concentration used in the initial inhibition screening. Eleven test drugs resulted in some MAO-B inhibitions and nine substances (2C-B, 2C-D, 2C-E, 2C-H, 2C-I, 2C-N, 2C-T-7, bk-2C-B, and bk-2C-I) induced a reduction in MAO-B activity that was highly significant (\*\*\*,  $P < 0.001$ ). However, only 2C-H reduced MAO-B activity by more than 50%, which resulted in a corresponding IC<sub>50</sub> value below 10  $\mu$ M (Table 1).

#### 3.2 | Determination and comparison of IC<sub>50</sub> values

To save time and costs, IC<sub>50</sub> values for MAO-A and B inhibition were only determined in cases where the test drugs revealed a statistically highly significant (\*\*\*,  $P < 0.001$ ) inhibition during the initial screening phase. All incubations for the IC<sub>50</sub> value determinations were performed in duplicate, in contrast to triplicate incubations during the initial MAO inhibition screening, to reduce workload and number of samples in accordance with the previous study.<sup>24</sup> In total, seven IC<sub>50</sub>

**TABLE 1** IC<sub>50</sub> values (standard errors) determined for 2C-based drugs of abuse and known monoamine oxidase (MAO) inhibitors. Reference plasma concentrations in μM were calculated from the published data (in μg/L). (PM: Postmortem; n.d.: Not determined)

Test Compound	Reference Plasma Concentration,		IC <sub>50</sub> Value, μM	
	μg/L	μM	MAO-A	MAO-B
2C-B	*		125 (1.1)	58 (1.3)
2C-D	*		n.d.	24 (1.4)
2C-E	*		n.d.	124 (1.2)
2C-H	*		n.d.	1.7 (1.1)
2C-I	*		125 (1.2)	55 (1.3)
2C-N	*		n.d.	66 (1.1)
2C-P	18 <sup>17</sup>	0.1	n.d.	n.d.
2C-T-2	*		n.d.	n.d.
2C-T-7	57 and 100 (heart and femoral blood, PM) <sup>19</sup>	0.2 and 0.4	46 (1.1)	180 (1.3)
2C-T-21	*		n.d.	n.d.
bk-2C-B	*		n.d.	14 (1.1)
bk-2C-I	*		n.d.	15 (1.1)
2C-B-FLY	*		19 (1.1)	n.d.
2C-E-FLY	*		18 (1.1)	n.d.
2C-EF-FLY	*		n.d.	n.d.
2C-I-FLY	*		13 (1.1)	n.d.
2C-T-7-FLY	*		10 (1.1)	n.d.
<i>Known inhibitors</i>				
5-IT	15–590 <sup>34</sup> 700–5,100 (PM) <sup>35</sup>	0.1–3.4 4.0–29	0.20 <sup>24</sup>	
Selegiline	0.3–1.5 <sup>36</sup>	0.002–0.01		0.017 <sup>24</sup>

\*No plasma concentrations reported.

values of MAO-A inhibitors and nine IC<sub>50</sub> values of MAO-B inhibitors were determined and listed in Table 1. For MAO-A inhibition, IC<sub>50</sub> values were determined between 10 (2C-T-7-FLY) and 125 μM (2C-B and 2C-I). For MAO-B inhibition, IC<sub>50</sub> values were found to range between 1.7 (2C-H) and 180 μM (2C-T-7).

As far as the potential clinical relevance of MAO inhibition based on IC<sub>50</sub> values was concerned, plasma concentrations obtained from the case report literature (Table 1) might be worthy of consideration even though only limited information is available. Usually, case reports involving fatal or non-fatal intoxications are the only information source and difficult to interpret due to individual variation and/or poly-drug intoxication. In those reports, dosage, time of ingestion, and route of application remain often unclear. Postmortem concentrations are particularly problematic as they can be affected by postmortem redistribution.<sup>26,27</sup> Although the presence of some 2Cs on the DOA market is documented,<sup>28,29</sup> few case reports involving drug consumption appear to be available. For example, plasma concentrations from individual patients have only been reported for 2C-P and 2C-T-7.<sup>17,19</sup> In the first case, a 19-year-old male ingested approximately 25 mg 2C-P, which was sold as 2C-B, and was admitted to the emergency department with severe hallucinations, mydriasis, tachycardia, agitation, and confusion.<sup>17</sup> In the second case, a 20-year-old male died after he had been insufflating approximately 35 mg of 2C-T-7 and quantification was subsequently performed in postmortem samples.<sup>19</sup> The IC<sub>50</sub> values determined in this study were higher than the plasma concentrations reported for 2C-P and 2C-T-7. However, as they were measured in individual cases, their significance remains unclear.

Shulgin and Shulgin published their experiences with numerous phenethylamines, which included information about synthesis, dosage, and duration of effects.<sup>8</sup> These data are available for all 2Cs tested in this study with exception of the two bk-2Cs and FLY analogs. For some compounds, such as 2C-D or 2C-N, higher doses were described than those estimated in the previously mentioned case reports. Consequently, higher doses are expected to lead to higher plasma concentrations. However, it must be considered that concentrations detectable in certain tissues are often higher than in plasma due to lipophilicity or active transport processes. A brain-to-plasma concentration ratio of 13.9 was described for 2C-B in rats.<sup>30</sup> Elevated concentrations in the liver, the main metabolizing organ, are also more than likely to be encountered.<sup>31</sup> From this perspective, a contribution to the clinical effects of MAO inhibition can perhaps not be excluded.

2C-B, 2C-I, and 2C-T-7 were identified as moderately potent MAO-A inhibitors with IC<sub>50</sub> values of 46 (2C-T-7) and 125 μM (2C-B and 2C-I). However, the corresponding FLYs were shown to be more potent MAO-A inhibitors with IC<sub>50</sub> values of 10 (2C-T-7-FLY), 13 (2C-I-FLY), and 19 μM (2C-B-FLY). As the deamination of 5-HT is predominantly catalyzed by MAO-A,<sup>32</sup> its inhibition is likely to contribute to increasing 5-HT levels, which could be clinically relevant. For example, in the case of 2C-I intoxication, 5-HT toxicity has been observed as a clinical feature.<sup>18</sup> The MAO-A activity related to different 2C-B or 2C-B-FLY concentrations is depicted in Figure 4. 2C-E-FLY provided an IC<sub>50</sub> value of 18 μM comparable to the above-mentioned FLYs, whereas 2C-EF-FLY showed only weak MAO-A inhibition during the initial inhibition screening procedure.

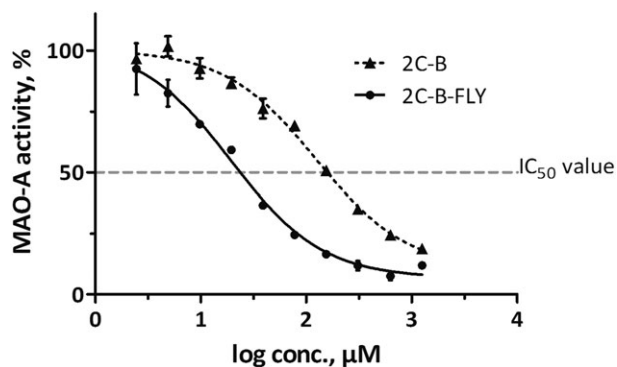


**FIGURE 4** MAO-A activity related to different test drug concentrations used for  $IC_{50}$  value determination. Data points represent the mean value of duplicate measurements ( $n = 2$ )

The FLYs were found to be inactive as MAO-B inhibitors with the exception of 2C-E-FLY, which resulted in weak MAO-B inhibition during the initial inhibition screening. In contrast, almost all classic 2Cs (apart from 2C-P and 2C-T-21), and the two bk-2Cs showed MAO-B inhibition potential. While 2C-B and 2C-I moderately inhibited MAO-B with  $IC_{50}$  values of 58 and 55  $\mu$ M, respectively, the inhibition by bk-2C-B and bk-2C-I was found to be more potent resulting in  $IC_{50}$  values of 14 and 15  $\mu$ M, respectively. These findings revealed that the replacement of bromine by iodine did not have a strong impact on MAO-A or B inhibition. The MAO-B activity related to different 2C-I or bk-2C-I concentrations is depicted in Figure 5.

2C-H was shown to be the most potent MAO-B inhibitor with an  $IC_{50}$  value of 1.7  $\mu$ M. However, Shulgin and Shulgin reported 2C-H to only result in weak psychoactive effects in animal assays.<sup>8</sup> In comparison, 2C-D and 2C-E revealed higher  $IC_{50}$  values of 24 and 124  $\mu$ M, respectively, whereas 2C-P only provided weak MAO-B inhibition potential during the initial inhibition screening. The MAO-B inhibitory potency of 2C-N ( $IC_{50}$  value 66  $\mu$ M) was comparable to that of 2C-B or 2C-I.

A previous study identified the MAO and cytochrome P450 isoforms involved in the deamination of 2C-B, 2C-D, 2C-E, 2C-I, 2C-T-2, and 2C-T-7.<sup>33</sup> MAO-A and B were shown to be the predominant enzymes involved in formation of their aldehydes and the studied 2Cs had a higher affinity to MAO-A than B.<sup>33</sup> As the present study identified these compounds with exception of 2C-T-2 as inhibitors of MAO-B, a competitive inhibition mechanism might be possible.

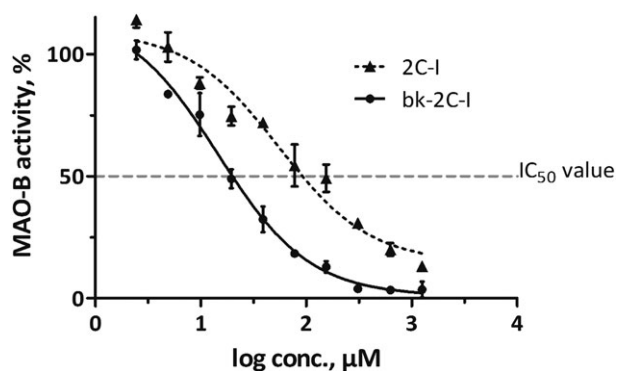


**FIGURE 5** MAO-B activity related to different test drug concentrations used for  $IC_{50}$  value determination. Data points represent the mean value of duplicate measurements ( $n = 2$ )

Nevertheless, as some 2Cs and 2C-B-FLY were described to have affinities to 5-HT receptor subtypes within the nM range,<sup>9,11-14</sup> MAO  $IC_{50}$  values within the  $\mu$ M range are expected to play only a minor role in the pharmacological effects after consumption of recreational doses. However, a contribution of MAO inhibition to the clinical effects observed in intoxication cases cannot be excluded.

## 4 | CONCLUSIONS

The presented study identified various 2C- and FLY-related test drugs as MAO inhibitors. A previously published inhibition assay was successfully applied for initial inhibition screening followed by  $IC_{50}$  value determinations. The FLYs were identified as MAO-A inhibitors, whereas the classic 2Cs with or without beta-keto functionality exhibited MAO-B inhibition potential. 2C-T-7-FLY and 2C-H were identified as the most potent MAO-A or B inhibitors with  $IC_{50}$  values of 10 and 1.7  $\mu$ M, respectively. Estimation of the clinical relevance of MAO inhibition based on  $IC_{50}$  values, however, was challenging given the lack of information regarding plasma concentrations of these test drugs. Nevertheless, the extent to which the clinical pharmacology of the evaluated test drugs involves MAO inhibition warrants further investigation.

## ACKNOWLEDGEMENTS

The authors would like to thank Thomas P. Bambauer and Armin A. Weber for their support. SDB gratefully extends gratitude to Stephen Chapman (Isomer Design, Toronto, Canada) for support.

## CONFLICT OF INTEREST

The authors declare that there are no conflicts of interest.

## ORCID

Simon D. Brandt  <http://orcid.org/0000-0001-8632-5372>

Hans H. Maurer  <http://orcid.org/0000-0003-4579-4660>

Markus R. Meyer  <http://orcid.org/0000-0003-4377-6784>

## REFERENCES

- World drug report 2018. UNODC; 2018. <https://www.unodc.org/wdr2018/index.html>. Accessed 10/07/2018.
- World drug report 2018. Booklet 3. Analysis of drug markets - opioids, cocaine, cannabis, synthetic drugs. UNODC; 2018. [https://www.unodc.org/wdr2018/prelaunch/WDR18\\_Booklet\\_3\\_DRUG\\_MARKETS.pdf](https://www.unodc.org/wdr2018/prelaunch/WDR18_Booklet_3_DRUG_MARKETS.pdf). Accessed 10/07/2018.
- Wagmann L, Maurer HH. Bioanalytical methods for new psychoactive substances. *Handb Exp Pharmacol*. 2018.
- Zamengo L, Frison G, Bettin C, Sciarone R. Understanding the risks associated with the use of new psychoactive substances (NPS): high variability of active ingredients concentration, mislabelled preparations, multiple psychoactive substances in single products. *Toxicol Lett*. 2014;229(1):220-228.
- Logan BK, Mohr ALA, Friscia M, et al. Reports of adverse events associated with use of novel psychoactive substances, 2013-2016: a review. *J Anal Toxicol*. 2017;41(7):573-610.
- Fentanils and synthetic cannabinoids: driving greater complexity into the drug situation. An update from the EU early warning system. EMCDDA; 2018. <http://www.emcdda.europa.eu/system/files/publications/8870/2018-2489-td0118414enn.pdf>. Accessed 10/07/2018.

7. Meyer MR. New psychoactive substances: an overview on recent publications on their toxicodynamics and toxicokinetics. *Arch Toxicol.* 2016;90(10):2421-2444.
8. Shulgin A, Shulgin A. *Pihkal, a chemical love story.* Berkley (CA): Transform Press; 1991.
9. Monte AP, Marona-Lewicka D, Parker MA, Wainscott DB, Nelson DL, Nichols DE. Dihydrobenzofuran analogues of hallucinogens. 3. Models of 4-substituted (2,5-dimethoxyphenyl) alkylamine derivatives with rigidified methoxy groups. *J Med Chem.* 1996;39(15):2953-2961.
10. Dean BV, Stellpflug SJ, Burnett AM, Engebretsen KM. 2C or not 2C: phenethylamine designer drug review. *J Med Toxicol.* 2013;9(2):172-178.
11. Johnson MP, Mathis CA, Shulgin AT, Hoffman AJ, Nichols DE. [125I]-2-(2,5-dimethoxy-4-iodophenyl) aminoethane ([125I]-2C-I) as a label for the 5-HT<sub>2</sub> receptor in rat frontal cortex. *Pharmacol Biochem Behav.* 1990;35(1):211-217.
12. Villalobos CA, Bull P, Saez P, Cassels BK, Huidobro-Toro JP. 4-Bromo-2,5-dimethoxyphenethylamine (2C-B) and structurally related phenylethylamines are potent 5-HT<sub>2A</sub> receptor antagonists in *Xenopus laevis* oocytes. *Br J Pharmacol.* 2004;141(7):1167-1174.
13. Fantegrossi WE, Harrington AW, Eckler JR, et al. Hallucinogen-like actions of 2,5-dimethoxy-4-(n)-propylthiophenethylamine (2C-T-7) in mice and rats. *Psychopharmacology (Berl).* 2005;181(3):496-503.
14. Power JD, Kavanagh P, O'Brien J, et al. Test purchase, identification and synthesis of 2-amino-1-(4-bromo-2, 5-dimethoxyphenyl)Ethan-1-one (bk-2C-B). *Drug Test Anal.* 2015;7(6):512-518.
15. Lobos M, Borges Y, Gonzalez E, Cassels BK. The action of the psychoactive drug 2C-B on isolated rat thoracic aorta. *Gen Pharmacol.* 1992;23(6):1139-1142.
16. Nagai F, Nonaka R, Satoh Hisashi Kamimura K. The effects of non-medically used psychoactive drugs on monoamine neurotransmission in rat brain. *Eur J Pharmacol.* 2007;559(2-3):132-137.
17. Stoller A, Dolder PC, Bodmer M, et al. Mistaking 2C-P for 2C-B: what a difference a letter makes. *J Anal Toxicol.* 2017;41(1):77-79.
18. Bosak A, LoVecchio F, Levine M. Recurrent seizures and serotonin syndrome following "2C-I" ingestion. *J Med Toxicol.* 2013;9(2):196-198.
19. Curtis B, Kemp P, Harty L, Choi C, Christensen D. Postmortem identification and quantitation of 2,5-dimethoxy-4-n-propylthiophenethylamine using GC-MSD and GC-NPD. *J Anal Toxicol.* 2003;27(7):493-498.
20. Scott KR, Power JD, McDermott SD, et al. Identification of (2-aminopropyl) indole positional isomers in forensic samples. *Drug Test Anal.* 2014;6(7-8):598-606.
21. Texter KB, Waymach R, Kavanagh PV, et al. Identification of pyrolysis products of the new psychoactive substance 2-amino-1-(4-bromo-2,5-dimethoxyphenyl) ethanone hydrochloride (bk-2C-B) and its iodo analogue bk-2C-I. *Drug Test Anal.* 2018;10(1):229-236.
22. Nichols DE. Chemistry and structure-activity relationships of psychedelics. *Curr Top Behav Neurosci.* 2018;36:1-43.
23. Chauret N, Gauthier A, Nicoll-Griffith DA. Effect of common organic solvents on in vitro cytochrome P450-mediated metabolic activities in human liver microsomes. *Drug Metab Dispos.* 1998;26(1):1-4.
24. Wagmann L, Brandt SD, Kavanagh PV, Maurer HH, Meyer MR. In vitro monoamine oxidase inhibition potential of alpha-methyltryptamine analog new psychoactive substances for assessing possible toxic risks. *Toxicol Lett.* 2017;272:84-93.
25. Helfer AG, Michely JA, Weber AA, Meyer MR, Maurer HH. Orbitrap technology for comprehensive metabolite-based liquid chromatographic-high resolution-tandem mass spectrometric urine drug screening - exemplified for cardiovascular drugs. *Anal Chim Acta.* 2015;891:221-233.
26. Shintani-Ishida K, Saka K, Nakamura M, Yoshida KI, Ikegaya H. Experimental study on the postmortem redistribution of the substituted phenethylamine, 25B-NBOMe. *J Forensic Sci.* 2018;63(2):588-591.
27. Staeheli SN, Gascho D, Ebert LC, Kraemer T, Steuer AE. Time-dependent postmortem redistribution of morphine and its metabolites in blood and alternative matrices-application of CT-guided biopsy sampling. *Int J Leg Med.* 2017;131(2):379-389.
28. King LA. New phenethylamines in Europe. *Drug Test Anal.* 2014;6(7-8):808-818.
29. Report on the risk assessment of 2C-I, 2C-T-2 and 2C-T-7 in the framework of the joint action on new synthetic drugs. EMCDDA; 2004. <http://www.emcdda.europa.eu/html.cfm/index33353EN.html>. Accessed 10/07/2018.
30. Rohanova M, Palenicek T, Balikova M. Disposition of 4-bromo-2,5-dimethoxyphenethylamine (2C-B) and its metabolite 4-bromo-2-hydroxy-5-methoxyphenethylamine in rats after subcutaneous administration. *Toxicol Lett.* 2008;178(1):29-36.
31. Li R, Niosi M, Johnson N, et al. A study on pharmacokinetics of bosentan with systems modeling, part 1: translating systemic plasma concentration to liver exposure in healthy subjects. *Drug Metab Dispos.* 2018;46(4):346-356.
32. Tipton KF. 90 years of monoamine oxidase: some progress and some confusion. *J Neural Transm (Vienna).* 2018.
33. Theobald DS, Maurer HH. Identification of monoamine oxidase and cytochrome P450 isoenzymes involved in the deamination of phenethylamine-derived designer drugs (2C-series). *Biochem Pharmacol.* 2007;73(2):287-297.
34. Backberg M, Beck O, Hulten P, Rosengren-Holmberg J, Helander A. Intoxications of the new psychoactive substance 5-(2-aminopropyl) indole (5-IT): a case series from the Swedish STRIDA project. *Clin Toxicol (Phila).* 2014;52(6):618-624.
35. Report on the risk assessment of 5-(2-aminopropyl) indole in the framework of the council decision on new psychoactive substances. EMCDDA; 2014. [http://www.emcdda.europa.eu/publications/risk-assessment/5-IT\\_en](http://www.emcdda.europa.eu/publications/risk-assessment/5-IT_en). Accessed 10/07/2018.
36. Barrett JS, Rohatagi S, DeWitt KE, Morales RJ, DiSanto AR. The effect of dosing regimen and food on the bioavailability of the extensively metabolized, highly variable drug eldepryl((R)) (selegiline hydrochloride). *Am J Ther.* 1996;3(4):298-313.

**How to cite this article:** Wagmann L, Brandt SD, Stratford A, Maurer HH, Meyer MR. Interactions of phenethylamine-derived psychoactive substances of the 2C-series with human monoamine oxidases. *Drug Test Anal.* 2018;1-7. <https://doi.org/10.1002/dta.2494>



**3.4. AN EASY AND FAST ADENOSINE 5'-DIPHOSPHATE QUANTIFICATION PROCEDURE BASED ON HYDROPHILIC INTERACTION LIQUID CHROMATOGRAPHY-HIGH RESOLUTION TANDEM MASS SPECTROMETRY FOR DETERMINATION OF THE IN VITRO ADENOSINE 5'-TRIPHOSPHATASE ACTIVITY OF THE HUMAN BREAST CANCER RESISTANCE PROTEIN ABCG2<sup>45</sup>**

**(DOI: 10.1016/j.chroma.2017.09.034)**





# An easy and fast adenosine 5'-diphosphate quantification procedure based on hydrophilic interaction liquid chromatography-high resolution tandem mass spectrometry for determination of the in vitro adenosine 5'-triphosphatase activity of the human breast cancer resistance protein ABCG2



Lea Wagmann, Hans H. Maurer, Markus R. Meyer\*

Department of Experimental and Clinical Toxicology, Institute of Experimental and Clinical Pharmacology and Toxicology, Saarland University, D-66421 Homburg, Saar, Germany

## ARTICLE INFO

### Article history:

Received 29 June 2017

Received in revised form 1 September 2017

Accepted 15 September 2017

Available online 18 September 2017

### Keywords:

ADP quantification

HILIC-HR-MS/MS

hBCRP ATPase

hBCRP substrate

hBCRP inhibitor

HIV protease inhibitors

## ABSTRACT

Interactions with the human breast cancer resistance protein (hBCRP) significantly influence the pharmacokinetic properties of a drug and can even lead to drug-drug interactions. As efflux pump from the ABC superfamily, hBCRP utilized energy gained by adenosine 5'-triphosphate (ATP) hydrolysis for the transmembrane movement of its substrates, while adenosine 5'-diphosphate (ADP) and inorganic phosphate were released. The ADP liberation can be used to detect interactions with the hBCRP ATPase. An ADP quantification method based on hydrophilic interaction liquid chromatography (HILIC) coupled to high resolution tandem mass spectrometry (HR-MS/MS) was developed and successfully validated in accordance to the criteria of the guideline on bioanalytical method validation by the European Medicines Agency. ATP and adenosine 5'-monophosphate were qualitatively included to prevent interferences. Furthermore, a setup consisting of six sample sets was evolved that allowed detection of hBCRP substrate or inhibitor properties of the test compound. The hBCRP substrate sulfasalazine and the hBCRP inhibitor orthovanadate were used as controls. To prove the applicability of the procedure, the effect of amprenavir, indinavir, nelfinavir, ritonavir, and saquinavir on the hBCRP ATPase activity was tested. Nelfinavir, ritonavir, and saquinavir were identified as hBCRP ATPase inhibitors and none of the five HIV protease inhibitors turned out to be an hBCRP substrate. These findings were in line with a previous publication.

© 2017 Elsevier B.V. All rights reserved.

## 1. Introduction

Membrane transporters such as the human breast cancer resistance protein (hBCRP, also known as ABCG2 or MXR) are gaining more and more attention not only during development, but also for better understanding of pharmacokinetics and drug interactions [1]. In 2010, the International Transporter Consortium (ITC) highlighted the importance of seven key membrane transporters in drug development because of their major influence on the pharmacokinetic, safety, and efficacy profiles of drugs [1]. In 2012, the European Medicines Agency (EMA) and Food and Drug Administration (FDA) included these transport proteins in their guidelines on the investigation of drug interactions [2,3].

One of the transporters highlighted by the ITC is hBCRP, an adenosine 5'-triphosphate (ATP)-dependent efflux pump from the ABC superfamily, closely related to P-glycoprotein [1]. hBCRP is not only highly expressed in several cancer cells, where it was initially discovered, but also in normal human tissues including the small intestine, liver, brain endothelium, and placenta. It plays therefore an important role in the absorption, elimination, and tissue distribution of drugs and other xenobiotics [4]. For the transmembrane movement of its substrates, hBCRP utilized energy gained by ATP hydrolysis, while adenosine 5'-diphosphate (ADP) and inorganic phosphate are released [5].

Besides more complicated models such as cell-based assays, intact organs, or transporter-deficient animals, membrane-based systems were often used to identify hBCRP substrates or inhibitors. Substrate-dependent ATP hydrolysis has been measured to evaluate the interactions with some ABC transporters usually by colorimetric analysis of the inorganic phosphate release [1]. Unfor-

\* Corresponding author.

E-mail address: [markus.meyer@uks.eu](mailto:markus.meyer@uks.eu) (M.R. Meyer).

tunately, this reaction can be disturbed by colored samples [6]. Another approach, the analysis of not consumed ATP, was measured by a bioluminescence reaction using luciferase [7]. This method is also known to be interference-prone, particularly due to substrate instability [8]. Furthermore, the linear range of the reaction is below the concentrations expected in the reaction mixtures and all incubated samples had to be diluted prior to analysis [7]. So far, only a few studies were published using LC–MS for quantification of ADP [9–12] but none of them were applicable for the direct measurement of ADP in *in vitro* hBCRP ATPase activity studies.

Therefore, the aim of the present study was the development of such a method using hydrophilic-interaction liquid chromatography (HILIC) coupled to high resolution tandem mass spectrometry (HR-MS/MS) for ADP quantification and detection of ATP and adenosine 5'-monophosphate (AMP). The workup and analysis should be validated in accordance to international guidelines for bioanalytical procedures [13]. Furthermore, the applicability of the developed setup should be demonstrated by determining the influence of five HIV protease inhibitors on the *in vitro* hBCRP ATPase activity, from which were already data available for comparison [14].

## 2. Materials and methods

### 2.1. Chemicals and enzymes

The baculovirus-infected insect cell microsomes (Supersomes) containing human complementary DNA-expressed BCRP (Arg482, 5 mg protein/mL) and wild-type Supersomes without hBCRP (control membrane, 5 mg protein/mL) used as negative control were obtained from Corning (Amsterdam, The Netherlands). After delivery, Supersomes were thawed at 37 °C, aliquoted, snap-frozen in liquid nitrogen, and stored at –80 °C until use.

AMP disodium salt, ADP sodium salt, ATP magnesium salt, guanosine 5'-diphosphate (GDP) sodium salt, uridine 5'-phosphate (UDP) sodium salt hydrate, sulfasalazine, sodium orthovanadate, amprenavir, indinavir, nelfinavir, ritonavir, saquinavir mesylate, ammonium acetate, MES hydrate, and Trizma base were obtained from Sigma-Aldrich (Taufkirchen, Germany), formic acid (MS grade) from Fluka (Neu-Ulm, Germany), acetonitrile, methanol (both LC–MS grade), and all other chemicals from VWR (Darmstadt, Germany).

Stock solutions were prepared in bidistilled water for sodium orthovanadate (10 mM), AMP, ADP, ATP, GDP, and UDP (20 mM, respectively) or in methanol for sulfasalazine (0.5 mg/mL), amprenavir, indinavir, nelfinavir, ritonavir, and saquinavir (1 mg/mL, respectively). Stock solutions were aliquoted and stored at –20 °C until use.

### 2.2. HILIC-HR-MS/MS apparatus

A Thermo Fisher Scientific (TF, Dreieich, Germany) Dionex Ultimate 3000 Rapid Separation (RS) LC system with a quaternary UltiMate 3000 RS pump and an UltiMate 3000 RS autosampler was used and controlled by the TF Chromeleon software version 6.80. It was coupled to a TF Q-Exact Plus equipped with a heated electrospray ionization II source (HESI-II). The gradient elution was performed on a Macherey-Nagel (Düren, Germany) HILIC Nucleodur column (125 × 3 mm, 3 µm) using aqueous ammonium acetate (200 mM, eluent A) and acetonitrile containing 0.1% (v/v) formic acid (eluent B). The flow rate was set to 700 µL/min and an isocratic elution with a duration of 6 min using 65% eluent B was performed at 40 °C column temperature, maintained by a Dionex UltiMate 3000 RS analytical column heater. The injection volume for all samples was 1 µL. HESI-II conditions were as already described

before [15]: sheath gas, 60 arbitrary units (AU); auxiliary gas, 10 AU; spray voltage, 4.00 kV; heater temperature, 320 °C; ion transfer capillary temperature, 320 °C; and S-lens RF level, 60.0. Mass calibration was done prior to analysis according to the manufacturer's recommendations using external mass calibration. For evaluating the chromatographic separation, a full scan experiment was used with the following scan parameters: polarity, negative; in-source collision-induced dissociation (CID), 0 eV; microscan, 1; resolution, 35,000; automatic gain control (AGC) target, 1e6; maximum injection time (IT), 120 ms; and acquisition range, 100–600 *m/z*. The final quantification was performed using a targeted single ion monitoring (t-SIM) and a subsequent data-dependent MS<sup>2</sup> (dd-MS<sup>2</sup>) mode with an inclusion list containing the exact masses of negatively charged AMP (*m/z* 346.0558), ADP (*m/z* 426.0221), and ATP (*m/z* 505.9885). The settings for the t-SIM mode were as follows: polarity, negative; in-source CID, 0 eV; microscan, 1; resolution, 35,000; AGC target, 5e4; maximum IT, 100 ms; and isolation window, 4 *m/z*. The cycle time for the t-SIM was 2.3 Hz. The settings for the dd-MS<sup>2</sup> mode were as follows: microscan, 1; resolution, 35,000; AGC target, 2e5; maximum IT, 100 ms; isolation window, 4 *m/z*; and dynamic exclusion, 4 s. Limited by the dynamic exclusion, the cycle time for the dd-MS<sup>2</sup> was set to 0.25 Hz. Quantification was performed using t-SIM, while dd-MS<sup>2</sup> was only used for identification. TF Xcalibur Qual Browser 2.2 software was used for data handling. The settings for automated peak integration were as follows: mass tolerance, 5 ppm; peak detection algorithm, ICIS; area noise factor, 5; and peak noise factor, 300. GraphPad Prism 5.00 (GraphPad Software, San Diego, USA) was used for statistical evaluation.

### 2.3. Method validation

The ADP quantification method was validated in accordance to the "Guideline on bioanalytical method validation" published by the EMA [13]. Briefly, the method was tested for selectivity (using ten blank samples containing 0.2 mg/mL control membrane with and without ATP, respectively), carry-over (using a blank sample without ATP following the high quality control, QC), lower limit of quantification (LLOQ, equal to the lowest calibration standard), within-run accuracy and precision (analyzed in a single run six samples per level at four concentration levels: LLOQ QC, low QC, medium QC, and high QC), between-run accuracy and precision (analyzed in three different runs on three different days six samples per level at four concentration levels: LLOQ QC, low QC, medium QC, and high QC), dilution integrity (analyzed five samples spiked above the calibration range and diluted by factor five with blank matrix), matrix effect (using six samples with matrix and six samples without matrix at two concentration levels: low QC and high QC), and stability of processed samples in the autosampler (analyzed immediately after preparation and again after 24 h in the autosampler, three samples per level at two concentration levels: low QC and high QC). The calibration consisted of six concentration points (given in Table 1) equally distributed over the entire range. The concentrations of LLOQ QC, low QC, medium QC, and high QC were as follows: 50, 125, 250, and 375 µM. Calibration standards and QCs were prepared from different stock solutions that were serially diluted with bidistilled water to obtain the final concentrations. Control membrane, diluted to a final concentration of 0.2 mg/mL with 50 mM Tris-MES buffer (pH 6.8), was used for sample preparation. Unless otherwise stated, 4 mM ATP was also present in the samples, which were not incubated. The final volume was 30 µL. Finally, the samples were diluted with the same volume of acetonitrile, centrifuged for 2 min at 10,000 × g, the supernatant was transferred to an autosampler vial, and analyzed by HILIC-HR-MS/MS. For quantification, the mean ADP area was used calculated after running each sample twice.

**Table 1**  
Calibrator concentrations for ADP quantification and mean coefficient of determination ( $R^2$ ,  $\pm$ coefficient of variation, CV).

	Calibrator						mean $R^2$ ( $\pm$ CV)
	1	2	3	4	5	6	
ADP conc., $\mu$ M	50	100	200	300	400	500	0.9849 ( $\pm$ 0.5)

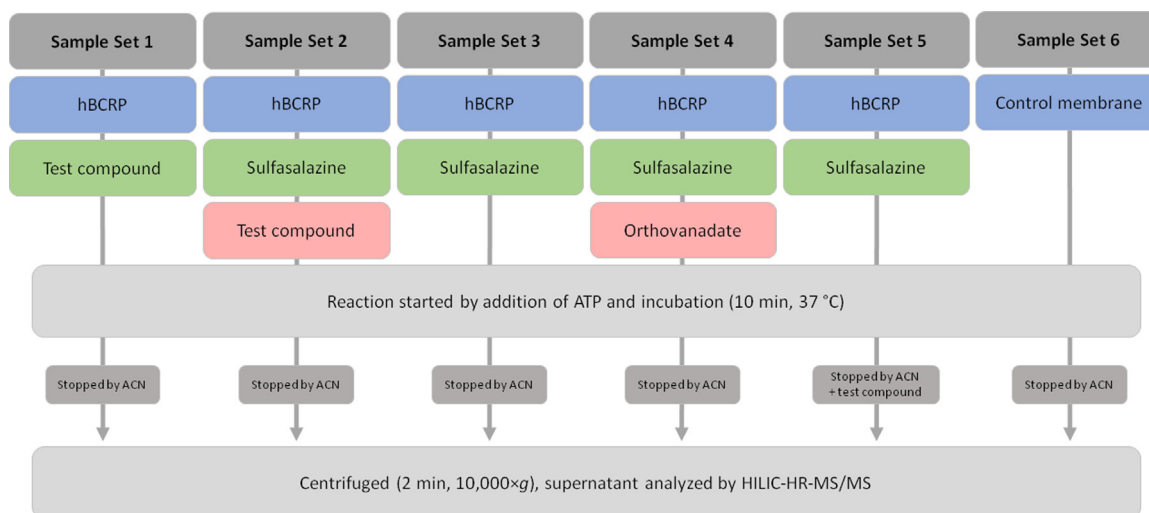


**Fig. 1.** Incubation scheme for detection of human breast cancer resistance protein (hBCRP) ATPase activity using six sample sets (ATP: adenosine 5'-triphosphate, ACN: acetonitrile).

After completed validation, all analytical runs consisted of two blank samples, the calibration standards in duplicate, three levels of QC samples (low, medium, and high) in duplicate, and the study samples. All samples were analyzed twice and the mean ADP area minus mean ADP area in blank samples was used for quantification. All calculations were done using GraphPad Prism 5.00 software.

#### 2.4. Incubation conditions for detection of hBCRP ATPase activity

Reaction conditions were adapted from Sarkadi et al. [16] with the following modifications. All reactions were carried out in 500  $\mu$ L reaction tubes. Sulfasalazine, a known hBCRP substrate [17], was diluted with bidistilled water and used at a final concentration of 10  $\mu$ M to ascertain appropriate incubation conditions. To check the protein dependency of the ATPase activity, the content of hBCRP membrane was varied between 0.1 and 0.8 mg/mL. To check the time dependency of the ATPase activity, incubation duration was varied between 5 and 60 min. To check the ATP dependency of the ATPase activity, ATP content was varied between 0.25 and 4 mM. All incubations were conducted in duplicate.

Final incubation mixtures contained 0.2 mg/mL hBCRP membrane and 4 mM ATP, as well as an hBCRP substrate or a mixture of an hBCRP substrate and an hBCRP inhibitor. ATP and substrate/inhibitor were diluted with bidistilled water and hBCRP membrane with Tris-MES buffer prior to incubations. The reaction was started by addition of ATP and stopped after 10 min of incubation at 37 °C by addition of 30  $\mu$ L of ice-cold acetonitrile. The mixture was centrifuged for 2 min at 10,000  $\times$  g, the supernatant transferred to an autosampler vial, and analyzed by HILIC-HR-MS/MS.

Incubations with sulfasalazine and 400  $\mu$ M sodium orthovanadate, an inhibitor of ABC efflux pumps such as hBCRP [17], were also conducted.

#### 2.5. Application for determination of interactions with HIV protease inhibitors

To test the influence of amprenavir, indinavir, nelfinavir, ritonavir, and saquinavir on hBCRP ATPase activity, six different sample sets consisting of three samples each were used as shown in Fig. 1. Incubation conditions were the same as described above. Sample set one contained one of the test compounds, set two one of the test compounds and sulfasalazine, sets three and five only sulfasalazine, set four sulfasalazine and orthovanadate, and set six none of these substances. All reactions were started by addition of ATP and sample sets one to five contained hBCRP membrane, while sample set six contained control membrane. Reactions of sample sets one to four and six were stopped by addition of pure acetonitrile, while acetonitrile used for set five contained the test compounds in addition. The HIV protease inhibitors were diluted with bidistilled water prior to incubations and had a final concentration of 50  $\mu$ M. The ADP formation in sets one to five minus ADP formation in set six was then compared to each other. For statistical analysis of data, a one-way ANOVA followed by Dunnett's multiple comparison test with set three as reference group (significance level,  $P < 0.05$ , 95% confidence intervals) was used.

### 3. Results and discussion

#### 3.1. Development of the method

For ABC transporters such as hBCRP, the transport process is associated with ATP binding and hydrolysis to provide energy for substrate translocation [4]. In the presence of ATP and a substrate, the hBCRP ATPase is activated and ATP consumed, while ADP and inorganic phosphate are released. If membrane fragments expressing the investigated transporter are used measurement of the substrate translocation is not possible, but the ATPase activity can be used as marker for interactions with hBCRP. Colorimetric anal-

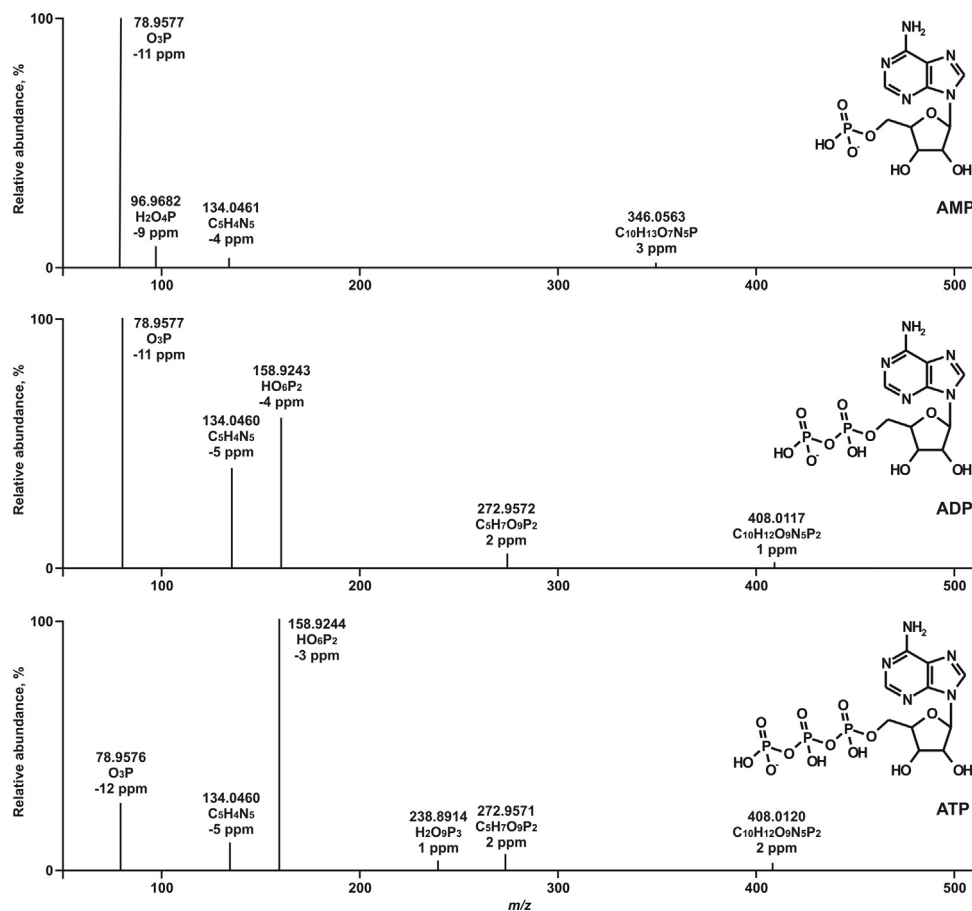


Fig. 2. Chemical structures and HR-MS/MS spectra of adenosine 5'-monophosphate (AMP), adenosine 5'-diphosphate (ADP), and adenosine 5'-triphosphate (ATP).

ysis of the inorganic phosphate may provide a simple and practical approach [1]. As ATP has to be present in excess to be not the limiting factor of the reaction, the quantification of remaining ATP after termination is another possibility [7]. However, as already mentioned, both methods have several limitations such as disturbance by colored samples and substrate instability [6,8]. Thus, the current method used hBCRP membranes and targeted the quantification of ADP that was not used as marker for determination of ATPase activity before. Furthermore, none of the described methods used the high flexibility and sensitivity of HR-MS/MS. HILIC was shown to provide sufficient retention and separation of small and polar compounds [18,19], but also of the highly polar adenosine nucleotides [12,20]. However, the method by Dowood et al. was developed to quantify 3'-phosphoadenosine-5'-phosphosulfate, while ADP and ATP were only qualitatively included to prevent interferences [20]. Li et al. quantified ADP, ATP, and four other cofactors in *E. coli* cells [12], but the linear range for ADP was below the concentrations that were expected in incubations with hBCRP membranes. Furthermore, the procedure was not validated in accordance to international guidelines and solid phase extraction followed by an analytical run time of 37 min would be far too time-consuming to screen a high number of samples for interactions with the hBCRP ATPase activity [12].

Chemical structures and HR-MS/MS spectra of AMP, ADP, and ATP are given in Fig. 2. Except for AMP, the mass of the precursor ion could not be detected in the HR-MS/MS spectrum but the substances could be differentiated thanks to specific fragments anyway. To ensure chromatographic separation, a mixture of the pure substance solutions was used containing AMP, ADP, and ATP in water:acetonitrile 1:1 (v/v) at a concentration of 2 mM, each.

After successful separation, two peaks appeared in the t-SIM chromatogram of ADP as shown in Fig. 3A and both were most likely identified to be ADP based on the dd-MS<sup>2</sup> spectrum. If ADP was injected alone, only one peak @ 3.5 min was detected. As the second ADP peak @ 4.0 min appeared only in solutions containing also ATP or exclusively ATP, this was most probably due to in-source fragmentation of ATP to ADP. However, as both peaks were chromatographically separated, it was possible to only integrate the prior one and use its area for ADP quantification in all samples.

To correct experimental variability, an internal standard structurally similar to ADP such as GDP should be added. Unfortunately, even changes in the ratio of the eluents and an increased run time did not lead to complete separation of the analytes and addition of GDP caused tailing of the ADP signal, probably as result of column saturation during co-elution. Therefore, UDP was tested as internal standard. Surprisingly, the UDP signal increased with an increasing amount of ADP in the sample for unclear reasons. As these two compounds with structural similarity to ADP did not provide any benefit, no internal standard was used instead and results were still sufficient but to correct fluctuations during analysis, all samples were run twice and the mean ADP area was used.

### 3.2. Method validation

The analytical procedure based on HILIC-HR-MS/MS in t-SIM mode with a subsequent dd-MS<sup>2</sup> mode allowed detection and identification of AMP, ADP, and ATP (Fig. 4). While AMP and ATP were only qualitatively included, the quantification of ADP was successfully validated in accordance to the criteria of an international guideline [13]. To avoid imprecision in ADP quantification by per-

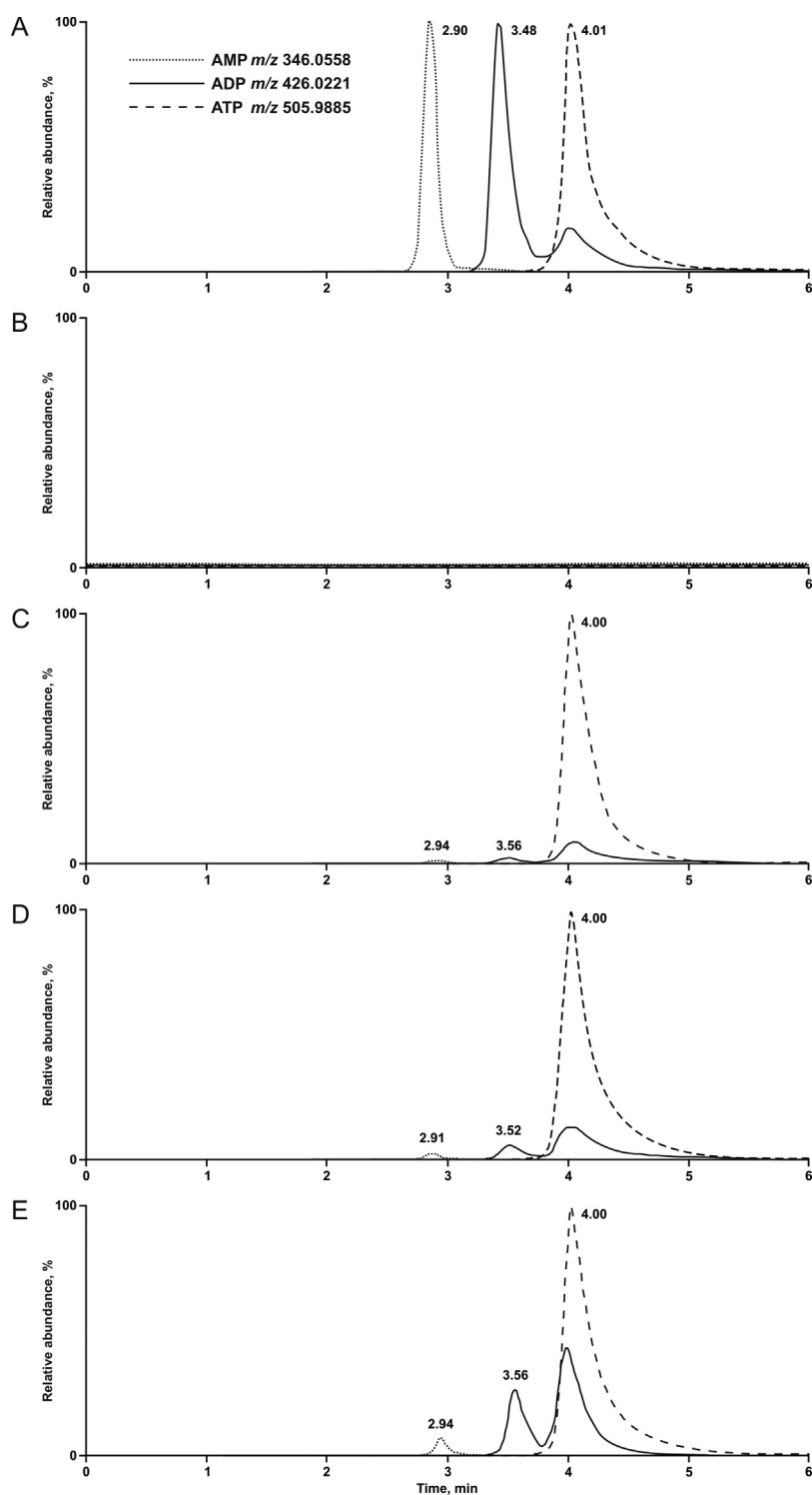


**Fig. 3.** Targeted-SIM chromatograms of adenosine 5'-monophosphate (AMP), adenosine 5'-diphosphate (ADP), and adenosine 5'-triphosphate (ATP) in a mixture of pure sample solutions (2 mM, each; A), a blank sample (B), a blank sample spiked with 4 mM ATP (C), a LLOQ QC (50  $\mu$ M ADP and 4 mM ATP; D), and a high QC (375  $\mu$ M ADP and 4 mM ATP; E).

manent MS<sup>2</sup> recording, dynamic exclusion of 4 s was used, what allowed repeated MS<sup>2</sup> recording of the same precursor ion only after 4 s had passed. Experimental variability during analysis was corrected by duplicate analysis of each sample and calculation of the mean ADP area. Mean coefficient of determination for calibration curves are given in Table 1. Curve was fitted using linear regression without weighting.

The LLOQ was set equal to the lowest calibration standard as the practically relevant concentration range were way above the real LOQ. The method was selective at LLOQ levels if no ATP was contained in the analyzed samples as shown in Fig. 3B. In presence of ATP, ADP was detectable (Fig. 3C). ADP was already contained in the ATP pure substance solution as well. Therefore, it could either be an impurity in the ATP pure substance, that is isolated from a microbial source by the manufacturer, or formed during ATP dissolving.

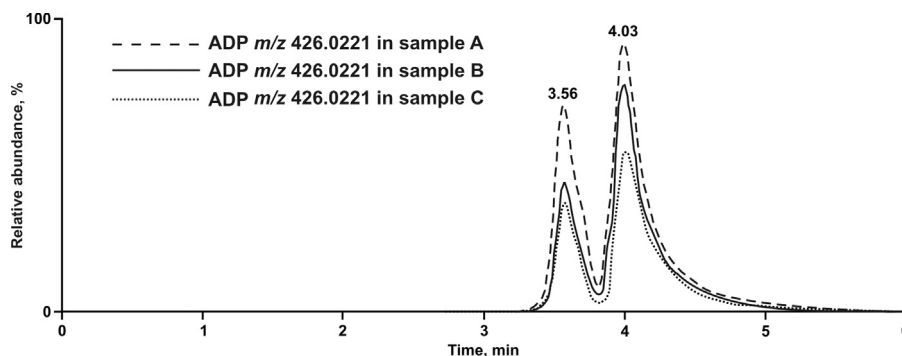


**Fig. 4.** Overlaid targeted-SIM chromatograms of adenosine 5'-diphosphate (ADP) in incubated samples containing adenosine 5'-triphosphate (ATP, 4 mM), hBCRP membrane (0.2 mg/mL), and an hBCRP substrate (10  $\mu$ M sulfasalazine; sample A), additionally an hBCRP inhibitor (400  $\mu$ M orthovanadate; sample B) or ATP (4 mM) and control membrane (0.2 mg/mL; sample C). The peaks @ 3.56 min were used for ADP quantification, while peaks @ 4.03 min were most likely caused by in-source fragmentation of ATP.

**Table 2**

Validation results for ADP quantification method: within-run and between-run accuracy and precision.

	LLOQ QC	low QC	med QC	high QC
Within-run accuracy, %	9	6	3	14
Between-run accuracy, %	7	8	10	10
Within-run precision, %	4	3	3	3
Between-run precision, %	4	7	4	3

ATP is known to be stable for months in aqueous solution stored at  $-15^{\circ}\text{C}$  and only for approximately one week at  $0^{\circ}\text{C}$  [21]. Therefore, it was necessary to use always a freshly thawed ATP aliquot and to prepare two blank samples with ATP and to subtract the ADP area detected in these samples from the ADP area detected in all following samples. No carry-over was observed. The LLOQ for ADP was defined as 50  $\mu\text{M}$ , which is the lowest ADP concentration that can be quantified reliably. The mean within-run and between-run accuracies ranged from 3 to 14% and were within 20% of the nominal values for the LLOQ QC and within 15% for the low, medium, and high QC samples. The mean within-run and between-run precisions ranged from 3 to 7%. Precisions were within 20% for the LLOQ QC and within 15% for the low, medium, and high QC samples. Accuracy and precision data are summarized in Table 2. To investigate the matrix effect, the ratio of the peak area in presence of matrix to the peak area in absence of matrix was used. Those matrix factors were 1.5 and 1.3 for low and high QC levels with coefficients of variation of 9% and 6%, respectively, and thus not greater than 15%. Chromatograms of a LLOQ QC and a high QC can be found in Fig. 3D and E, respectively. Fig. 3C–E show also, that AMP was detectable in samples containing ADP and/or ATP, even if they were not fortified with AMP. This was most likely due to an impurity in the pure substances of ADP and/or ATP. Processed samples provided stability in the autosampler for at least 24 h, corresponding to the maximum duration of the analytical runs, as mean concentrations of low and high QC levels were within  $\pm 15\%$  of the nominal values.

### 3.3. Detection of hBCRP ATPase activity

The hBCRP substrate sulfasalazine was used to demonstrate the detectability of ADP formed in *in vitro* incubations by hBCRP ATPase activity. Incubation time and enzyme concentration were varied and final conditions set in the linear range of ADP formation. Further incubations were therefore conducted with 0.2 mg/mL hBCRP membrane for 10 min. To avoid non-specific protein binding, the protein concentrations were chosen as low as analytically possible as recommended by Baranczewski et al. [22]. The dependency of the ATP concentration was also tested because ATP should not be the limiting factor of the reaction. The highest amount of ADP was

formed with 4 mM ATP. The final incubation conditions were similar to the hBCRP membrane manufacturer's recommendations, but the protein concentration could be chosen lower than suggested, thanks to the high sensitivity of HR-MS/MS reducing the risk of non-specific protein binding, as well as material costs.

As ADP was also detected in incubations without sulfasalazine, the basal ATPase activity was determined. Therefore, hBCRP membranes were incubated with the hBCRP inhibitor orthovanadate in presence of sulfasalazine. The amount of formed ADP was comparable to that formed in incubations with control membrane. Control membranes provided constant, reproducible ATP consumption that was independent of the presence of other substances, such as sulfasalazine or orthovanadate. Therefore, the amount of ADP formed in incubations with control membrane could be used as blank samples and subtracted from that formed in incubations with hBCRP membrane.

### 3.4. Effect of HIV protease inhibitors on hBCRP ATPase activity

The experimental setup with six different sample sets (Fig. 1) allowed identification of hBCRP ATPase activity activators as well as inhibitors. Therefore, set one was used as activator test set and set two as inhibitor test set. Set three provided the activator positive control, using a known hBCRP substrate leading to activation of the hBCRP ATPase activity, and set four the inhibitor positive control. The ADP formation in set three was set to 100% hBCRP ATPase activity and the ADP formation in set four was below 10%, suggesting almost complete hBCRP ATPase activity inhibition. Set five allowed exclusion of mass spectral ion suppression or enhancement effects on the ADP detection caused by the test compounds [23]. Those interfering samples were mandatory, as only the adenosine nucleotides were monitored by the analytical method and co-eluting analytes could lead to false positive or false negative results. For the five HIV protease inhibitors, no analytical interferences could be detected. A one-way ANOVA followed by Dunnett's multiple comparison test was used to decide whether ADP formation in sets one, two, four, or five was statistically significantly different from ADP formation in set three. Similar initial screening strategies were published by Dinger et al. and Wagmann et al. to identify CYP or MAO inhibitors, respectively [19,24]. ATPase activity in sample sets one and two are given in Fig. 5. Out of five test compounds, none could activate the hBCRP ATPase in a way comparable to sulfasalazine. Furthermore, amprenavir and indinavir were shown to have no hBCRP ATPase activity inhibition potential, while nelfinavir, ritonavir, and saquinavir were identified as hBCRP ATPase activity inhibitors. These results are in line with findings of Gupta et al. who studied hBCRP substrate or inhibitor properties of those five HIV protease inhibitors with human embryonic

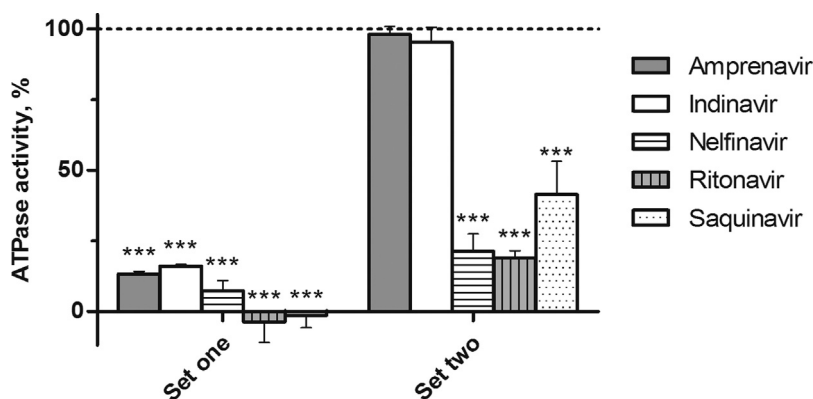


**Fig. 5.** Effect of 50  $\mu$ M amprenavir, indinavir, nelfinavir, ritonavir, or saquinavir on hBCRP ATPase activity. Sample set one contained human breast cancer resistance protein (hBCRP) membrane, adenosine 5'-triphosphate (ATP), and one of the HIV protease inhibitors, while sample set two contained sulfasalazine in addition. Percentage of activity represented the percentage of adenosine 5'-diphosphate (ADP) formation in relation to hBCRP ATPase activator positive control incubations only with sulfasalazine (100%). Values are expressed as mean and were tested for significance ( $n=3$ , \*\*\*,  $P<0.001$ , \*\*,  $P<0.01$ , \*  $P<0.1$  for ADP formation in incubations with test compound versus ADP formation in activator positive control incubations).

kidney cells stably expressing hBCRP by measuring intracellular mitoxantrone fluorescence using flow cytometry [14].

#### 4. Conclusion

The presented method was the first using ADP quantification by HILIC-HR-MS/MS to detect in vitro hBCRP ATPase activity. The workup and analysis were validated according to international guidelines. Due to its high sensitivity, only small amounts of hBCRP membrane were needed, thus, reducing the risk of non-specific protein binding as well as material costs. Sample preparation by protein precipitation was simple and fast and the analysis time of 6 min for one analytical run allowed high throughput. Nevertheless, some shortcomings should be considered. The used orbitrap-based mass spectrometer is rather expensive and therefore not available for everyone but the use of a triple quadrupole mass spectrometer might be an alternative. Furthermore, no internal standard could be recommended as all tested compounds turned out to be inappropriate but ADP quantification could still be successfully performed.

The approach was successfully applied to study interactions between hBCRP and five HIV protease inhibitors. Nelfinavir, ritonavir, and saquinavir were identified as hBCRP ATPase activity inhibitors, while amprenavir and indinavir did not inhibit hBCRP ATPase activity. None of the five HIV protease inhibitors turned out to be an hBCRP substrate. These findings were in line with published data [14]. Therefore, this approach should be able to predict possible interactions between the hBCRP ATPase and compounds of interest.

#### Acknowledgements

The authors like to thank Achim T. Caspar, Sascha K. Manier, Julian A. Michely, Lilian H. J. Richter, and Armin A. Weber for their support and fruitful discussion.

#### References

- [1] C. International Transporter, K.M. Giacomini, S.M. Huang, D.J. Tweedie, L.Z. Benet, K.L. Brouwer, X. Chu, A. Dahlin, R. Evers, V. Fischer, K.M. Hillgren, K.A. Hoffmaster, T. Ishikawa, D. Keppler, R.B. Kim, C.A. Lee, M. Niemi, J.W. Polli, Y. Sugiyama, P.W. Swaan, J.A. Ware, S.H. Wright, S.W. Yee, M.J. Zamek-Gliszczynski, L. Zhang, Membrane transporters in drug development, *Nat. Rev. Drug Discov.* 9 (2010) 215–236.
- [2] FDA, Guidance for Industry Drug Interaction Studies Journal, (2012) <https://www.fda.gov/downloads/drugs/guidancecomplianceregulatoryinformation/guidances/ucm292362.pdf>, 08/31/2017.
- [3] EMA, Guideline on the investigation of drug interactions, Journal, CPMP/EWP/560/95/Rev. 1 Corr. 2\*\* (2012) [http://www.ema.europa.eu/docs/en\\_GB/document\\_library/Scientific\\_guideline/2012/07/WC500129606.pdf](http://www.ema.europa.eu/docs/en_GB/document_library/Scientific_guideline/2012/07/WC500129606.pdf), 08/31/2017.
- [4] Z. Ni, Z. Bikadi, M.F. Rosenberg, Q. Mao, Structure and function of the human breast cancer resistance protein (BCRP/ABCG2), *Curr. Drug Metab.* 11 (2010) 603–617.
- [5] B. Sarkadi, L. Homolya, G. Szakacs, A. Varadi, Human multidrug resistance ABCB and ABCG transporters: participation in a chemoinnity defense system, *Physiol. Rev.* 86 (2006) 1179–1236.
- [6] G.C. Upreti, Colorimetric estimation of inorganic phosphate in colored and/or turbid biological samples: assay of phosphohydrolases, *Anal. Biochem.* 137 (1984) 485–492.
- [7] M.R. Meyer, T. Orschiadt, H.H. Maurer, Michaelis-Menten kinetic analysis of drugs of abuse to estimate their affinity to human P-glycoprotein, *Toxicol. Lett.* 217 (2013) 137–142.
- [8] Z.M. Kaskova, A.S. Tsarkova, I.V. Yampolsky, 1001 lights: luciferins, luciferases, their mechanisms of action and applications in chemical analysis, biology and medicine, *Chem. Soc. Rev.* 45 (2016) 6048–6077.
- [9] J. Klawitter, V. Schmitz, J. Klawitter, D. Leibfritz, U. Christians, Development and validation of an assay for the quantification of 11 nucleotides using LC/LC-electrospray ionization-MS, *Anal. Biochem.* 365 (2007) 230–239.
- [10] Y. Jiang, C. Sun, X. Ding, D. Yuan, K. Chen, B. Gao, Y. Chen, A. Sun, Simultaneous determination of adenine nucleotides, creatine phosphate and creatine in rat liver by high performance liquid chromatography-electrospray ionization-tandem mass spectrometry, *J. Pharm. Biomed. Anal.* 66 (2012) 258–263.
- [11] R.L. Cordell, S.J. Hill, C.A. Ortori, D.A. Barrett, Quantitative profiling of nucleotides and related phosphate-containing metabolites in cultured mammalian cells by liquid chromatography tandem electrospray mass spectrometry, *J. Chromatogr. B Analyt. Technol. Biomed. Life Sci.* 871 (2008) 115–124.
- [12] Z. Li, A. Yang, Y. Li, P. Liu, Z. Zhang, X. Zhang, W. Shui, Targeted cofactor quantification in metabolically engineered *E. coli* using solid phase extraction and hydrophilic interaction liquid chromatography-mass spectrometry, *J. Chromatogr. B Analyt. Technol. Biomed. Life Sci.* 1014 (2016) 107–115.
- [13] EMA, Guideline on bioanalytical method validation, Journal, EMEA/CHMP/EWP/192217/2009 Rev.1 Corr. 2 (2011) [http://www.ema.europa.eu/docs/en\\_GB/document\\_library/Scientific\\_guideline/2011/08/WC500109686.pdf](http://www.ema.europa.eu/docs/en_GB/document_library/Scientific_guideline/2011/08/WC500109686.pdf), 08/31/2017.
- [14] A. Gupta, Y. Zhang, J.D. Unadkat, Q. Mao, HIV protease inhibitors are inhibitors but not substrates of the human breast cancer resistance protein (BCRP/ABCG2), *J. Pharmacol. Exp. Ther.* 310 (2004) 334–341.
- [15] A.G. Helfer, J.A. Michely, A.A. Weber, M.R. Meyer, H.H. Maurer, Orbitrap technology for comprehensive metabolite-based liquid chromatographic-high resolution-tandem mass spectrometric urine drug screening – exemplified for cardiovascular drugs, *Anal. Chim. Acta* 891 (2015) 221–233.
- [16] B. Sarkadi, E.M. Price, R.C. Boucher, U.A. Germann, G.A. Scarborough, Expression of the human multidrug resistance cDNA in insect cells generates a high activity drug-stimulated membrane ATPase, *J. Biol. Chem.* 267 (1992) 4854–4858.
- [17] M. Jani, P. Szabo, E. Kis, E. Molnar, H. Glavinas, P. Krajcsi, Kinetic characterization of sulfasalazine transport by human ATP-binding cassette G2, *Biol. Pharm. Bull.* 32 (2009) 497–499.
- [18] A.E. Steuer, M.I. Boxler, L. Stock, T. Kraemer, Inhibition potential of 3 4-methylenedioxyamphetamine (MDMA) and its metabolites on the in vitro monoamine oxidase (MAO)-catalyzed deamination of the neurotransmitters serotonin and dopamine, *Toxicol. Lett.* 243 (2016) 48–55.
- [19] L. Wagmann, S.D. Brandt, P.V. Kavanagh, H.H. Maurer, M.R. Meyer, In vitro monoamine oxidase inhibition potential of alpha-methyltryptamine analog

- new psychoactive substances for assessing possible toxic risks, *Toxicol. Lett.* 272 (2017) 84–93.
- [20] R.K. Dowood, R. Adusumalli, E. Tykesson, E. Johnsen, E. Lundanes, K. Prydz, S.R. Wilson, Determination of 3'-phosphoadenosine-5'-phosphosulfate in cells and Golgi fractions using hydrophilic interaction liquid chromatography-mass spectrometry, *J. Chromatogr. A* 1470 (2016) 70–75.
- [21] R.M.C. Dawson, *Data for Biochemical Research*, 3rd ed., Oxford University Press, New York, NY, 1986.
- [22] P. Baranczewski, A. Stanczak, K. Sundberg, R. Svensson, A. Wallin, J. Jansson, P. Garberg, H. Postlind, Introduction to in vitro estimation of metabolic stability and drug interactions of new chemical entities in drug discovery and development, *Pharmacol. Rep.: PR* 58 (2006) 453–472.
- [23] D. Remane, M.R. Meyer, D.K. Wissenbach, H.H. Maurer, Ion suppression and enhancement effects of co-eluting analytes in multi-analyte approaches: systematic investigation using ultra-high-performance liquid chromatography/mass spectrometry with atmospheric-pressure chemical ionization or electrospray ionization, *Rapid Commun. Mass Spectrom.* 24 (2010) 3103–3108.
- [24] J. Dinger, M.R. Meyer, H.H. Maurer, In vitro cytochrome P450 inhibition potential of methylenedioxy-derived designer drugs studied with a two-cocktail approach, *Arch. Toxicol.* 90 (2016) 305–318.

**3.5. INHIBITION AND STIMULATION OF THE HUMAN BREAST CANCER RESISTANCE PROTEIN AS IN VITRO PREDICTOR OF DRUG-DRUG-INTERACTIONS OF DRUGS OF ABUSE<sup>46</sup>**

**(DOI: 10.1007/s00204-018-2276-y)**





# Inhibition and stimulation of the human breast cancer resistance protein as in vitro predictor of drug–drug interactions of drugs of abuse

Lea Wagmann<sup>1</sup> · Hans H. Maurer<sup>1</sup> · Markus R. Meyer<sup>1</sup>

Received: 21 May 2018 / Accepted: 30 July 2018 / Published online: 6 August 2018  
© Springer-Verlag GmbH Germany, part of Springer Nature 2018

## Abstract

Transporter-mediated drug–drug interactions (DDI) may induce adverse clinical events. As drugs of abuse (DOA) are marketed without preclinical safety studies, only very limited information about interplay with membrane transporters are available. Therefore, 13 DOA of various classes were tested for their in vitro affinity to the human breast cancer resistance protein (hBCRP), an important efflux transporter. As adenosine 5'-triphosphate (ATP) hydrolysis is crucial for hBCRP activity, adenosine 5'-diphosphate (ADP) formation was measured and used as in vitro marker for hBCRP ATPase activity. ADP quantification was performed by hydrophilic interaction liquid chromatography coupled to high-resolution tandem mass spectrometry and its amount in test compound incubations was compared to that in reference incubations using the hBCRP substrate sulfasalazine or the hBCRP inhibitor orthovanadate. If DOA caused stimulation or inhibition, further investigations such as Michaelis–Menten kinetic modeling or  $IC_{50}$  value determination were conducted. Among the tested DOA, seven compounds showed statistically significant hBCRP ATPase stimulation. The entactogen 3,4-BDB and the plant alkaloid mitragynine were identified as strongest stimulators. Their affinity to the hBCRP ATPase was lower than that of sulfasalazine but comparable to that of rosuvastatin, another hBCRP model substrate. Five DOA showed statistically significant hBCRP ATPase inhibition. Determination of  $IC_{50}$  values identified the synthetic cannabinoid receptor agonists JWH-200 and WIN 55,212-2 as the strongest inhibitors comparable to orthovanadate. The present study clearly demonstrated that tested DOA show in part high affinities to the hBCRP within the range of model substrates or inhibitors. Thus, there is a risk of hBCRP-mediated DDI, which needs to be considered in clinical settings.

**Keywords** Drugs of abuse · hBCRP · Drug–drug interactions · Mass spectrometry · HILIC

## Introduction

Efflux transporters such as the human breast cancer resistance protein (hBCRP) can significantly influence absorption, distribution, and excretion of drugs. In analogy to its close relative P-glycoprotein (P-gp), the hBCRP is primarily present in sites critical for drug disposition, such as epithelia of the intestine or liver and the endothelium of the blood–brain barrier (International Transporter C et al. 2010). Consequently, it decisively codetermines not only bioavailability

and thus therapeutic efficacy but also drug–drug interactions (DDI), which can increase toxicity and encourage adverse drug reactions.

Interactions occur if translocation of a drug is influenced by a second compound either via inhibition or induction of the transport protein (Muller and Fromm 2011). Significantly increased plasma concentrations of hBCRP substrates after oral co-administration of an hBCRP inhibitor are described (Kruijtzter et al. 2002; Wang et al. 2018) and clinically relevant effects are expected in case of narrow therapeutic windows and toxic properties. However, it is important to note that transporter-based interactions may result in concentration changes of the substrate in a particular tissue without affecting the plasma concentration of the substrate followed by local toxic effects (Endres et al. 2006). This demonstrates the complexity of identifying toxicity mechanisms in vivo and underlines the importance of

✉ Markus R. Meyer  
markus.meyer@uks.eu

<sup>1</sup> Department of Experimental and Clinical Toxicology, Institute of Experimental and Clinical Pharmacology and Toxicology, Center for Molecular Signaling (PZMS), Saarland University, 66421 Homburg, Germany

investigations of drug–transporter interactions in early stages of drug development.

As the impact of transporters on clinically relevant DDI is now generally recognized to be equal to that of drug metabolizing enzymes (Mao et al. 2018), new drug candidates are recommended to be routinely checked for interactions with the hBCRP and further transport proteins (International Transporter C et al. 2010). Guidelines on the investigation of drug interactions were, for example, published by the European Medicines Agency (EMA) or the Food and Drug Administration (EMA 2012; FDA 2017). Unfortunately, only scarce information is available for interplay between the hBCRP and drugs of abuse (DOA), which are marketed without preclinical safety studies. hBCRP inhibition was only described for the abused alkaloid ibogaine and the plant cannabinoids cannabiniol, cannabidiol, and delta 9-tetrahydrocannabinol (Holland et al. 2007; Tournier et al. 2010) demonstrating that DOA have to be considered. However, nothing is known about interactions with the so-called new psychoactive substances and profound toxicological risk assessment is ruled out. Sold as in part legal alternatives to drugs under international control with similar structures and effects, these compounds pose an outstanding risk as they proliferate at an unprecedented rate reaching almost 500 different substances in 2015 (UNODC 2017).

Therefore, the aim of the present study was to test 13 DOA with various chemical structures (Fig. 1) for their influence on the hBCRP. Primarily, *in vitro* experiments are recommended to identify potential factors influencing drug disposition, to elucidate potential DDI mechanisms,

and to yield kinetic parameters for use in further studies (FDA 2017). Cell-based assays or membrane-based systems are suitable to get a first indication of hBCRP involvement. The latter is usually based on measurement of substrate-dependent adenosine 5'-triphosphate (ATP) hydrolysis, as the presence of ATP is crucial for an hBCRP-mediated transport. Thanks to this linking between substrate transport and catalytic activity followed by release of adenosine 5'-diphosphate (ADP) and inorganic phosphate, the ATPase activity can be used as *in vitro* marker for hBCRP transport (Sarkadi et al. 2006). Because of its simplicity and reproducibility, the ATPase assay is one of the most widely used *in vitro* models for identification of compounds that interact with the hBCRP (Sarkadi et al. 2006).

Recently, a validated ADP quantification method based on hydrophilic interaction liquid chromatography coupled to high-resolution tandem mass spectrometry (HILIC–HRMS/MS) was published and successfully applied for determination of the *in vitro* hBCRP ATPase activity in the presence of five HIV protease inhibitors (Wagmann et al. 2017b). This method in combination with the presented initial hBCRP ATPase activity screening procedure (Fig. 2) was applied in the current study for DOA testing at three different concentrations (5, 50, and 500  $\mu\text{M}$ ) to get a first impression of their ATPase stimulation or inhibition potential. Further data were generated and used to calculate Michaelis–Menten kinetic parameters or  $\text{IC}_{50}$  values in case of stimulation or inhibition, respectively. We also investigated a model inhibitor (orthovanadate) and two model substrates (sulfasalazine and rosuvastatin) to clearly demonstrate suitable experimental

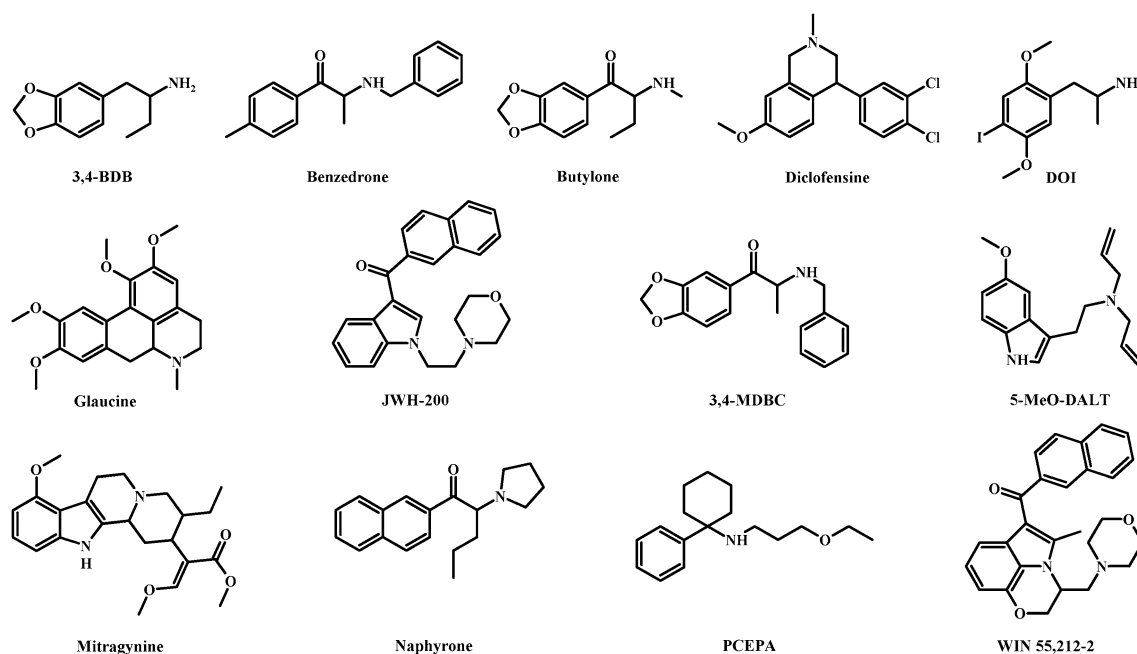
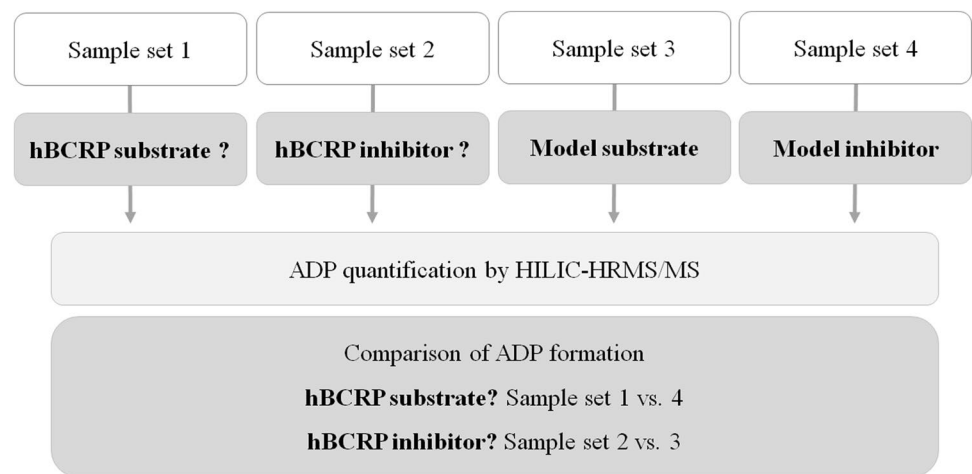


**Fig. 1** Chemical structures of the investigated drugs of abuse

**Fig. 2** Simplified scheme of the initial hBCRP ATPase activity screening procedure



conditions and to compare their data with those elucidated for the DOA.

## Materials and methods

### Chemicals and enzymes

Baculovirus-infected insect cell microsomes (Supersomes) containing complementary DNA-expressed hBCRP (Arg482, 5 mg protein/mL) and wild-type Supersomes without hBCRP (control membrane, 5 mg protein/mL) used as negative control were obtained from Corning (Amsterdam, The Netherlands). After delivery, Supersomes were thawed at 37 °C, aliquoted, snap-frozen in liquid nitrogen, and stored at –80 °C until use. ADP sodium salt, ATP magnesium salt, sulfasalazine, rosuvastatin, sodium orthovanadate, ammonium acetate, MES hydrate, and TRIS base were obtained from Sigma-Aldrich (Taufkirchen, Germany), formic acid (MS grade) from Fluka (Neu-Ulm, Germany), acetonitrile, methanol (both LC–MS grade), and all other chemicals from VWR (Darmstadt, Germany).

The test compounds *R,S*-1-(3,4-methylenedioxyphenyl)-2-butamine (3,4-BDB) and 1-[2-(4-morpholinyl)ethyl]-1*H*-indol-3-yl-(1-naphthyl)methanone (JWH-200) were supplied by Lipomed AG (Arlesheim, Switzerland), *R,S*-2-(benzylamino)-1-(4-methylphenyl)-1-propanone (benzedrone), diclofensine, *R,S*-1-(1,3-benzodioxol-5-yl)-2-(benzylamino)-1-propanone (3,4-MDBC), and *R,S*-1-(2-naphthyl)-2-(1-pyrrolidinyl)-1-pentanone (naphyrone) by LG Chemicals (Teddington, UK), *R,S*-1-(1,3-benzodioxol-5-yl)-2-(methylamino)-1-butanone (butylone) HCl by <http://www.EU-Legals.com> (currently not available) before it was scheduled, *R,S*-1-(4-iodo-2,5-dimethoxyphenyl)-2-propanamine (DOI) by Sigma-Aldrich, and [(3*R*)-5-methyl-3-(4-morpholinylmethyl)-2,3-dihydro[1,4]oxazino[2,3,4-*hi*]indol-6-yl](1-naphthyl)methanone

(WIN 55,212) mesylate by Chiron AS (Trondheim, Norway). (6*aS*)-1,2,9,10-Tetramethoxy-6-methyl-5,6,6*a*,7-tetrahydro-4*H*-dibenzo[de,g]quinoline (glaucine) HBr was obtained from Oskar Tropitzsch (Marktredwitz, Germany), *N*-(1-phenylcyclohexyl)-3-ethoxypropanamine (PCEPA) HCl was provided by the Hessisches Landeskriminalamt (Wiesbaden, Germany), and methyl(*E*)-2-[(2*S*,3*S*,12*bS*)-3-ethyl-8-methoxy-1,2,3,4,6,7,12,12*b*-octahydroindolo[2,3-*a*]quinolizin-2-yl]-3-methoxyprop-2-enoate (mitragynine) by the Department of Forensic Medicine, Johannes Gutenberg University (Mainz, Germany), where it was isolated from kratom leaves obtained from head&nature (Regensburg, Germany) (Philipp et al. 2009). *N*-allyl-*N*-[2-(5-methoxy-1*H*-indol-3-yl)ethyl]-2-propen-1-amine (5-MeO-DALT) was synthesized by use of established methods (Brandt et al. 2008) and provided by the School of Pharmacy and Biomolecular Sciences, John Moores University (Liverpool, UK).

### Preparation of stock solutions

Stock solutions were prepared in bidistilled water for sodium orthovanadate (10 mM), ADP, and ATP (20 mM, respectively) or in methanol for sulfasalazine (0.5 mg/mL), rosuvastatin, and the test compounds (1 mg/mL, respectively). Stock solutions were aliquoted and stored at –20 °C until use. To ensure that the organic solvent content in the final incubation mixtures was not higher than 3% (Chauret et al. 1998), methanolic stock solutions were gently evaporated under nitrogen at 70 °C and resolved in water/methanol (8:2, v/v) in a final concentration of 15 mM prior to incubations. To exclude negative impacts on the analytes' concentration, their peak areas in a concentration of 0.5 mM diluted with acetonitrile from the methanolic stock solutions or the resolved solutions were compared. The MS settings were the same as described before (Helfer et al. 2015). A peak area decrease of 30% was defined as tolerable and this criterion was fulfilled for all test compound solutions.

## HILIC–HRMS/MS apparatus

A Thermo Fisher Scientific (TF, Dreieich, Germany) Dionex UltiMate 3000 Rapid Separation (RS) UHPLC system with a quaternary UltiMate 3000 RS pump and an UltiMate 3000 RS autosampler was used and controlled by the TF Chromeleon software version 6.80. It was coupled to a TF Q-Exactive Plus mass spectrometer equipped with a heated electrospray ionization II source (HESI-II). Conditions and settings were the same as described previously (Wagmann et al. 2017b). Briefly, gradient elution was performed on a Macherey–Nagel (Düren, Germany) HILIC Nucleodur column (125 × 3 mm, 3 μm) using aqueous ammonium acetate (200 mM, eluent A) and acetonitrile containing 0.1% (v/v) formic acid (eluent B). The flow rate was set to 700 μL/min and an isocratic elution with a duration of 6 min using 65% eluent B was performed at 40 °C column temperature, maintained by a Dionex UltiMate 3000 RS analytical column heater. The injection volume for all samples was 1 μL. HESI-II conditions were: sheath gas, 60 arbitrary units (AU); auxiliary gas, 10 AU; spray voltage, 4.00 kV; heater temperature, 320 °C; ion transfer capillary temperature, 320 °C; and S-lens RF level, 60.0. Mass calibration was done prior to analysis according to the manufacturer's recommendations using external mass calibration. ADP quantification was performed using a targeted single ion monitoring (t-SIM) and a subsequent data-dependent MS<sup>2</sup> (dd-MS<sup>2</sup>) mode with an inclusion list containing the exact masses of negatively charged adenosine 5'-monophosphate (AMP, *m/z* 346.0558), ADP (*m/z* 426.0221), and ATP (*m/z* 505.9885). The settings for the t-SIM mode were as follows: microscan, 1; resolution, 35,000; AGC target, 5e4; maximum IT, 100 ms; and isolation window, 4 *m/z*. The settings for the dd-MS<sup>2</sup> mode were as follows: microscan, 1; resolution, 35,000; AGC target, 2e5; maximum IT, 100 ms; isolation window, 4 *m/z*; and dynamic exclusion, 4 s. The TF Xcalibur Qual Browser 2.2 software was used for data handling. The settings for automated peak integration were as follows: mass tolerance, 5 ppm; peak detection algorithm, ICIS; area noise factor, 5; and peak noise factor, 300. GraphPad QuickCalcs (GraphPad Software, San Diego, USA) was used for outlier detection (<http://graphpad.com/quickcalcs/grubbs1>), while the GraphPad Prism 5.00 software was used for statistical evaluation.

Before analysis of study samples, two blank samples, six levels of calibration standards in duplicate, and three levels of quality control (QC) samples in duplicate were measured. ADP concentrations of calibrators and QC samples are given in Table 1. Blank samples only contained control membranes

(0.2 mg/mL) and ATP (4 mM), while calibrators and QC samples contained the particular ADP amount as well. Prior to analysis, they were diluted with acetonitrile (1:1, v/v). These samples as well as the study samples were analyzed twice and the mean ADP area minus mean ADP area in blank samples or blank incubations was used for quantification (Wagmann et al. 2017b).

## Initial hBCRP ATPase activity screening

To check whether the test compounds had an influence on the hBCRP ATPase activity, four different sample sets consisting of three samples each were used. A simplified scheme of the hBCRP ATPase activity screening procedure is given in Fig. 2. Setup and incubation conditions were the same as previously described with minor modifications (Wagmann et al. 2017b). Briefly, sample set one contained hBCRP membrane, ATP, and one of the test compounds, while sample set two additionally contained sulfasalazine. Sample set three consisted of hBCRP membrane, ATP, and sulfasalazine, while sample set four contained orthovanadate in addition. All reactions were started by the addition of ATP and stopped after 10 min of incubation at 37 °C by addition of 30 μL of ice-cold acetonitrile. The mixture was centrifuged for 2 min at 10,000×*g*, the supernatant transferred to an autosampler vial, and analyzed by HILIC–HRMS/MS. Prior to incubations, hBCRP membrane was diluted with TRIS-MES buffer (pH 6.8), while ATP, sulfasalazine, orthovanadate, and the test compounds were diluted with bidistilled water. The final concentrations were 0.2 mg/mL hBCRP, 4 mM ATP, 10 μM sulfasalazine, and 400 μM orthovanadate. Three different concentration levels of the test compounds were used (5, 50, and 500 μM). Furthermore, a blank set consisting of three samples only containing ATP and control membranes (0.2 mg/mL) were incubated and measured. ADP in these blank incubations was subtracted from ADP in all other sample sets. In addition, an interference set consisting of three samples containing hBCRP membrane, ATP, and sulfasalazine were incubated and the reactions were stopped with acetonitrile containing one of the test compounds in a concentration of 500 μM instead of pure acetonitrile.

Finally, ADP was quantified and its formation in set three was always set to 100% and ADP formation in all the sample sets was compared to each other. To detect ATPase stimulation, set one was compared to set four, while set two was compared to set three to detect ATPase inhibition (Fig. 2). ADP formation in the interference set should be equal to that in set three. To decide whether detected ADP formation differences

**Table 1** ADP concentrations of calibrators and quality control (QC) samples

	Calibrator						QC sample		
	1	2	3	4	5	6	Low	Medium	High
ADP conc., μM	50	100	200	300	400	500	125	250	375

were statistically significant or not, a one-way ANOVA was performed followed by Dunnett's multiple comparison test ( $***P < 0.001$ ,  $**P < 0.01$ ,  $*P < 0.05$ ) using the GraphPad Prism 5.00 software. Further investigations of kinetic constants and/or  $IC_{50}$  values of the test compounds were only conducted if a significant difference of at least  $P < 0.01$  was detected for a minimum of one concentration level.

## Kinetic studies

The kinetic constants were derived from incubations with hBCRP membranes. Substrate concentrations were chosen to allow modeling of enzyme kinetics and were always between 0.005 and 500  $\mu\text{M}$ . ATP (4 mM) was additionally contained in the final incubation mixtures. Incubation time and hBCRP membrane concentration were chosen to be in the linear range of ADP formation and final conditions, as given in Table 2. Blank incubations only contained hBCRP membrane and ATP and the ADP amount found in these incubations was subtracted from ADP in the other incubations. All incubations were performed in triplicate. Kinetic constants were calculated by ADP quantification using a calibration curve (Table 1). Enzyme kinetic constants were estimated by nonlinear curve fitting using the GraphPad Prism 5.00 software. The Michaelis–Menten equation (Eq. 1) was used to calculate apparent  $K_m$  and  $V_{max}$  values, where  $v$  is the initial reaction velocity,  $S$  is the substrate concentration,  $V_{max}$  is the maximal reaction velocity, and  $K_m$  is the substrate concentration at half  $V_{max}$ :

$$v = \frac{V_{max} \times S}{K_m + S} \quad (1)$$

## Determination of $IC_{50}$ values

Inhibitors were incubated at ten different concentrations (5, 10, 20, 39, 78, 156, 313, 625, 1250, and 2500  $\mu\text{M}$ ), with exception of JWH-200 and WIN 55,212-2, which could not be incubated at 2500  $\mu\text{M}$  due to insufficient solubility. Sulfasalazine (10  $\mu\text{M}$ ), ATP (4 mM), and hBCRP membrane (0.2 mg/mL) were additionally contained in the final incubation mixtures. Control incubations without

inhibitor and blank incubations were also prepared. Blank incubations only contained control membranes and ATP. The ADP amount found in these incubations was subtracted from ADP in the other incubations. All incubation conditions were the same as described for the initial hBCRP ATPase activity screening. All incubations were conducted in duplicate. The  $IC_{50}$  values were calculated by plotting the metabolite formation (relative to the control incubations) over the logarithm of the inhibitor concentration using GraphPad Prism 5.00.

## Results

### Initial hBCRP ATPase activity screening

ADP was quantified and its formation in the different sample sets (Fig. 2) was compared. ADP formation in sample set three (set to 100% hBCRP ATPase activity) and the interference set were found to be not significantly different. Residual hBCRP ATPase activity in sample set four containing sulfasalazine and orthovanadate ranged always between 1 and 8%.

Results for detection of hBCRP ATPase stimulators are given in Table 3. In total, rosuvastatin and seven DOA demonstrated hBCRP ATPase stimulation potential. In comparison with these incubations, rosuvastatin showed statistically significant higher ADP formation in all tested concentrations. The DOA butylone, DOI, JWH-200, and mitragynine also activated the hBCRP ATPase in all tested concentration levels, while 3,4-BDB only showed an effect in the highest concentration, WIN 55,212-2 in the lowest concentration, and diclofenac at the lowest and the medium concentration. However, detected stimulation by rosuvastatin or DOA was lower than that detected in sample set three caused by 10  $\mu\text{M}$  sulfasalazine.

Results for detection of hBCRP ATPase inhibitors are given in Table 4. In total, five DOA provided an hBCRP ATPase inhibition potential. In comparison with incubations with sulfasalazine alone, all of these compounds showed statistically significant reduction of ADP formation at their highest concentration level. Only JWH-200 and WIN 55,212-2 also showed an effect at medium concentration.

### Kinetic studies

The enzyme kinetic curves of sulfasalazine and rosuvastatin are depicted in Fig. 3. Kinetic curves of 3,4-BDB and mitragynine are given in Fig. 4.  $K_m$  and  $V_{max}$  values are summarized in Table 5.

**Table 2** Incubation time and hBCRP membrane concentration for determination of kinetic constants

Test compound	Incubation time, min	hBCRP conc., mg/mL
3,4-BDB	30	0.4
Mitragynine	30	0.4
Sulfasalazine	10	0.2
Rosuvastatin	30	0.2

**Table 3** Initial hBCRP ATPase activity screening results for detection of hBCRP ATPase stimulation

Test compound	ADP formation, %		
	5 $\mu$ M	50 $\mu$ M	500 $\mu$ M
Rosuvastatin	30 (2)***	41 (3)***	34 (3)***
3,4-BDB	19 (13)	13 (8)	32 (3)***
Benzedrone	23 (3)*	16 (1)	15 (7)
Butylone	27 (2)**	29 (3)**	34 (2)***
Diclofensine	31 (4)***	26 (3)**	11 (2)
DOI	29 (7)**	30 (6)***	26 (2)**
Glaucine	13 (5)	16 (7)	16 (7)
JWH-200	16 (4)***	29 (1)***	17 (1)***
3,4-MDBC	20 (2)	21 (3)*	18 (4)
5-MeO-DALT	13 (5)	16 (7)	16 (7)
Mitragynine	27 (2)***	39 (1)***	25 (9)**
Naphyrone	7 (2)	32 (9)*	30 (1)
PCEPA	18 (2)	15 (3)	21 (1)*
WIN 55,212-2	12 (1)**	6 (1)	4 (5)

Percentage ADP formation (percentage error in brackets) represented ADP formation in incubations containing one of the test compounds in relation with incubations containing the hBCRP model substrate sulfasalazine (10  $\mu$ M). Significant differences in comparison with reference incubations containing sulfasalazine and the hBCRP model inhibitor orthovanadate (400  $\mu$ M) are marked by asterisks (\*\*\*  $P < 0.001$ , \*\*  $P < 0.01$ , \*  $P < 0.05$ )

**Table 4** Initial hBCRP ATPase activity screening results for detection of hBCRP ATPase inhibition

Test compound	ADP formation, %		
	5 $\mu$ M	50 $\mu$ M	500 $\mu$ M
Rosuvastatin	126 (21)	129 (11)	84 (1)
3,4-BDB	95 (8)	71 (13)	36 (16)***
Benzedrone	96 (3)	92 (9)	73 (3)*
Butylone	126 (3)*	107 (14)	74 (1)*
Diclofensine	93 (12)	97 (12)	20 (3)***
DOI	110 (4)	105 (4)	88 (7)
Glaucine	67 (9)	74 (21)	82 (3)
JWH-200	78 (10)	30 (16)***	22 (16)***
3,4-MDBC	103 (1)	106 (17)	112 (25)
5-MeO-DALT	81 (17)	86 (19)	84 (2)
Mitragynine	86 (6)	72 (11)	31 (2)***
Naphyrone	99 (9)	102 (7)	85 (5)
PCEPA	74 (8)	102 (1)	77 (10)
WIN 55,212-2	84 (4)	32 (3)***	25 (2)***

Percentage ADP formation (percentage error in brackets) represented ADP formation in incubations containing one of the test compounds and the hBCRP model substrate sulfasalazine (10  $\mu$ M) in relation with incubations containing only sulfasalazine and significant differences are marked by asterisks (\*\*\*  $P < 0.001$ , \*\*  $P < 0.01$ , \*  $P < 0.05$ )

## Determination of IC<sub>50</sub> values

IC<sub>50</sub> values of orthovanadate and the five DOA are given in Table 6. The determined IC<sub>50</sub> values were between 13 and 359  $\mu$ M. Amongst the DOA, the synthetic cannabinoid receptor agonists JWH-200 and WIN 55,212-2 provided the lowest IC<sub>50</sub> values, comparable to that of orthovanadate.

## Discussion

As already mentioned, hBCRP ATPase activity is a widely used in vitro model to get a first impression of interactions between test compounds and efflux transporters. As ATP hydrolysis is substrate-dependent, ATPase activity increases in the presence of transported substrates, while noncompetitive inhibitors reduce the ATPase activity of the investigated transport protein (Sarkadi et al. 2006). If ATP is hydrolyzed, inorganic phosphate and ADP are released. The latter can be quantified and used as in vitro marker for hBCRP ATPase activity (Wagmann et al. 2017b). Direct analysis of the product ADP, by use of HILIC–HRMS/MS, is less interference prone than colorimetric measurement of inorganic phosphate or bioluminescence-based analysis of residual ATP (Kaskova et al. 2016; Upreti 1984). However, drawbacks of the ATPase assay include inconsistency between ATPase activity and the transport rate of some substrates and inhibitors, a high incidence of false positives and negatives, and the requirement of high substrate concentrations (International Transporter C et al. 2010). Nevertheless, notable advantages are simplicity, reproducibility, and particularly cost-effectiveness, as hBCRP expressing membrane fragments can be used, which are cheaper than membrane vesicles or cell culture experiments.

To extend the knowledge surrounding interactions between DOA and the hBCRP, 13 DOA were tested for their influence on the hBCRP ATPase. These test compounds belonged to various DOA classes, for example, stimulants, entactogens, or synthetic cannabinoid receptor agonists and provided different chemical structures (Fig. 1). All of them were shown previously to be stimulators of the P-gp ATPase and/or P-gp inhibitors using polarized cell monolayers (Meyer et al. 2013, 2015). As a broad overlap between P-gp and hBCRP substrates was described (Hira and Terada 2018), these compounds were now investigated for their influence on the hBCRP ATPase.

The used initial hBCRP ATPase activity screening setup was already successfully applied for investigation of five HIV protease inhibitors. Amongst them, three were identified as hBCRP inhibitors (Wagmann et al. 2017b). However, none of them showed hBCRP ATPase stimulation, and therefore, the known stimulator rosuvastatin (Huang et al. 2006) was used as control. As only adenosine phosphates

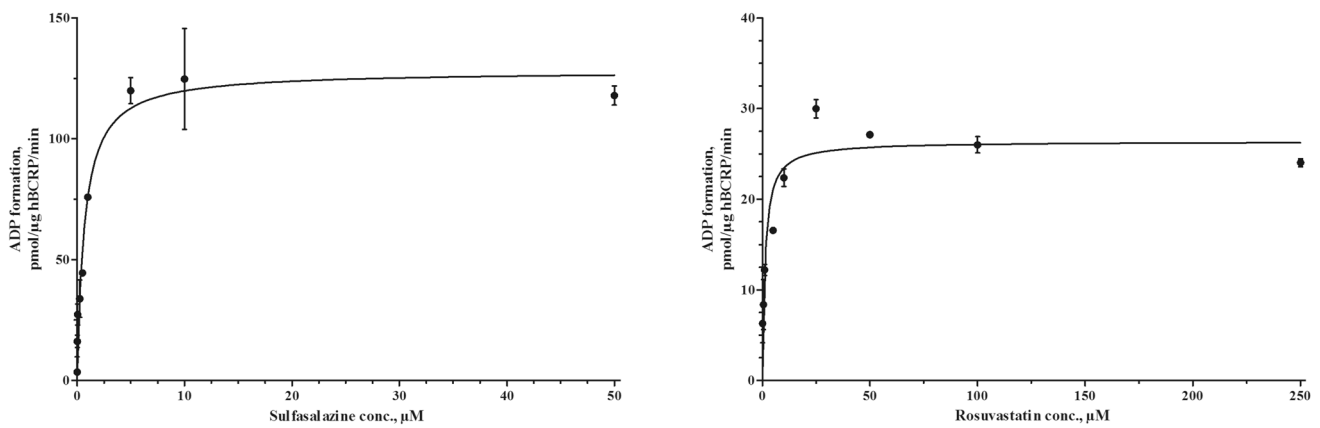


**Fig. 3** Kinetic curves modeled after incubation of different concentrations of sulfasalazine (left: 10 min incubation time, in presence of 4 mM ATP and 0.2 mg/mL hBCRP,  $n=3$ ) or rosuvastatin (right: 30 min incubation time, in presence of 4 mM ATP and 0.2 mg/mL hBCRP,  $n=3$ )

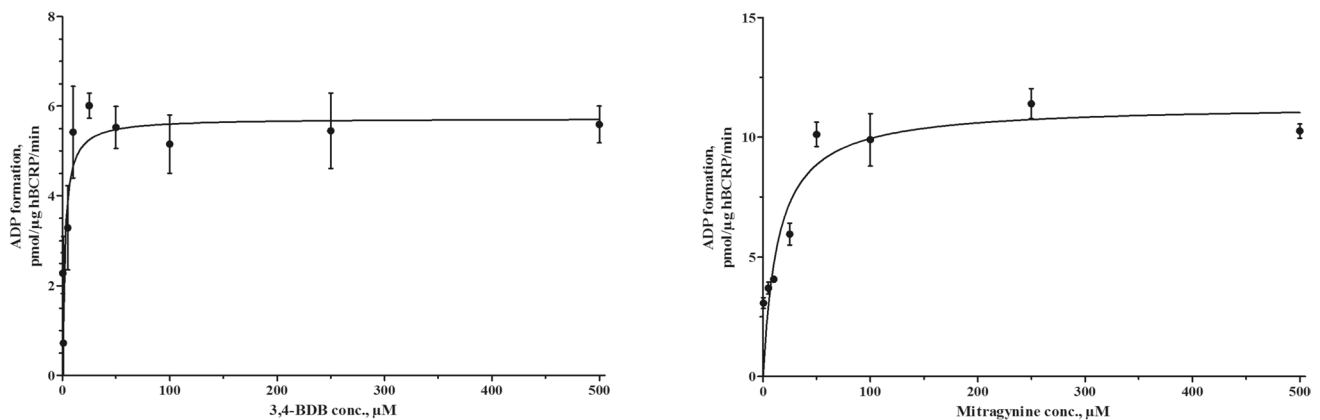


**Fig. 4** Kinetic curves modeled after incubation of different concentrations of 3,4-BDB (left: 30 min incubation time, in presence of 4 mM ATP and 0.4 mg/mL hBCRP,  $n=3$ ) or mitragynine (right: 30 min incubation time, in presence of 4 mM ATP and 0.4 mg/mL hBCRP,  $n=3$ )

**Table 5**  $K_m$  and  $V_{max}$  values of tested drugs of abuse, sulfasalazine, and rosuvastatin

Test compound	$K_m$ , $\mu\text{M}$	$V_{max}$ , pmol/ $\mu\text{g}$ hBCRP/min
3,4-BDB	$2.3 \pm 1$	$5.7 \pm 0.5$
Mitragynine	$14 \pm 3$	$11 \pm 0.6$
Sulfasalazine	$0.68 \pm 0.1$	$128 \pm 6$
Rosuvastatin	$1.2 \pm 0.3$	$26 \pm 1$

were analytically detected, it was mandatory to investigate the influence of all test compounds on the ADP MS signal. Both enhancement or suppression of the ADP signal could lead to errors in assessing a compound's hBCRP substrate or inhibitor properties. However, no analytical interferences were detected as the ADP formation in the interference set and sample set three were always similar. Furthermore, sample set four provided minimal residual hBCRP ATPase

activity what confirmed almost complete hBCRP inhibition by orthovanadate.

The EMA defined that in case of DDI, one compound acts as victim drug and the other one as perpetrator drug. The victim drug is the compound affected by DDI, while the perpetrator drug is that one, which affects the pharmacokinetic and/or pharmacodynamic properties of the victim drug (EMA 2012). In the context of hBCRP-mediated interactions, an hBCRP substrate would rather act as victim, while an inhibitor would be the perpetrator. Both possibilities should be considered and investigated, and therefore, hBCRP ATPase stimulators as well as inhibitors should be identified.

According to the previous study, ADP formation in sample set one was initially compared to that in sample set three to detect hBCRP ATPase stimulators (Wagmann et al. 2017b). ADP formation in rosuvastatin incubations was found to be significantly lower than ADP formation in sample set three, indicating that rosuvastatin was either

**Table 6** Test compounds, reference plasma concentrations, and IC<sub>50</sub> values (percentage error in brackets) for inhibition of hBCRP ATPase activity (*PM* post-mortem, *DUID* driving under the influence of drug)

Test compound	Common plasma concentration		IC <sub>50</sub> value, μM
	μg/L	μM	
Drugs of abuse			
3,4-BDB	106 (PM) (Carter et al. 2000)	0.6	143 (1)
Diclofensine	5 (Strojny and de Silva 1985)	0.02	113 (1)
JWH-200	0.1–28 <sup>a</sup> (DUID cases)	0.0003–0.07 <sup>a</sup>	19 (8)
	0.1–320 <sup>a</sup> (intoxications)	0.0003–0.8 <sup>a</sup>	
	0.1–199 <sup>a</sup> (PM) (Karinen et al. 2015)	0.0003–0.5 <sup>a</sup>	
	3–10 <sup>a</sup> (Toennes et al. 2017)	0.008–0.03 <sup>a</sup>	
Mitragynine	19–105 (Trakulsrichai et al. 2015)	0.05–0.3	359 (1)
WIN 55,212-2	0.1–28 <sup>a</sup> (DUID cases)	0.0002–0.07 <sup>a</sup>	15 (8)
	0.1–320 <sup>a</sup> (intoxications)	0.0002–0.8 <sup>a</sup>	
	0.1–199 <sup>a</sup> (PM) (Karinen et al. 2015)	0.0002–0.5 <sup>a</sup>	
	3–10 <sup>a</sup> (Toennes et al. 2017)	0.007–0.02 <sup>a</sup>	
Known inhibitor			
Orthovanadate	–	–	13 (8)

<sup>a</sup>No plasma concentrations published, listed concentrations were published for other synthetic cannabinoid receptor agonists

no or a weaker hBCRP substrate than sulfasalazine. However, sulfasalazine is widely accepted as ideal hBCRP probe substrate (Jani et al. 2009), causing intense hBCRP ATPase stimulation, which is probably stronger than that caused by other hBCRP substrates. Therefore, ADP formation in sample set one was compared to that in sample set four instead of sample set three to identify also weaker hBCRP ATPase stimulators than sulfasalazine. This alignment had no influence on the negative assessment of the hBCRP ATPase stimulation properties of the HIV protease inhibitors, which were previously reported to be no hBCRP substrates (Gupta et al. 2004). Even if rosuvastatin and seven DOA were shown to have hBCRP ATPase stimulation properties, maximum ATPase activity was always less than 50% of that caused by sulfasalazine. As already mentioned above, the hBCRP ATPase stimulation caused by sulfasalazine was expected to be more pronounced than that generated by other hBCRP substrates. The findings are in line with this assumption. As the highest hBCRP ATPase activities were mainly caused by the medium test compound concentration (50 μM), the occurrence of substrate-dependent inhibition at higher concentrations is likely.

To identify potential hBCRP ATPase inhibitors, ADP formation in sample set two was compared to that in sample set three. Five DOA were shown to have hBCRP ATPase inhibition potential. To reduce the hBCRP ATPase activity rather high concentrations of 3,4-BDB, diclofensine, or mitragynine were needed, compared to lower concentrations of JWH-200 or WIN 55,212-2. It is notable that all of these inhibitory substances also showed stimulating properties in the initial hBCRP ATPase activity screening, what could indicate a partial competitive inhibition mechanism.

However, in case of rosuvastatin, no inhibitory properties were detected in co-incubations with sulfasalazine.

The initial hBCRP ATPase activity screening demonstrated that only selected DOA had an influence on the hBCRP ATPase activity. As only these substances were further investigated by kinetic studies or IC<sub>50</sub> value determination, time and costs could be saved. Such prescreening procedures were already successfully applied to detect interactions with other enzymes (Dinger et al. 2016; Wagmann et al. 2017a).

The Michaelis–Menten kinetics of sulfasalazine and rosuvastatin (Fig. 3) were modeled as controls to demonstrate that the chosen incubation conditions were suitable. Determined  $K_m$  values were similar to published  $K_m$  values for sulfasalazine (0.70 μM) (Jani et al. 2009) or rosuvastatin (10.8 μM) (Huang et al. 2006), respectively. Not only the  $K_m$  value of sulfasalazine was lower than that of rosuvastatin but also its  $V_{max}$  value was higher. Both parameters indicated that sulfasalazine is a stronger hBCRP substrate than rosuvastatin, as already assumed after the initial hBCRP ATPase activity screening. Concerning DOA, 3,4-BDB provided a  $K_m$  value comparable to that of rosuvastatin, while the  $K_m$  value of mitragynine was higher. Determined  $V_{max}$  values of the test compounds were lower than  $V_{max}$  values of the model substrates indicating a slower transport rate of the DOA. Although butylone, diclofensine, DOI, JWH-200, and WIN 55,212-2 showed initial activity in the screening studies, enzyme kinetics could finally not be modeled due to insufficient activities.

For presumed hBCRP ATPase inhibitors, the inhibitor concentration at which the enzyme activity is reduced by 50% should be determined. This concentration is expressed as IC<sub>50</sub> value. To demonstrate that chosen incubation

conditions were suitable, the  $IC_{50}$  value of the model inhibitor orthovanadate was determined and comparable to that described in the literature (20  $\mu$ M) (Ishikawa et al. 2003). In addition,  $IC_{50}$  values of five DOA were determined. To predict a potential clinical relevance of the hBCRP inhibition based on  $IC_{50}$  values, expected plasma concentrations (given in Table 6) should be considered. Unfortunately, only limited information concerning DOA plasma concentrations is available. In general, case reports are the only information source and interpretation is difficult due to single cases, polytoxicomania, or post-mortem concentrations that are affected by post-mortem redistribution (Staeheli et al. 2017). In case of 3,4-BDB, only a single post-mortem concentration was published, and in this case, 2.1 mg/L amphetamine and 0.4 mg/L *N*-methyl-1-(3,4-methylenedioxyphenyl)-2-butamine (3,4-MBDB) were additionally detected (Carter et al. 2000). Diclofensine is abused due to central stimulating properties, but was originally developed as antidepressant (Meyer et al. 2015). Published concentrations were derived from a controlled experiment after intake of doses common for antidepressant therapy (Strojny and de Silva 1985) and are, therefore, not necessarily equal to doses in case of abuse. Mitragynine concentrations were determined in ten chronic kratom users with the aim of investigating its pharmacokinetics (Trakulsrichai et al. 2015). As plasma concentrations after intake of JWH-200 or WIN 55,212-2 have not yet been determined, those published for over 20 other synthetic cannabinoid receptor agonists such as JWH-018, JWH-122, or JWH-203 were used. The given concentrations derived from a trial to investigate JWH-018 pharmacokinetics, driving under the influence of drug cases, intoxications, or autopsies (Karinen et al. 2015; Toennes et al. 2017). This fact and the large number of different synthetic cannabinoid receptor agonists explained the broad concentration ranges. In summary, expected DOA plasma concentrations were lower than the determined  $IC_{50}$  values. Therefore, a clinical effect seemed rather unlikely. However, it must be considered that concentrations in certain tissues are often higher than in plasma. This is, for example, more than likely in the liver, the main metabolizing organ. Thus, the occurrence of local DDI (Endres et al. 2006) followed by local toxicity cannot be excluded, especially not after intake of high doses.

## Conclusions

The present study was the first to describe the influence of a broad range of new DOA on the hBCRP ATPase activity. A recently published ADP quantification method and the initial hBCRP ATPase activity screening procedure were successfully applied for DOA testing. The results demonstrated that DOA can act as hBCRP ATPase stimulators or inhibitors. 3,4-BDB and mitragynine were shown to have an hBCRP

ATPase stimulation potential. Thanks to the determination of kinetic parameters, their transport is expected to be slower than that of the model substrates. Nevertheless, they could act as victim drug in case of co-consumption of an hBCRP inhibitor followed by potential (local) toxic effects. JWH-200 and WIN 55,212-2 were identified as hBCRP inhibitors comparably strong as the model inhibitor. Therefore, they could act as perpetrator drug, especially after intake of high doses. However, as in vitro studies only have a limited conclusiveness, further investigations are warranted to facilitate a more complete assessment.

**Acknowledgements** The authors like to thank Achim T. Caspar, Lilian H. J. Richter, Gabriele Ulrich, and Armin A. Weber for their support.

## Compliance with ethical standards

**Conflict of interest** The authors declare that they have no conflict of interest.

## References

- Brandt SD, Tirunaryanapuram SS, Freeman S et al (2008) Microwave-accelerated synthesis of psychoactive deuterated *N,N*-dialkylated- $[\alpha,\alpha,\beta,\beta\text{-d}_4]$ -tryptamines. *J Label Compd Radiopharm* 51(14):423–429
- Carter N, Ruttly GN, Milroy CM, Forrest AR (2000) Deaths associated with MBDB misuse. *Int J Leg Med* 113(3):168–170
- Chauret N, Gauthier A, Nicoll-Griffith DA (1998) Effect of common organic solvents on in vitro cytochrome P450-mediated metabolic activities in human liver microsomes. *Drug Metab Dispos* 26(1):1–4
- Dinger J, Meyer MR, Maurer HH (2016) In vitro cytochrome P450 inhibition potential of methylenedioxy-derived designer drugs studied with a two-cocktail approach. *Arch Toxicol* 90(2):305–318
- EMA (2012) Guideline on the investigation of drug interactions, vol CPMP/EWP/560/95/Rev. 1 Corr. 2\*\*, 2012 edn. European Medicines Agency, London. [http://www.ema.europa.eu/docs/en\\_GB/document\\_library/Scientific\\_guideline/2012/07/WC500129606.pdf](http://www.ema.europa.eu/docs/en_GB/document_library/Scientific_guideline/2012/07/WC500129606.pdf). Accessed 21 May 2018
- Endres CJ, Hsiao P, Chung FS, Unadkat JD (2006) The role of transporters in drug interactions. *Eur J Pharm Sci* 27(5):501–517
- FDA (2017) In vitro metabolism- and transporter-mediated drug–drug interaction studies, guidance for industry. FDA (Food and Drug Administration). <https://www.fda.gov/downloads/Drugs/GuidanceComplianceRegulatoryInformation/Guidances/UCM581965.pdf>. Accessed 21 May 2018
- Gupta A, Zhang Y, Unadkat JD, Mao Q (2004) HIV protease inhibitors are inhibitors but not substrates of the human breast cancer resistance protein (BCRP/ABCG2). *J Pharmacol Exp Ther* 310(1):334–341
- Helfer AG, Michely JA, Weber AA, Meyer MR, Maurer HH (2015) Orbitrap technology for comprehensive metabolite-based liquid chromatographic–high resolution–tandem mass spectrometric urine drug screening—exemplified for cardiovascular drugs. *Anal Chim Acta* 891:221–233
- Hira D, Terada T (2018) BCRP/ABCG2 and high-alert medications: biochemical, pharmacokinetic, pharmacogenetic, and clinical implications. *Biochem Pharmacol* 147:201–210

- Holland ML, Lau DT, Allen JD, Arnold JC (2007) The multidrug transporter ABCG2 (BCRP) is inhibited by plant-derived cannabinoids. *Br J Pharmacol* 152(5):815–824
- Huang L, Wang Y, Grimm S (2006) ATP-dependent transport of rosvastatin in membrane vesicles expressing breast cancer resistance protein. *Drug Metab Dispos* 34(5):738–742
- International Transporter C, Giacomini KM, Huang SM et al (2010) Membrane transporters in drug development. *Nat Rev Drug Discov* 9(3):215–236
- Ishikawa T, Kasamatsu S, Hagiwara Y, Mitomo H, Kato R, Sumino Y (2003) Expression and functional characterization of human ABC transporter ABCG2 variants in insect cells. *Drug Metab Pharmacokinet* 18(3):194–202
- Jani M, Szabo P, Kis E, Molnar E, Glavinas H, Krajcsi P (2009) Kinetic characterization of sulfasalazine transport by human ATP-binding cassette G2. *Biol Pharm Bull* 32(3):497–499
- Karinen R, Tuv SS, Oiestad EL, Vindenes V (2015) Concentrations of APINACA, 5F-APINACA, UR-144 and its degradant product in blood samples from six impaired drivers compared to previous reported concentrations of other synthetic cannabinoids. *Forensic Sci Int* 246:98–103
- Kaskova ZM, Tsarkova AS, Yampolsky IV (2016) 1001 lights: luciferins, luciferases, their mechanisms of action and applications in chemical analysis, biology and medicine. *Chem Soc Rev* 45(21):6048–6077
- Kruitjer CM, Beijnen JH, Rosing H et al (2002) Increased oral bioavailability of topotecan in combination with the breast cancer resistance protein and P-glycoprotein inhibitor GF120918. *J Clin Oncol* 20(13):2943–2950
- Mao Q, Lai Y, Wang J (2018) Drug Transporters in xenobiotic disposition and pharmacokinetic prediction. *Drug Metab Dispos* 46(5):561–566
- Meyer MR, Orschiedt T, Maurer HH (2013) Michaelis–Menten kinetic analysis of drugs of abuse to estimate their affinity to human P-glycoprotein. *Toxicol Lett* 217(2):137–142
- Meyer MR, Wagmann L, Schneider-Daum N et al (2015) P-glycoprotein interactions of novel psychoactive substances—stimulation of ATP consumption and transport across Caco-2 monolayers. *Biochem Pharmacol* 94(3):220–226
- Muller F, Fromm MF (2011) Transporter-mediated drug–drug interactions. *Pharmacogenomics* 12(7):1017–1037
- Philipp AA, Wissenbach DK, Zoerntlein SW, Klein ON, Kanogunsunthornrat J, Maurer HH (2009) Studies on the metabolism of mitragynine, the main alkaloid of the herbal drug Kratom, in rat and human urine using liquid chromatography-linear ion trap mass spectrometry. *J Mass Spectrom* 44(8):1249–1261
- Sarkadi B, Homolya L, Szakacs G, Varadi A (2006) Human multidrug resistance ABCB and ABCG transporters: participation in a chemoinnate defense system. *Physiol Rev* 86(4):1179–1236
- Staheli SN, Gascho D, Ebert LC, Kraemer T, Steuer AE (2017) Time-dependent postmortem redistribution of morphine and its metabolites in blood and alternative matrices-application of CT-guided biopsy sampling. *Int J Leg Med* 131(2):379–389
- Strojny N, de Silva JA (1985) Determination of diclofenac, an antidepressant agent, and its major metabolites in human plasma by high-performance liquid chromatography with fluorometric detection. *J Chromatogr* 341(2):313–331
- Toennes SW, Geraths A, Pogoda W et al (2017) Pharmacokinetic properties of the synthetic cannabinoid JWH-018 and of its metabolites in serum after inhalation. *J Pharm Biomed Anal* 140:215–222
- Tournier N, Chevillard L, Megarbane B, Pirnay S, Scherrmann JM, Declèves X (2010) Interaction of drugs of abuse and maintenance treatments with human P-glycoprotein (ABCB1) and breast cancer resistance protein (ABCG2). *Int J Neuropsychopharmacol* 13(7):905–915
- Trakulsrichai S, Sathirakul K, Auparakkitanon S et al (2015) Pharmacokinetics of mitragynine in man. *Drug Des Dev Ther* 9:2421–2429
- UNODC (2017) World drug report. United Nations publication. <https://www.unodc.org/wdr2017/index.html>. Accessed 21 May 2018
- Upreti GC (1984) Colorimetric estimation of inorganic phosphate in colored and/or turbid biological samples: assay of phosphohydrolases. *Anal Biochem* 137(2):485–492
- Wagmann L, Brandt SD, Kavanagh PV, Maurer HH, Meyer MR (2017a) In vitro monoamine oxidase inhibition potential of alpha-methyltryptamine analog new psychoactive substances for assessing possible toxic risks. *Toxicol Lett* 272:84–93
- Wagmann L, Maurer HH, Meyer MR (2017b) An easy and fast adenosine 5'-diphosphate quantification procedure based on hydrophilic interaction liquid chromatography–high resolution tandem mass spectrometry for determination of the in vitro adenosine 5'-triphosphatase activity of the human breast cancer resistance protein ABCG2. *J Chromatogr A* 1521:123–130
- Wang X, Zhang ZY, Arora S et al (2018) Effects of rolapitant administered intravenously or orally on the pharmacokinetics of digoxin (P-glycoprotein substrate) and sulfasalazine (breast cancer resistance protein substrate) in healthy volunteers. *J Clin Pharmacol* 58(2):202–211

## 4. DISCUSSION AND CONCLUSIONS

The presented studies clearly expanded the knowledge of interactions between abused psychoactive substances and the metabolic enzymes FMO3 and MAO or the transport protein BCRP. In the first study, different incubation settings were tested to identify FMO3 substrates by in vitro incubations and LC-IT-MS/MS. Neither heat inactivation, nor chemical inhibition using human liver microsomes led to satisfactory results. Therefore, single enzyme incubations were preferred for unambiguous identification of FMO3 substrates. An initial monooxygenases activity screening was conducted and five DOA were identified as FMO3, but also CYP substrates. Modeling of kinetic curves was followed by determination of kinetic parameters, which were successfully used to calculate the contribution of the different monooxygenases in the in vivo hepatic net clearance of the *N*-oxygenation products. This was realized by application of an extended relative activity factor approach, containing not only CYP enzymes, but also FMO3 for the first time. In case of *N,N*-diallyltryptamine and methamphetamine, FMO3 was identified as main enzyme involved in the formation of the *N*-oxygenation products and demonstrated its relevance in the metabolism of DOA.<sup>42</sup>

In the next studies, the MAO-A or B inhibition potential of AMT-derived NPS or 2C-series DOA was investigated. For this purpose, an inhibition assay based on in vitro incubations of recombinant MAO catalyzing the deamination of the non-selective MAO substrate kynuramine and HRMS/MS analysis after HILIC was successfully developed and validated. Due to the high sensitivity of the used apparatus, only minimal enzymes amounts were required, reducing costs and the risk of non-specific protein binding of analytes. The application of an initial MAO inhibition screening revealed AMT and all 13 analogs to be inhibitors of MAO-A, while four AMT

---

## DISCUSSION AND CONCLUSIONS

---

derivatives additionally inhibited MAO-B. Determination of  $IC_{50}$  values identified 7-methyl-AMT as most potent MAO-A inhibitor comparable to the model inhibitors harmine and harmaline. An investigation of the inhibition mode revealed 7-methyl-AMT to be a competitive MAO-A inhibitor.<sup>43</sup> The presented procedure was also successfully applied for investigation of 17 phenethylamines, which consisted of 12 classic 2C-series compounds and five FLY analogs. Thirteen test drugs showed inhibition potential for MAO-A and 11 inhibited MAO-B. The FLYs were identified as MAO-A inhibitors, whereas the classic 2C-series drugs exhibited MAO-B inhibition potential.<sup>44</sup> Determination of  $IC_{50}$  values demonstrated that AMT analogs provided lower values and could therefore be considered as stronger MAO inhibitors than 2C-series compounds. Nevertheless, an assessment of the clinical relevance of MAO inhibition after consumption was rather difficult as only scarce information concerning plasma concentrations of the investigated DOA was available. However, a contribution of MAO inhibition to the pharmacology of these DOA is likely.

For the measurement of ADP concentrations in in vitro incubations with the BCRP, an ADP quantification method based on HILIC-HRMS/MS was developed and successfully validated. During an initial activity screening, the BCRP ATPase activity in presence or absence of the test compound was assessed and applicability was demonstrated by the investigation of five HIV protease inhibitors.<sup>45</sup> This procedure was then applied for DOA testing. Seven DOA were shown to have BCRP ATPase stimulation potential. Kinetic curve modeling identified the entactogen 1-(3,4-methylenedioxyphenyl)-2-butamine and the plant alkaloid mitragynine as strongest stimulators of the BCRP ATPase, with an affinity comparable to that of the BCRP model substrate rosuvastatin. Five DOA were shown to have BCRP ATPase inhibition potential. Two synthetic cannabinoid receptor agonists provided the lowest

## DISCUSSION AND CONCLUSIONS

---

IC<sub>50</sub> values, comparable to that of the BCRP model inhibitor orthovanadate. The study demonstrated, that DOA potently stimulate or inhibit the BCRP ATPase comparable to model substrates or inhibitors. Therefore, it is likely that these DOA could be involved in the appearance of DDI. However, as in vitro studies have only a limited conclusiveness, further investigations are warranted to facilitate a more complete assessment of clinical effects.<sup>46</sup>



---

## 5. REFERENCES

1. UNODC. World Drug Report. In: UNODC, ed: United Nations publication; 2017. <http://www.unodc.org/wdr2017/>
2. Wagmann L, Maurer HH. Bioanalytical methods for new psychoactive substances. *Handb Exp Pharmacol*. 2018; DOI: 10.1007/164\_2017\_83
3. EMCDDA. European Drug Report 2018. *Publications of of the European Union*. 2018.  
[http://www.emcdda.europa.eu/system/files/publications/8585/20181816\\_TDAT18001ENN\\_PDF.pdf](http://www.emcdda.europa.eu/system/files/publications/8585/20181816_TDAT18001ENN_PDF.pdf)
4. Brandt SD, King LA, Evans-Brown M. The new drug phenomenon. *Drug Test Anal*. 2014;6(7-8):587-597.
5. Logan BK, Mohr ALA, Friscia M, et al. Reports of adverse events associated with use of novel psychoactive substances, 2013-2016: A Review. *J Anal Toxicol*. 2017;41(7):573-610.
6. Nelson ME, Bryant SM, Aks SE. Emerging drugs of abuse. *Dis Mon*. 2014;60(3):110-132.
7. Zamengo L, Frison G, Bettin C, Sciarrone R. Understanding the risks associated with the use of new psychoactive substances (NPS): high variability of active ingredients concentration, mislabelled preparations, multiple psychoactive substances in single products. *Toxicol Lett*. 2014;229(1):220-228.
8. Meyer MR. New psychoactive substances: an overview on recent publications on their toxicodynamics and toxicokinetics. *Arch Toxicol*. 2016;90(10):2421-2444.

## REFERENCES

---

9. Nordberg M, Duffus JH, Templeton DM. Glossary of terms used in toxicokinetics - (IUPAC Recommendations 2003). *Pure Appl Chem.* 2004;76(5):1033-1082.
10. EMA. Guideline on the investigation of drug interactions. In. Vol CPMP/EWP/560/95/Rev. 1 Corr. 2\*\* 2012 ed. London, UK: European Medicines Agency; 2012.  
[http://www.ema.europa.eu/docs/en\\_GB/document\\_library/Scientific\\_guideline/2012/07/WC500129606.pdf](http://www.ema.europa.eu/docs/en_GB/document_library/Scientific_guideline/2012/07/WC500129606.pdf)
11. FDA. In Vitro Metabolism- and Transporter- Mediated Drug-Drug Interaction Studies, Guidance for Industry. In: FDA (Food and Drug Administration); 2017.  
<https://www.fda.gov/downloads/Drugs/GuidanceComplianceRegulatoryInformation/Guidances/UCM581965.pdf>
12. Kennedy WK, Jann MW, Kutscher EC. Clinically significant drug interactions with atypical antipsychotics. *CNS Drugs.* 2013;27(12):1021-1048.
13. Spina E, Trifiro G, Caraci F. Clinically significant drug interactions with newer antidepressants. *CNS Drugs.* 2012;26(1):39-67.
14. Spina E, Santoro V, D'Arrigo C. Clinically relevant pharmacokinetic drug interactions with second-generation antidepressants: an update. *Clin Ther.* 2008;30(7):1206-1227.
15. Patsalos PN. Drug interactions with the newer antiepileptic drugs (AEDs)--part 1: pharmacokinetic and pharmacodynamic interactions between AEDs. *Clin Pharmacokinet.* 2013;52(11):927-966.
16. Patsalos PN. Drug interactions with the newer antiepileptic drugs (AEDs)--Part 2: pharmacokinetic and pharmacodynamic interactions between AEDs and

## REFERENCES

---

- drugs used to treat non-epilepsy disorders. *Clin Pharmacokinet.* 2013;52(12):1045-1061.
17. Lindsey WT, Stewart D, Childress D. Drug interactions between common illicit drugs and prescription therapies. *Am J Drug Alcohol Abuse.* 2012;38(4):334-343.
  18. Kumar S, Rao PS, Earla R, Kumar A. Drug-drug interactions between anti-retroviral therapies and drugs of abuse in HIV systems. *Expert Opin Drug Metab Toxicol.* 2015;11(3):343-355.
  19. Thompson RA, Isin EM, Ogese MO, Mettetal JT, Williams DP. Reactive metabolites: current and emerging risk and hazard assessments. *Chem Res Toxicol.* 2016;29(4):505-533.
  20. Strolin Benedetti M, Whomsley R, Baltés E. Involvement of enzymes other than CYPs in the oxidative metabolism of xenobiotics. *Expert Opinion on Drug Metabolism & Toxicology.* 2006;2(6):895-921.
  21. Kalgutkar AS, Dalvie D. Predicting toxicities of reactive metabolite-positive drug candidates. *Annu Rev Pharmacol Toxicol.* 2015;55:35-54.
  22. Mao Q, Lai Y, Wang J. Drug transporters in xenobiotic disposition and pharmacokinetic prediction. *Drug Metab Dispos.* 2018;46(5):561-566.
  23. International Transporter C, Giacomini KM, Huang SM, et al. Membrane transporters in drug development. *Nat Rev Drug Discov.* 2010;9(3):215-236.
  24. Cashman JR, Zhang J. Human flavin-containing monooxygenases. *Annu Rev Pharmacol Toxicol.* 2006;46:65-100.
  25. Cashman JR, Xiong YN, Xu L, Janowsky A. N-oxygenation of amphetamine and methamphetamine by the human flavin-containing monooxygenase (form

## REFERENCES

---

- 3): role in bioactivation and detoxication. *J Pharmacol Exp Ther.* 1999;288(3):1251-1260.
26. Wang CC, Billett E, Borchert A, Kuhn H, Ufer C. Monoamine oxidases in development. *Cell Mol Life Sci.* 2013;70(4):599-630.
27. Ramsay RR. Inhibitor design for monoamine oxidases. *Curr Pharm Des.* 2013;19(14):2529-2539.
28. Fisar Z. Drugs related to monoamine oxidase activity. *Prog Neuropsychopharmacol Biol Psychiatry.* 2016;69:112-124.
29. Tipton KF. 90 years of monoamine oxidase: some progress and some confusion. *J Neural Transm (Vienna).* 2018; DOI: 10.1007/s00702-018-1881-5
30. Brush DE, Bird SB, Boyer EW. Monoamine oxidase inhibitor poisoning resulting from Internet misinformation on illicit substances. *J Toxicol Clin Toxicol.* 2004;42(2):191-195.
31. Chai PR, Boyer EW. Serotonin Syndrome. In: *Critical Care Toxicology.* 2017:539-548.
32. Steuer AE, Boxler MI, Stock L, Kraemer T. Inhibition potential of 3,4-methylenedioxymethamphetamine (MDMA) and its metabolites on the in vitro monoamine oxidase (MAO)-catalyzed deamination of the neurotransmitters serotonin and dopamine. *Toxicol Lett.* 2016;243:48-55.
33. Herraiz T, Brandt SD. 5-(2-Aminopropyl)indole (5-IT): a psychoactive substance used for recreational purposes is an inhibitor of human monoamine oxidase (MAO). *Drug Test Anal.* 2014;6(7-8):607-613.
34. EMCDDA. Report on the risk assessment of 5-(2-aminopropyl)indole in the framework of the Council Decision on new psychoactive substances. In: Publications Office of the European Union, Luxembourg; 2014.
-

## REFERENCES

---

- [http://www.emcdda.europa.eu/system/files/publications/788/TDAK13002ENN-1\\_\\_462975.pdf](http://www.emcdda.europa.eu/system/files/publications/788/TDAK13002ENN-1__462975.pdf)
35. Nakanishi T, Ross DD. Breast cancer resistance protein (BCRP/ABCG2): its role in multidrug resistance and regulation of its gene expression. *Chin J Cancer*. 2012;31(2):73-99.
  36. Kruijtzter CM, Beijnen JH, Rosing H, et al. Increased oral bioavailability of topotecan in combination with the breast cancer resistance protein and P-glycoprotein inhibitor GF120918. *J Clin Oncol*. 2002;20(13):2943-2950.
  37. Wang X, Zhang ZY, Arora S, et al. Effects of rolapitant administered intravenously or orally on the pharmacokinetics of digoxin (P-glycoprotein substrate) and sulfasalazine (breast cancer resistance protein substrate) in healthy volunteers. *J Clin Pharmacol*. 2018;58(2):202-211.
  38. Ni Z, Bikadi Z, Rosenberg MF, Mao Q. Structure and function of the human breast cancer resistance protein (BCRP/ABCG2). *Curr Drug Metab*. 2010;11(7):603-617.
  39. Sarkadi B, Homolya L, Szakacs G, Varadi A. Human multidrug resistance ABCB and ABCG transporters: participation in a chemoimmunity defense system. *Physiol Rev*. 2006;86(4):1179-1236.
  40. Holland ML, Lau DT, Allen JD, Arnold JC. The multidrug transporter ABCG2 (BCRP) is inhibited by plant-derived cannabinoids. *Br J Pharmacol*. 2007;152(5):815-824.
  41. Tournier N, Chevillard L, Megarbane B, Pirnay S, Scherrmann JM, Declèves X. Interaction of drugs of abuse and maintenance treatments with human P-glycoprotein (ABCB1) and breast cancer resistance protein (ABCG2). *Int J Neuropsychopharmacol*. 2010;13(7):905-915.

## REFERENCES

---

42. Wagmann L, Meyer MR, Maurer HH. What is the contribution of human FMO3 in the *N*-oxygenation of selected therapeutic drugs and drugs of abuse? *Toxicol Lett.* 2016;258:55-70.
43. Wagmann L, Brandt SD, Kavanagh PV, Maurer HH, Meyer MR. In vitro monoamine oxidase inhibition potential of alpha-methyltryptamine analog new psychoactive substances for assessing possible toxic risks. *Toxicol Lett.* 2017;272:84-93.
44. Wagmann L, Maurer HH, Meyer MR. Interactions of phenethylamine-derived psychoactive substances of the 2C-series with human monoamine oxidases. *Drug Test Anal.* 2018; DOI: 10.1002/dta.2494.
45. Wagmann L, Maurer HH, Meyer MR. An easy and fast adenosine 5'-diphosphate quantification procedure based on hydrophilic interaction liquid chromatography-high resolution tandem mass spectrometry for determination of the in vitro adenosine 5'-triphosphatase activity of the human breast cancer resistance protein ABCG2. *J Chromatogr A.* 2017;1521:123-130.
46. Wagmann L, Maurer HH, Meyer MR. Inhibition and stimulation of the human breast cancer resistance protein as in vitro predictor of drug-drug interactions of drugs of abuse. *Arch Toxicol.* 2018;92(9):2875-2884.

## 6. ABBREVIATIONS

5-HT	serotonin
ABC	ATP-binding cassette
ADP	adenosine 5'-diphosphate
AMT	alpha-methyltryptamine
ATP	adenosine 5'-triphosphate
BCRP	breast cancer resistance protein
CYP	cytochrome P450
DDI	drug-drug interaction
DOA	drugs of abuse
FMO	flavin-containing monooxygenases
HILIC	hydrophilic interaction liquid chromatography
HR	high resolution
IT	ion trap
LC	liquid chromatography
MAO	monoamine oxidases
MDMA	3,4-methylenedioxymethamphetamine
MS/MS	tandem mass spectrometry
NPS	new psychoactive substances

## ABBREVIATIONS

---

## 7. SUMMARY

Besides traditional drugs of abuse (DOA), a steadily increasing number of new psychoactive substances (NPS) is available on the DOA market. In contrast to therapeutic drugs, DOA are marketed without (pre)clinical studies and their pharmacology is unknown. To expand the knowledge surrounding toxicokinetics of DOA, the affinity and/or inhibition potential of selected DOA towards metabolic enzymes such as monooxygenases or monoamine oxidases and the breast cancer resistance protein, an efflux transporter, was tested. In vitro incubations with recombinant human enzymes and/or human liver cell preparations followed by mass spectrometric analysis were the basis for all conducted experiments. During an initial monooxygenases activity screening, several DOA were shown to be substrate of FMO3, which was identified as main enzyme involved in the *N*-oxygenation of *N,N*-diallyltryptamine and methamphetamine. After development and validation of a procedure for detection of MAO inhibition, a broad range of AMT-derived NPS were identified as MAO-A inhibitors. Phenethylamines were also tested and the classic 2C-series drugs inhibited MAO-B, while their FLY analogs were identified as MAO-A inhibitors. For assessing the BCRP ATPase activity, a method for quantification of ADP in BCRP incubations by HILIC-HRMS/MS was developed and validated. Investigation of selected DOA demonstrated that they potently stimulated or inhibited the BCRP ATPase comparable to model substrates or inhibitors.

## SUMMARY

---

## 8. ZUSAMMENFASSUNG

Eine ständig wachsende Zahl sogenannter Neuer Psychoaktiver Substanzen (NPS) wird auf dem Drogenmarkt ohne Durchführung (prä)klinische Studien angeboten und ihre Pharmakologie und Toxikologie sind meist unbekannt. Zur Erforschung ihrer Toxikokinetik wurden Affinität und/oder Inhibitionspotential ausgewählter Drogen gegenüber metabolischen Enzymen wie Monoxygenasen oder Monoaminoxidasen und dem *breast cancer resistance protein* (BCRP), einem Effluxtransporter, mittels in vitro Inkubationen rekombinanter humaner Enzyme und/oder Leberzellpräparationen untersucht. Im Rahmen einer Monoxygenasen-Aktivitätsuntersuchung wurden mehrere Missbrauchsdrogen als FMO3 Substrate identifiziert und FMO3 daraufhin als hauptverantwortliches Enzym für die *N*-Oxygenierung von *N,N*-Diallyltryptamin und Methamphetamin nachgewiesen. Nach Entwicklung und Validierung eines massenspektrometrischen Verfahrens zum Nachweis von MAO Inhibition wurden zahlreiche AMT-verwandte NPS als MAO-A Inhibitoren identifiziert. Auch Phenethylamine wurden getestet. Die klassischen Verbindungen der 2C-Serie inhibierten MAO-B, ihre FLY Analoga aber MAO-A. Des Weiteren wurde zur Einschätzung der BCRP-ATPase-Aktivität eine Methode zur Quantifizierung von ADP in BCRP-Inkubaten mittels HILIC-HRMS/MS entwickelt und validiert. Die Untersuchung ausgewählter Missbrauchsdrogen belegte, dass diese die BCRP-ATPase vergleichbar stark stimulieren oder hemmen wie Modelsubstrate oder -inhibitoren.